Chapter 5

Moment Methods

"He who will not reason is a bigot; he who cannot is a fool; he who dares not is a slave."
William Drummond

5.1 Introduction

In Section 1.3.2, it was mentioned that most EM problems can be stated in terms of an inhomogeneous equation

$$L\Phi = g \tag{5.1}$$

where L is an operator which may be differential, integral or integro-differential, g is the known excitation or source function, and Φ is the unknown function to be determined. So far, we have limited our discussion to cases for which L is differential. In this chapter, we will treat L as an integral or integro-differential operator.

The *method of moments* (MOM) is a general procedure for solving Eq. (5.1). The method owes its name to the process of taking moments by multiplying with appropriate weighing functions and integrating, as discussed in Section 4.6. The name "method of moments" has its origin in Russian literature [1, 2]. In western literature, the first use of the name is usually attributed to Harrington [3]. The origin and development of the moment method are fully documented by Harrington [4, 5].

The method of moments is essentially the method of weighted residuals discussed in Section 4.6. Therefore, the method is applicable for solving both differential and integral equations.

The use of MOM in EM has become popular since the work of Richmond in 1965 and Harrington [7] in 1967. The method has been successfully applied to a wide variety of EM problems of practical interest such as radiation due to thin-wire elements and arrays, scattering problems, analysis of microstrips and lossy structures, propagation over an inhomogeneous earth, and antenna beam pattern, to mention a few. An updated review of the method is found in a paper by Ney [8]. The literature on MOM is already so large as to prohibit a comprehensive bibliography. A partial bibliography is provided by Adams [9].

The procedure for applying MOM to solve Eq. (5.1) usually involves four steps:

(1) derivation of the appropriate integral equation (IE),

(2) conversion (discretization) of the IE into a matrix equation using basis (or expansions) functions and weighting (or testing) functions,

(3) evaluation of the matrix elements, and

(4) solving the matrix equation and obtaining the parameters of interest.

The basic tools for step (2) have already been mastered in Section 4.6; in this chapter we will apply them to IEs rather than PDEs. Just as we studied PDEs themselves in Section 1.3.2, we will first study IEs.

5.2 Integral Equations

An integral equation is any equation involving unknown function Φ under the integral sign. Simple examples of integral equations are Fourier, Laplace, and Hankel transforms.

5.2.1 Classification of Integral Equations

Linear integral equations that are most frequently studied fall into two categories named after Fredholm and Volterra. One class is the Fredholm equations of the first, second, and third kind, namely,

$$f(x) = \int_a^b K(x,t)\Phi(t)\,dt\ , \tag{5.2}$$

$$f(x) = \Phi(x) - \lambda \int_a^b K(x,t)\Phi(t)\,dt\ , \tag{5.3}$$

$$f(x) = a(x)\Phi(x) - \lambda \int_a^b K(x,t)\Phi(t)\,dt\ , \tag{5.4}$$

where λ is a scalar (or possibly complex) parameter. Functions $K(x,t)$ and $f(x)$ and the limits a and b are known, while $\Phi(x)$ is unknown. The function $K(x,t)$ is known as the *kernel* of the integral equation. The parameter λ is sometimes equal to unity.

The second class of integral equations are the Volterra equations of the first, second, and third kind, namely,

$$f(x) = \int_a^x K(x,t)\Phi(t)\,dt\ , \tag{5.5}$$

$$f(x) = \Phi(x) - \lambda \int_a^x K(x,t)\Phi(t)\,dt\ , \tag{5.6}$$

$$f(x) = a(x)\Phi(x) - \lambda \int_a^x K(x,t)\Phi(t)\,dt\ , \tag{5.7}$$

with a variable upper limit of integration. If $f(x) = 0$, the integral equations (5.2) to (5.7) become homogeneous. Note that Eqs. (5.2) to (5.7) are all linear equations in that Φ enters the equations in a linear manner. An integral equation is nonlinear if Φ appears in the power of $n > 1$ under the integral sign. For example, the integral equation

$$f(x) = \Phi(x) - \int_a^b K(x,t)\Phi^2(t)\,dt \tag{5.8}$$

is nonlinear. Also, if limit a or b or the kernel $K(x,t)$ becomes infinite, an integral equation is said to be singular. Finally, a kernel $K(x,t)$ is said to be symmetric if $K(x,t) = K(t,x)$.

5.2.2 Connection Between Differential and Integral Equations

The above classification of one-dimensional integral equations arises naturally from the theory of differential equations, thereby showing a close connection between the integral and differential formulation of a given problem. Most ordinary differential equations can be expressed as integral equations, but the reverse is not true. While boundary conditions are imposed externally in differential equations, they are incorporated within an integral equation.

For example, consider the first order ordinary differential equation

$$\frac{d\Phi}{dx} = F(x,\Phi), \quad a \le x \le b \tag{5.9}$$

subject to $\Phi(a) =$ constant. This can be written as the Volterra integral of the second kind. Integrating Eq. (5.9) gives

$$\Phi(x) = \int_a^x F(t,\Phi(t))\,dt + c_1$$

where $c_1 = \Phi(a)$. Hence Eq. (5.9) is the same as

$$\Phi(x) = \Phi(a) + \int_a^x F(t,\Phi)\,dt \tag{5.10}$$

Any solution of Eq. (5.10) satisfies both Eq. (5.9) and the boundary conditions. Thus an integral equation formulation includes both the differential equation and the boundary conditions.

Similarly, consider the second order ordinary differential equation

$$\frac{d^2\Phi}{dx^2} = F(x, \Phi), \quad a \le x \le b \tag{5.11}$$

Integrating once yields

$$\frac{d\Phi}{dx} = \int_a^x F(x, \Phi(t))\, dt + c_1 \tag{5.12}$$

where $c_1 = \Phi'(a)$. Integrating Eq. (5.12) by parts,

$$\Phi(x) = c_2 + c_1 x + \int_a^x (x - t) F(x, \Phi(t))\, dt$$

where $c_2 = \Phi(a) - \Phi'(a)a$. Hence

$$\Phi(x) = \Phi(a) + (x - a)\Phi'(a) + \int_a^x (x - t) F(x, \Phi)\, dt \tag{5.13}$$

Again, we notice that the integral equation (5.13) represents both the differential equation (5.11) and the boundary conditions. We have only considered one-dimensional integral equations. Integral equations involving unknown functions in two or more space dimensions will be discussed later.

Example 5.1

Solve the Volterra integral equation

$$\Phi(x) = 1 + \int_0^x \Phi(t)\, dt \qquad \square$$

Solution

This can be solved directly or indirectly by finding the solution of the corresponding differential equation. To solve it directly, we differentiate both sides of the given integral equation. In general, given an integral

$$g(x) = \int_{\alpha(x)}^{\beta(x)} f(x, t)\, dt \tag{5.14}$$

with variable limits, we differentiate this using the Leibnitz rule, namely,

$$g'(x) = \int_{\alpha(x)}^{\beta(x)} \frac{\partial f(x, t)}{\partial x}\, dt + f(x, \beta)\beta' - f(x, \alpha)\alpha' \tag{5.15}$$

Differentiating the given integral equation, we obtain

$$\frac{d\Phi}{dx} = \Phi(x) \tag{5.16a}$$

or

$$\frac{d\Phi}{\Phi} = dx \tag{5.16b}$$

Integrating gives

$$\ln \Phi = x + \ln c_o$$

or

$$\Phi = c_o e^x$$

where $\ln c_o$ is the integration constant. From the given integral equation

$$\Phi(0) = 1 = c_o$$

Hence

$$\Phi(x) = e^x \tag{5.17}$$

is the required solution. This can be checked by substituting it into the given integral equation.

An indirect way of solving the integral equation is by comparing it with Eq. (5.10) and noting that

$$a = 0,\ \Phi(a) = \Phi(0) = 1$$

and that $F(x, \Phi) = \Phi(x)$. Hence the corresponding first order differential equation is

$$\frac{d\Phi}{dx} = \Phi, \quad \Phi(0) = 1$$

which is the same as Eq. (5.16), and the solution in Eq. (5.17) follows. ∎

Example 5.2

Find the integral equation corresponding to the differential equation

$$\Phi''' - 3\Phi'' - 6\Phi' + 8\Phi = 0$$

subject to $\Phi''(0) = \Phi'(0) = \Phi(0) = 1$. □

Solution

Let $\Phi''' = F(\Phi, \Phi, \phi, x) = 3\Phi'' + 6\Phi' - 8\Phi$. Integrating both sides,

$$\Phi'' = 3\Phi' + 6\Phi - 8\int_0^x \Phi(t)\,dt + c_1 \tag{5.18}$$

where c_1 is determined from the initial values, i.e.,

$$1 = 3 + 6 + c_1 \quad \rightarrow \quad c_1 = -8$$

Integrating both sides of Eq. (5.18) gives

$$\Phi' = 3\Phi + 6\int_o^x \Phi(t)\,dt - 8\int_0^x (x-t)\Phi(t)\,dt - 8x + c_2 \tag{5.19}$$

where

$$1 = 3 + c_2 \quad \rightarrow \quad c_2 = -2$$

Finally, we integrate both sides of Eq. (5.19) to get

$$\Phi = 3\int_o^x \Phi(t)\,dt + 6\int_o^x (x-t)\Phi(t)\,dt - 4\int_o^x (x-t)^2\Phi(t)\,dt - 4x^2 - 2x + c_3$$

where $1 = c_3$. Thus the integral equation equivalent to the given differential equation is

$$\Phi(x) = 1 - 2x - 4x^2 + \int_o^x \left[3 + 6(x-t) - 4(x-t)^2\right]\Phi(t)\,dt \qquad \blacksquare$$

5.3 Green's Functions

A more systematic means of obtaining an IE from a PDE is by constructing an auxiliary function known as the *Green's function*[1] for that problem [10]–[13]. The Green's function, also known as the *source function* or *influence function,* is the kernel function obtained from a linear boundary value problem and forms the essential link between the differential and integral formulations. Green's function also provides a method of dealing with the source term (g in $L\Phi = g$) in a PDE. In other words, it provides an alternative approach to the series expansion method of Section 2.7 for solving inhomogeneous boundary-value problems by reducing the inhomogeneous problem to a homogeneous one.

To obtain the field caused by a distributed source by the Green's function technique, we find the effects of each elementary portion of source and sum them up. If $G(\mathbf{r}, \mathbf{r}')$ is the field at the observation point (or field point) $\mathbf{r}$ caused by a unit point source at the source point $\mathbf{r}'$, then the field at $\mathbf{r}$ by a source distribution $g(\mathbf{r}')$ is the integral of $g(\mathbf{r}')G(\mathbf{r}, \mathbf{r}')$ over the range of $\mathbf{r}'$ occupied by the source. The function G is the Green's function. Thus, physically, the Green's function $G(\mathbf{r}, \mathbf{r}')$ represents the potential at $\mathbf{r}$ due to a unit point charge at $\mathbf{r}'$. For example, the solution to the Dirichlet problem

$$\begin{aligned} \nabla^2\Phi &= g \quad \text{in} \quad R \\ \Phi &= f \quad \text{on} \quad B \end{aligned} \tag{5.20}$$

[1] Named after George Green (1793–1841), an English mathematician.

is given by

$$\Phi = \int_R g\left(\mathbf{r}'\right) G\left(\mathbf{r}, \mathbf{r}'\right)\, dv' + \oint_B f \frac{\partial G}{\partial n} dS \tag{5.21}$$

where n denotes the outward normal to the boundary B of the solution region R. It is obvious from Eq. (5.21) that the solution Φ can be determined provided the Green's function G is known. So the real problem is not that of finding the solution but that of constructing the Green's function for the problem.

Consider the linear second order PDE

$$L\Phi = g \tag{5.22}$$

We define the Green's function corresponding to the differential operator L as a solution of the point source inhomogeneous equation

$$LG\left(\mathbf{r}, \mathbf{r}'\right) = \delta\left(\mathbf{r}, \mathbf{r}'\right) \tag{5.23}$$

where $\mathbf{r}$ and $\mathbf{r}'$ are the position vectors of the field point (x, y, z) and source point (x', y', z'), respectively, and $\delta(\mathbf{r}, \mathbf{r}')$ is the Dirac delta function, which vanishes for $\mathbf{r} \neq \mathbf{r}'$ and satisfies

$$\int \delta\left(\mathbf{r}, \mathbf{r}'\right) g\left(\mathbf{r}'\right)\, dv' = g(\mathbf{r}) \tag{5.24}$$

From Eq. (5.23), we notice that the Green function $G(\mathbf{r}, \mathbf{r}')$ can be interpreted as the solution to the given boundary value problem with the source term g replaced by the unit impulse function. Thus $G(\mathbf{r}, \mathbf{r}')$ physically represents the response of the linear system to a unit impulse applied at the point $\mathbf{r} = \mathbf{r}'$.

The Green's function has the following properties [13]:

(a) G satisfies the equation $LG = 0$ except at the source point $\mathbf{r}'$, i.e.,

$$LG\left(\mathbf{r}, \mathbf{r}'\right) = \delta\left(\mathbf{r}, \mathbf{r}'\right) \tag{5.23}$$

(b) G is symmetric in the sense that

$$G\left(\mathbf{r}, \mathbf{r}'\right) = G\left(\mathbf{r}', \mathbf{r}\right) \tag{5.25}$$

(c) G satisfies that prescribed boundary value f on B, i.e.,

$$G = f \ \text{ on } \ B \tag{5.26}$$

(d) The directional derivative $\partial G/\partial n$ has a discontinuity at $\mathbf{r}'$ which is specified by the equation

$$\lim_{\epsilon \to 0} \oint_S \frac{\partial G}{\partial n}\, dS = 1 \tag{5.27}$$

where n is the outward normal to the sphere of radius ϵ as shown in Fig. 5.1, i.e.,

$$\left|\mathbf{r} - \mathbf{r}'\right| = \epsilon^2$$

Property (b) expresses the *principle of reciprocity*; it implies that an exchange of source and observer does not affect G. The property is proved by Myint–U [13] by applying Green's second identity in conjunction with Eq. (5.23) while property (d) is proved by applying divergence theorem along with Eq. (5.23).

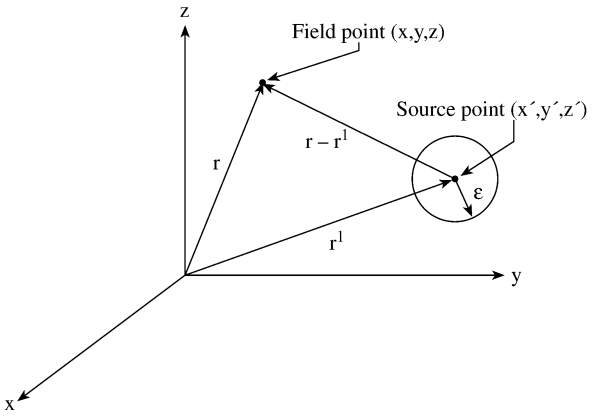

Figure 5.1
Illustration of the field point (x, y, z) **and source point** (x', y', z')**.**

5.3.1 For Free Space

We now illustrate how to construct the free space Green's function G corresponding to a PDE. It is usually convenient to let G be the sum of a particular integral of the inhomogeneous equation $LG = g$ and the solution of the associated homogeneous equation $LG = 0$. In other words, we let

$$G\left(\mathbf{r}, \mathbf{r}'\right) = F\left(\mathbf{r}, \mathbf{r}'\right) + U\left(\mathbf{r}, \mathbf{r}'\right) \tag{5.28}$$

where F, known as the free-space Green's function or fundamental solution, satisfies

$$LF = \delta\left(\mathbf{r}, \mathbf{r}'\right) \text{ in } R \tag{5.29}$$

and U satisfies

$$LU = 0 \text{ in } R \tag{5.30}$$

so that by superposition $G = F + U$ satisfies Eq. (5.23). Also $G = f$ on the boundary B requires that

$$U = -F + f \text{ on } B \tag{5.31}$$

Notice that F need not satisfy the boundary condition.

We apply this to two specific examples. First, consider the two-dimensional problem for which

$$L = \frac{\partial^2}{\partial x^2} + \frac{\partial^2}{\partial y^2} = \nabla^2 \tag{5.32}$$

The corresponding Green's function $G(x, y; x', y')$ satisfies

$$\nabla^2 G\left(x, y; x', y'\right) = \delta\left(x - x'\right)\delta\left(y - y'\right) \tag{5.33}$$

Hence, F must satisfy

$$\nabla^2 F = \delta\left(x - x'\right)\delta\left(y - y'\right)$$

For $\rho = [(x - x')^2 + (y - y')^2]^{1/2} > 0$, i.e., for $x \neq x'$, $y \neq y'$,

$$\nabla^2 F = \frac{1}{\rho}\frac{\partial}{\partial \rho}\left(\rho \frac{\partial F}{\partial \rho}\right) = 0 \tag{5.34}$$

which is integrated twice to give

$$F = A \ln \rho + B \tag{5.35}$$

Applying the property in Eq. (5.27)

$$\lim_{\epsilon \to 0} \oint \frac{dF}{d\rho}\, dl = \lim_{\epsilon \to 0} \int_0^{2\pi} \frac{A}{\rho} \rho\, d\phi = 2\pi A = 1$$

or $A = \dfrac{1}{2\pi}$. Since B is arbitrary, we may choose $B = 0$. Thus

$$F = \frac{1}{2\pi} \ln \rho$$

and

$$G = F + U = \frac{1}{2\pi} \ln \rho + U \tag{5.36}$$

We choose U so that G satisfies prescribed boundary conditions.

For the three-dimensional problem,

$$L = \nabla^2 = \frac{\partial^2}{\partial x^2} + \frac{\partial^2}{\partial y^2} + \frac{\partial^2}{\partial z^2} \tag{5.37}$$

and the corresponding Green's function $G(x, y, z; x', y', z')$ satisfies

$$LG\left(x, y, z; x', y', z'\right) = \delta\left(x - x'\right)\delta\left(y - y'\right)\delta\left(z - z'\right) \tag{5.38}$$

Hence, F must satisfy

$$\begin{aligned} \nabla^2 F &= \delta\left(x - x'\right)\delta\left(y - y'\right)\delta\left(z - z'\right) \\ &= \delta\left(\mathbf{r} - \mathbf{r}'\right) \end{aligned}$$

For $\mathbf{r} \neq \mathbf{r}'$,

$$\nabla^2 F = \frac{1}{r^2}\frac{d}{dr}\left(r^2 \frac{dF}{dr}\right) = 0 \tag{5.39}$$

which is integrated twice to yield

$$F = -\frac{A}{r} + B \tag{5.40}$$

Applying Eq. (5.27),

$$1 = \lim_{\epsilon \to 0} \oint \frac{dF}{dr}\, dS = \lim_{\epsilon \to 0} \int_0^{2\pi} \int_0^{\pi} \frac{A}{r^2} r^2 \sin\phi \, d\theta \, d\phi = 4\pi A$$

or $A = \dfrac{1}{4\pi}$. Choosing $B = 0$ leads to

$$F = -\frac{1}{4\pi r}$$

and

$$G = F + U = -\frac{1}{4\pi r} + U \tag{5.41}$$

where U is chosen so that G satisfies prescribed boundary conditions.

Table 5.1 lists some Green functions that are commonly used in the solution of EM-related problems. It should be observed from Table 5.1 that the form of the three-dimensional Green's function for the steady-state wave equation tends to the Green's function for Laplace's equation as the wave number k approaches zero. It is also worthy of remark that each of the Green's functions in closed form as in Table 5.1 can be expressed in series form. For example, the Green's function

$$\begin{aligned} F &= -\frac{j}{4} H_0^{(1)} \left(k \left| \boldsymbol{\rho} - \boldsymbol{\rho}' \right| \right) \\ &= -\frac{j}{4} H_0^{(1)} \left(k \left[\rho^2 + \rho'^2 - 2\rho\rho' \cos\left(\phi - \phi'\right) \right]^{1/2} \right) \end{aligned} \tag{5.42}$$

can be written in series form as

$$F = \begin{cases} -\dfrac{j}{4} \displaystyle\sum_{n=-\infty}^{\infty} H_n^{(1)} \left(k\rho'\right) J_n(k\rho) e^{-jn(\phi - \phi')}, & \rho < \rho' \\ -\dfrac{j}{4} \displaystyle\sum_{n=-\infty}^{\infty} H_n^{(1)}(k\rho) J_n \left(k\rho'\right) e^{-jn(\phi - \phi')}, & \rho > \rho' \end{cases} \tag{5.43}$$

This is obtained from addition theorem for Hankel functions [14]. It should be noted that Green's functions are very difficult to construct in an explicit form except for the simplest shapes of domain.

With the aid of the Green's function, we can construct the integral equation corresponding to Poisson's equation in three dimensions

$$\nabla^2 V = -\frac{\rho_v}{\epsilon} \tag{5.44}$$

as

$$V = \int \frac{\rho_v}{\epsilon} G\left(\mathbf{r}, \mathbf{r}'\right) dv'$$

Table 5.1 Free-Space Green's Functions

Operator equation	Laplace's equation	Steady-state Helmholtz's (or wave) equation[1]	Modified steady-state Helmholtz's (or wave) equation
Solution Region	$\nabla^2 G = \delta(\mathbf{r}, \mathbf{r}')$	$\nabla^2 G + k^2 G = \delta(\mathbf{r}, \mathbf{r}')$	$\nabla^2 G - k^2 G = \delta(\mathbf{r}, \mathbf{r}')$
1- dimensional	no solution for $(-\infty, \infty)$	$-\frac{j}{2k}\exp\left(jk\left\|x-x'\right\|\right)$	$-\frac{1}{2k}\exp\left(-k\left\|x-x'\right\|\right)$
2-dimensional	$\frac{1}{2\pi}\ln\left\|\rho-\rho'\right\|$	$-\frac{j}{4}H_0^{(1)}(k\|\rho-\rho'\|)$	$-\frac{1}{2\pi}K_o\left(k\left\|\rho-\rho'\right\|\right)$
3-dimensional	$-\frac{1}{4\pi(\mathbf{r}-\mathbf{r}')}$	$-\frac{\exp(jk\|\mathbf{r}-\mathbf{r}'\|)}{4\pi\|\mathbf{r}-\mathbf{r}'\|}$	$-\frac{\exp(-k\|\mathbf{r}-\mathbf{r}'\|)}{4\pi\|\mathbf{r}-\mathbf{r}'\|}$

[1] The wave equation has the time factor $e^{j\omega t}$ so that $k = \omega\sqrt{\mu\epsilon}$.

or

$$V = \int \frac{\rho_v \, dv'}{4\pi\epsilon r} \tag{5.45}$$

Similarly, the integral equation corresponding to Helmholtz's equation in three dimensions

$$\nabla^2\Phi + k^2\Phi = g \tag{5.46}$$

as

$$\Phi = \int gG\left(\mathbf{r}, \mathbf{r}'\right) \, dv'$$

or

$$\Phi = \int \frac{ge^{jkr} \, dv'}{4\pi r} \tag{5.47}$$

where an outgoing wave is assumed.

5.3.2 For Domain with Conducting Boundaries

The Green's functions derived so far are useful if the domain is free space. When the domain is bounded by one or more grounded planes, there are two ways to obtain Green's function:

(a) the method of images [12], [15]–[22] and

(b) the eigenfunction expansion [12, 16, 17], [22]–[30].

(a) Method of Images

The method of images is a powerful technique for obtaining the field due to one or more sources with conducting boundary planes. If a point charge q is at some distance h from a grounded conducting plane, the boundary condition imposed by the plane on the resulting potential field may be satisfied by replacing the plane with an "image charge" $-q$ located at a position which is the mirror location of q. Using this idea to obtain the Green's function is perhaps best illustrated with an example.

Consider the region between the ground planes at $y = 0$ and $y = h$ as shown in Fig. 5.2. The Green's function $G(x, y; x', y')$ is the potential at the point (x, y), which results when a unit line charge of 1 C/m is placed at the point (x', y'). If no ground planes were present, the potential at distance ρ from a unit line charge would be

$$V(\rho) = \frac{1}{4\pi\epsilon} \ln \rho^2 \tag{5.48}$$

In order to satisfy the boundary conditions on the ground planes, an infinite set of images is derived as shown in Fig. 5.2. The potential due to such a sequence of line charges (including the original) within the strip is the superposition of an infinite series of images:

$$\begin{aligned} G\left(x, y; x', y'\right) = \frac{1}{4\pi\epsilon} \Bigg(& \ln\left[\left(x - x'\right)^2 + \left(y + y'\right)^2\right] - \ln\left[\left(x - x'\right)^2 + \left(y + y'\right)^2\right] \\ & + \sum_{n=1}^{\infty} (-1)^n \Big\{ \ln\left[\left(x - x'\right)^2 + \left(y + y' - 2nh\right)^2\right] \\ & - \ln\left[\left(x - x'\right)^2 + \left(y - y' - 2nh\right)^2\right] \\ & + \ln\left[\left(x - x'\right)^2 + \left(y + y' - 2nh\right)^2\right] \\ & - \ln\left[\left(x - x'\right)^2 + \left(y - y' - 2nh\right)^2\right] \Big\} \Bigg) \\ = \frac{1}{4\pi\epsilon} & \sum_{n=-\infty}^{\infty} \ln\left[\frac{\left(x - x'\right)^2 + \left(y + y' - 2nh\right)^2}{(x - x')^2 + (y - y' - 2nh)^2}\right] \end{aligned} \tag{5.49}$$

This series converges slowly and is awkward for numerical computation. It can be summed to give [15]

$$G\left(x, y; x', y'\right) = \frac{1}{4\pi\epsilon} \ln\left[\frac{\sinh^2\left(\frac{\pi(x-x')}{2h}\right) + \sin^2\left(\frac{\pi(y+y')}{2h}\right)}{\sinh^2\left(\frac{\pi(x-x')}{2h}\right) + \sin^2\left(\frac{\pi(y-y')}{2h}\right)}\right] \tag{5.50}$$

This expression can be shown to satisfy the appropriate boundary conditions along the ground plane, i.e., $G(x, y; x', y') = 0$ at $y = 0$ or $y = h$. Note that G has exactly one singularity at $x = x',\ y = y'$ in the region $0 \le y \le h$.

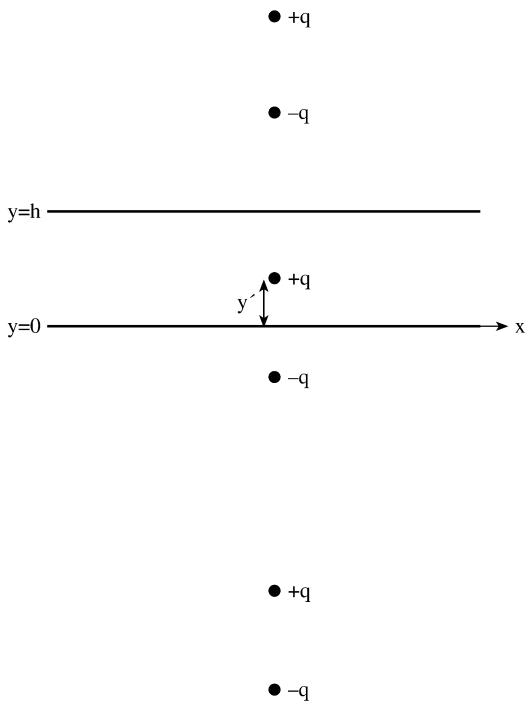

Figure 5.2
A single charge placed between two conducting planes produces the same potential as does the system of image charges when no conducting planes are present.

In order to evaluate an integral involving $G(x, y; x', y')$ in Eq. (5.50), it is convenient to take out the singular portion of the unit source function. We rewrite Eq. (5.50) as

$$G\left(x, y; x', y'\right) = -\frac{1}{4\pi\epsilon} \ln\left[\left(x - x'\right)^2 + \left(y + y'\right)^2\right] + g\left(x, y; x', y'\right) \qquad (5.51)$$

where

$$g\left(x, y; x', y'\right) =$$

$$\frac{1}{4\pi\epsilon} \ln\left[\frac{\left[\left(x - x'\right)^2 \left(y - y'\right)^2\right]\left[\sinh^2\left(\frac{\pi\left(x-x'\right)}{2h}\right) + \sin^2\left(\frac{\pi\left(y+y'\right)}{2h}\right)\right]}{\sinh^2\left(\frac{\pi\left(x-x'\right)}{2h}\right) + \sin^2\left(\frac{\pi\left(y-y'\right)}{2h}\right)}\right] \qquad (5.52)$$

Note that $g(x, y; x', y')$ is finite everywhere in $0 \leq y \leq h$. The integral involving g is evaluated numerically, while the one involving the singular logarithmic term is evaluated analytically with the aid of integral tables.

The method of images has been applied in derivating the Green's functions for multiconductor transmission lines [18]–[20] and planar microwave circuits [16, 17, 21]. The method is restricted to the shapes enclosed by boundaries that are straight conductors.

(b) Eigenfunction Expansion

This method is suitable for deriving the Green's function for differential equations whose homogeneous solution is known. The Green's function is represented in terms of a series of orthonormal functions that satisfy the boundary conditions associated with the differential equation. To illustrate the eigenfunction expansion procedure, suppose we are interested in the Green's function for the wave equation

$$\frac{\partial^2 \Psi}{\partial x^2} + \frac{\partial^2 \Psi}{\partial y^2} + k^2 \Psi = 0 \tag{5.53}$$

subject to

$$\frac{\partial \Psi}{\partial n} = 0 \quad \text{or} \quad \Psi = 0 \tag{5.54}$$

Let the eigenfunctions and eigenvalues of Eq. (5.53) that satisfy Eq. (5.54) be Ψ_j and k_j, respectively, i.e.,

$$\nabla^2 \Psi_j + k_j^2 \Psi_j = 0 \tag{5.55}$$

Assuming that Ψ_j form a complete set of orthonormal functions,

$$\int_S \Psi_j^* \Psi_i \, dxdy = \begin{cases} 1, & j = i \\ 0, & j \neq i \end{cases} \tag{5.56}$$

where the asterisk $(*)$ denotes complex conjugation. $G(x, y; x', y')$ can be expanded in terms of Ψ_j, i.e.,

$$G\left(x, y; x', y'\right) = \sum_{j=1}^{\infty} a_j \Psi_j(x, y) \tag{5.57}$$

Since the Green's function must satisfy

$$\left(\nabla^2 + k^2\right) G\left(x, y; x', y'\right) = \delta\left(x - x'\right) \, \delta\left(y - y'\right) \, , \tag{5.58}$$

substituting Eqs. (5.55) and (5.57) into Eq. (5.58), we obtain

$$\sum_{j=1}^{\infty} a_j \left(k^2 - k_j^2\right) \Psi_j = \delta\left(x - x'\right) \, \delta\left(y - y'\right) \tag{5.59}$$

Multiplying both sides by Ψ_i^* and integrating over the region S gives

$$\sum_{j=1}^{\infty} a_j \left(k^2 - k_j^2\right) \int_S \Psi_j \Psi_i^* \, dx dy = \Psi_i^* \left(x', y'\right) \tag{5.60}$$

Imposing the orthonormal property in Eq. (5.56) leads to

$$a_i \left(k^2 - k_i^2\right) = \Psi_i^* \left(x', y'\right)$$

or

$$a_i = \frac{\Psi_i^* \left(x', y'\right)}{\left(k^2 - k_i^2\right)} \tag{5.61}$$

Thus

$$G\left(x, y; x', y'\right) = \sum_{j=1}^{\infty} \frac{\Psi_j(x, y) \Psi_j^* \left(x', y'\right)}{\left(k^2 - k_j^2\right)} \tag{5.62}$$

The eigenfunction expansion approach has been applied to derive the Green's functions for plane conducting boundaries such as rectangular box and prism [22], planar microwave circuits [16, 17, 25], multilayered dielectric structures [23, 24], waveguides [28], and surfaces of revolution [27]. The approach is limited to separable coordinate systems since the requisite eigenfunctions can be determined for only these cases.

Example 5.3

Construct a Green's function for

$$\nabla^2 V = 0$$

subject to $V(a, \phi) = f(\phi)$ within a circular disk $\rho \leq a$. □

Solution

Since $g = 0$, the solution is obtained from Eq. (5.21) as

$$V = \oint_C f \frac{\partial G}{\partial n} \, dl \tag{5.63}$$

where the circle C is the boundary of the disk as shown in Fig. 5.3. Let

$$G = F + U \ ,$$

where F is already found to be

$$F = \frac{1}{2\pi} \ln \left|\rho - \rho'\right| \ ,$$

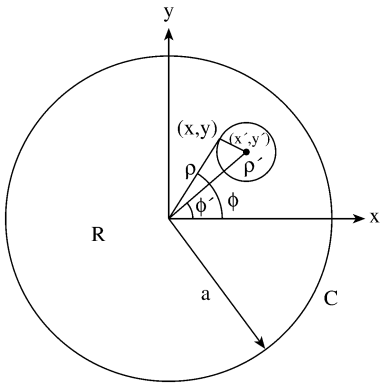

Figure 5.3
A disk of radius a.

i.e.,

$$F\left(\rho, \phi; \rho', \phi'\right) = \frac{1}{4\pi} \ln\left[\rho'^2 + \rho'^2 - 2\rho\rho' \cos\left(\phi - \phi'\right)\right] \tag{5.64}$$

The major problem is finding U. But

$$\nabla^2 U = 0 \quad \text{in } R \tag{5.65a}$$

with

$$U = -F \quad \text{on} \quad C$$

or

$$U\left(a, \phi; \rho', \phi'\right) = -\frac{1}{4\pi} \ln\left[a^2 + \rho'^2 - 2a\rho' \cos\left(\phi - \phi'\right)\right] \tag{5.65b}$$

Thus U can be found by solving the PDE in Eq. (5.65a) subject to the condition in Eq. (5.65b). Applying the separation of variables method,

$$U = \frac{A_0}{2} \sum_{n=1}^{\infty} \rho^n \left[A_n \cos n\phi + B_n \sin n\phi\right] \tag{5.66}$$

The term ρ^{-n} is not included since U must be bounded at $\rho = 0$. To impose the boundary condition in Eq. (5.65b) on the solution in Eq. (5.66), we first express Eq. (5.65b) in Fourier series using the identity

$$\sum_{n=1}^{\infty} \frac{z^n}{n} \cos n\theta = \int_0^z \frac{\cos\theta - \lambda}{1 + \lambda^2 - 2\lambda\cos\theta}\, d\lambda = -\frac{1}{2} \ln\left[1 + z^2 - 2z\cos\theta\right] \tag{5.67}$$

Hence Eq. (5.65b) becomes

$$U\left(a,\phi;\rho',\phi'\right) = -\frac{1}{4\pi}\ln a^2\left[1+\left(\rho'/a\right)^2-\frac{2\rho'}{a}\cos\left(\phi-\phi'\right)\right]$$
$$= -\frac{1}{2\pi}\ln a+\frac{1}{2\pi}\sum_{n=1}^{\infty}\left[\frac{\rho'}{a}\right]^n\frac{\cos n\left(\phi-\phi'\right)}{n}$$
$$= -\frac{1}{2\pi}\ln a+\frac{1}{2\pi}\sum_{n=1}^{\infty}\left[\frac{\rho'}{a}\right]^n\cdot$$
$$\frac{\left(\cos n\phi\cos n\phi'+\sin n\phi\sin n\phi'\right)}{n} \tag{5.68}$$

Comparing Eq. (5.66) with Eq. (5.68) at $\rho = a$, we obtain the coefficients A_n and B_n as

$$\frac{A_0}{2} = -\frac{1}{2\pi}\ln a$$
$$a^n A_n = \frac{1}{2\pi n}\left[\frac{\rho'}{a}\right]^n\cos n\phi'$$
$$a^n B_n = \frac{1}{2\pi n}\left[\frac{\rho'}{a}\right]^n\sin n\phi'$$

Thus Eq. (5.66) becomes

$$U\left(\rho,\phi;\rho',\phi'\right) = -\frac{1}{2\pi}\ln a+\frac{1}{2\pi}\sum_{n=1}^{\infty}\left[\frac{\rho'}{a}\right]^n\left[\frac{\rho}{a}\right]^n\frac{\cos n\left(\phi-\phi'\right)}{n}$$
$$= -\frac{1}{2\pi}\ln a-\frac{1}{4\pi}\ln\left[1+\left[\frac{\rho\rho'}{a^2}\right]^2-\frac{2\rho\rho'}{a^2}\cos\left(\phi-\phi'\right)\right] \tag{5.69}$$

From Eqs. (5.64) and Eq. (5.69), we obtain the Green's function as

$$G = \frac{1}{4\pi}\ln\left[\rho^2+\rho'^2-2\rho\rho'\cos\left(\phi-\phi'\right)\right]$$
$$-\frac{1}{4\pi}\ln\left[a^2+\frac{\rho'^2\rho^2}{a^2}-2\rho\rho'\cos\left(\phi-\phi'\right)\right] \tag{5.70}$$

An alternative means of constructing the Green's function is the method of images. Let us obtain Eq. (5.70) using the method of images. Let

$$G\left(P,P'\right) = \frac{1}{2\pi}\ln r+U$$

The problem reduces to finding the induced field U, which is harmonic within the disk and is equal to $-\frac{1}{2\pi}\ln r$ on C. Let P' be the singular point of Green's function

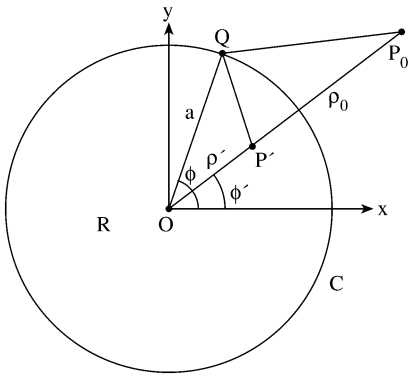

Figure 5.4
The image point P_o of P' with respect to circle C so that $OP'.OP_o = OQ = a^2$ and OQP' and OP_oQ are similar triangles.

and let P_o be the image of P' with respect to the circle C as shown in Fig. 5.4. The triangles OQP' and OQP_0 are similar because the angle at O is common and the sides adjacent to it are proportional. Thus

$$\frac{\rho'}{a} = \frac{a}{\rho_o} \quad \rightarrow \quad \rho'\rho_o = a^2 \tag{5.71}$$

That is, the product of OP' and OP_o is equal to the square of the radius OQ. At a point Q on C, it is evident from Fig. 5.4 that

$$r_{QP'} = \frac{\rho'}{a} r_{QP_o}$$

Therefore,

$$U = -\frac{1}{2\pi} \ln \frac{\rho' r_{PP_o}}{a} \tag{5.72}$$

and

$$G = \frac{1}{2\pi} \ln r_{PP'} - \frac{1}{2\pi} \ln \frac{\rho'}{a} r_{PP_o} \tag{5.73}$$

Since $r_{PP'}$ is the distance between $P(\rho, \phi)$ and $P'(\rho', \phi')$ while r_{PP_o} is the distance between $P(\rho, \phi)$ and $P_o(\rho'_o, \phi) = P_o(a^2/\rho', \phi)$,

$$r^2_{PP'} = \rho^2 + \rho'^2 - 2\rho\rho' \cos\left(\phi - \phi'\right) ,$$
$$r^2_{PP_o} = \rho^2 + \frac{a^4}{\rho'^2} - 2\rho\frac{a^2}{\rho'} \cos\left(\phi - \phi'\right)$$

Substituting these in Eq. (5.73), we obtain

$$G = \frac{1}{4\pi} \ln\left[\rho^2 + \rho'^2 - 2\rho\rho' \cos\left(\phi - \phi'\right)\right] - \frac{1}{4\pi} \ln\left[a^2 + \frac{\rho'^2\rho^2}{a^2} - 2\rho\rho' \cos\left(\phi - \phi'\right)\right] \tag{5.74}$$

which is the same as Eq. (5.70). From Eq. (5.70) or (5.74), the directional derivative $\partial G/\partial n = (\nabla G \cdot \mathbf{a}_n)$ on C is given by

$$\left.\frac{\partial G}{\partial \rho'}\right|_{\rho'=a} = \frac{2a - 2\rho\cos\left(\phi - \phi'\right)}{4\pi\left[a^2 + \rho^2 - 2a\rho\cos\left(\phi - \phi'\right)\right]} - \frac{\frac{2\rho^2}{a} - 2\rho\cos\left(\phi - \phi'\right)}{4\pi\left[a^2 + \rho^2 - 2a\rho\cos\left(\phi - \phi'\right)\right]},$$

$$= \frac{a^2 - \rho^2}{2\pi a\left[a^2 + \rho^2 - 2a\rho\cos\left(\phi - \phi'\right)\right]}$$

Hence the solution in Eq. (5.63) becomes (with $dl = a d\phi'$)

$$V(\rho, \phi) = \frac{1}{2\pi} \int_0^{2\pi} \frac{\left(a^2 - \rho^2\right) f\left(\phi'\right) d\phi'}{\left[a^2 + \rho^2 - 2a\rho\cos\left(\phi - \phi'\right)\right]} \tag{5.75}$$

which is known as *Poisson's integral formula*. ∎

Example 5.4

Obtain the solution for the Laplace operator on unbounded half-space, $z \leq 0$ with the condition $V(z = 0) = f$. □

Solution

Again the solution is

$$V = \oint_S f \frac{\partial G}{\partial n}\, dS$$

where S is the plane $z = 0$. We let

$$G = \frac{1}{4\pi\left|\mathbf{r} - \mathbf{r}'\right|} + U,$$

so that the major problem is reduced to finding U. Using the method of images, it is easy to see that the image point of $P'(x', y', z')$ is $P_o(x', y', -z')$ as shown in Fig. 5.5. Hence

$$U = -\frac{1}{4\pi\left|\mathbf{r} - \mathbf{r}_o\right|}$$

and

$$G = \frac{1}{4\pi\left|\mathbf{r} - \mathbf{r}'\right|} - \frac{1}{4\pi\left|\mathbf{r} - \mathbf{r}_o\right|},$$

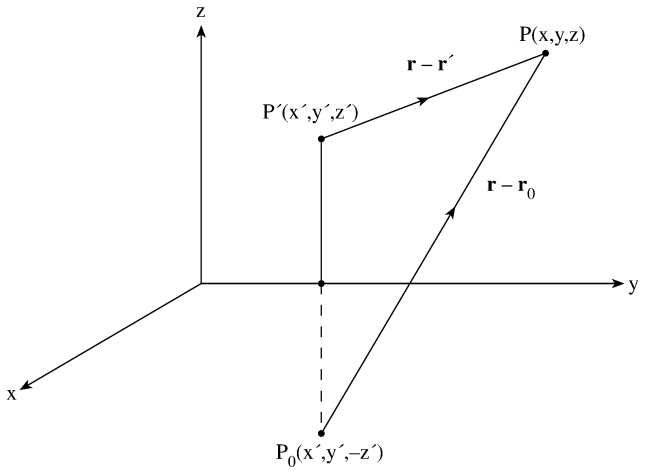

Figure 5.5
Half-space problem of Example 5.4.

where

$$|\mathbf{r}-\mathbf{r}'| = \left[(x-x')^2+(y-y')^2+(z-z')^2\right]^{1/2}$$
$$|\mathbf{r}-\mathbf{r}_o| = \left[(x-x')^2+(y-y')^2+(z+z')^2\right]^{1/2}$$

Notice that G reduces to zero at $z=0$ and has the required singularity at $P'(x',\, y',\, z')$. The directional derivative $\partial G/\partial n$ on plane $z=0$ is

$$\left.\frac{\partial G}{\partial z'}\right|_{z'=0} = \frac{1}{4\pi}\left[\frac{(z-z')}{|\mathbf{r}-\mathbf{r}'|^3}+\frac{(z+z')}{|\mathbf{r}-\mathbf{r}_o|^3}\right]\Bigg|_{z'=0}$$
$$= \frac{z}{2\pi\left[(x-x')^2+(y-y')^2+z^2\right]^{3/2}}$$

Hence

$$V(x,\,y,\,z) = \frac{1}{2\pi}\int_{-\infty}^{\infty}\int_{-\infty}^{\infty}\frac{zf\,(x',\,y')\,dx'dy'}{\left[(x-x')^2+(y-y')^2+z^2\right]^{3/2}} \quad \blacksquare$$

Example 5.5
Using Green's function, construct the solution for Poisson's equation

$$\frac{\partial^2 V}{\partial x^2}+\frac{\partial^2 V}{\partial y^2} = f(x,\,y)$$

subject to the boundary conditions

$$V(0, y) = V(a, y) = V(x, 0) = V(x, b) = 0 \qquad \square$$

Solution

According to Eq. (5.21), the solution is

$$V(x, y) = \int_0^b \int_0^a f\left(x', y'\right) G\left(x, y; x', y'\right)\, dx'dy' \tag{5.76}$$

so that our problem is essentially that of obtaining the Green's function $G(x, y; x', y')$. The Green's function satisfies

$$\frac{\partial^2 G}{\partial x^2} + \frac{\partial^2 G}{\partial y^2} = \delta\left(x - x'\right)\delta\left(y - y'\right) \tag{5.77}$$

To apply the series expansion method of finding G, we must first determine eigenfunctions $\Psi(x, y)$ of Laplace's equation, i.e.,

$$\nabla^2 \Psi = \lambda \Psi$$

where Ψ satisfies the boundary conditions. It is evident that the normalized eigenfunctions are

$$\Psi_{mn} = \frac{2}{\sqrt{ab}} \sin\frac{m\pi x}{a} \sin\frac{n\pi y}{b}$$

with the corresponding eigenvalues

$$\lambda_{mn} = -\left(\frac{m^2\pi^2}{a^2} + \frac{n^2\pi^2}{b^2}\right)$$

Thus,

$$G\left(x, y; x', y'\right) = \frac{2}{\sqrt{ab}} \sum_{m=1}^{\infty} \sum_{n=1}^{\infty} A_{mn}\left(x', y'\right) \sin\frac{m\pi x}{a} \sin\frac{n\pi y}{b} \tag{5.78}$$

The expansion coefficients, A_{mn} are determined by substituting Eq. (5.78) into Eq. (5.77), multiplying both sides by $\sin\frac{m\pi x}{a}\sin\frac{n\pi y}{b}$ and integrating over $0 < x < a,\ 0 < y < b$. Using the orthonormality property of the eigenfunctions and the shifting property of the delta function results in

$$-\left(\frac{m^2\pi^2}{a^2} + \frac{n^2\pi^2}{b^2}\right) A_{mn} = \frac{2}{\sqrt{ab}} \sin\frac{m\pi x'}{a} \sin\frac{n\pi y'}{b}$$

Obtaining A_{mn} from this and substituting in Eq. (5.78) gives

$$G\left(x, y; x', y'\right) = -\frac{4}{ab} \sum_{m=1}^{\infty} \sum_{n=1}^{\infty} \frac{\sin\frac{m\pi x}{a} \sin\frac{m\pi x'}{a} \sin\frac{n\pi y}{b} \sin\frac{n\pi y'}{b}}{m^2\pi^2/a^2 + n^2\pi^2/b^2} \tag{5.79}$$

Another way of obtaining Green's function is by means of a single series rather than a double summation in Eq. (5.79). It can be shown that [28, 29]

$$G(x, y; x', y') = \begin{cases} -\frac{2}{\pi}\sum_{n=1}^{\infty} \frac{\sin\frac{n\pi x}{b}\sinh\frac{n\pi(a-x')}{b}\sin\frac{n\pi y}{b}\sinh\frac{n\pi y'}{b}}{n\sinh\frac{n\pi a}{b}}, & x < x' \\ -\frac{2}{\pi}\sum_{n=1}^{\infty} \frac{\sinh\frac{n\pi x'}{b}\sinh\frac{n\pi(a-x)}{b}\sin\frac{n\pi y}{b}\sinh\frac{n\pi y'}{b}}{n\sinh\frac{n\pi a}{b}}, & x > x' \end{cases} \tag{5.80}$$

By Fourier series expansion, it can be verified that the expressions in Eqs. (5.79) and (5.80) are identical. Besides the factor $\frac{1}{\epsilon}$, the Green's function in Eq. (5.79) or Eq. (5.80) gives the potential V due to a unit line source at (x', y') in the region $0 < x < a,\ 0 < y < b$ as shown in Fig. 5.6. ∎

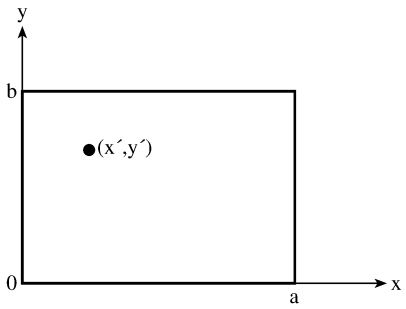

Figure 5.6
Line source in a rectangular region.

Example 5.6

An infinite line source I_z is located at (ρ', ϕ') in a wedge waveguide shown in Fig. 5.7. Derive the electric field due to the line. □

Solution

Assuming the time factor $e^{j\omega t}$, the z-component of **E** for the TE mode satisfies the wave equation

$$\nabla^2 E_z + k^2 E_z = j\omega\mu I_z \tag{5.81}$$

with

$$\frac{\partial E_z}{\partial n} = 0$$

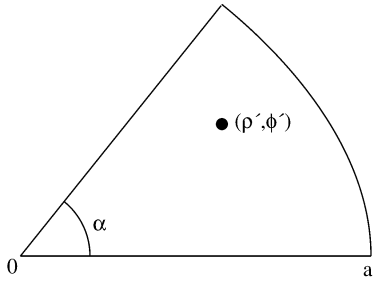

Figure 5.7
Line source in a waveguide.

where $k = \omega\sqrt{\mu\epsilon}$ and n is the outward unit normal at any point on the periphery of the cross section. The Green's function for this problem satisfies

$$\nabla^2 G + k^2 G = j\omega\mu\delta\left(\rho - \rho'\right) \tag{5.82}$$

with

$$\frac{\partial G}{\partial n} = 0$$

so that the solution to Eq. (5.81) is

$$E_z = j\omega\mu \int_S I_z\left(\rho', \phi'\right) G\left(\rho, \phi; \rho', \phi'\right)\, dS \tag{5.83}$$

To determine the Green's function $G(\rho, \phi; \rho', \phi')$, we find Ψ_i so that Eq. (5.62) can be applied. The boundary condition $\dfrac{\partial G}{\partial n} = 0$ implies that

$$\frac{1}{\rho}\frac{\partial G}{\partial \phi}\bigg|_{\phi=0} = 0 = \frac{1}{\rho}\frac{\partial G}{\partial \phi}\bigg|_{\phi=\alpha} = \frac{\partial G}{\partial \rho}\bigg|_{\rho=a} \tag{5.84}$$

The set of functions which satisfy the boundary conditions are

$$\Psi_{m\nu}(\rho, \phi) = J_\nu\left(k_{m\nu}\rho\right)\cos\nu\phi \tag{5.85}$$

where

$$\nu = n\pi/\alpha, \quad n = 0, 1, 2, \ldots\,, \tag{5.86a}$$

$k_{m\nu}$ are chosen to satisfy

$$\frac{\partial}{\partial\rho} J_\nu\left(k_{m\nu}\rho\right)\bigg|_{\rho=a} = 0\,, \tag{5.86b}$$

and the subscript m is used to denote the mth root of Eq. (5.86b); m can take the value zero for $n = 0$. The functions $\Psi_{m\nu}$ are orthogonal if and only if ν is an integer

which implies that ν is an integral multiple of α. Let $\alpha = \pi/\ell$, where ℓ is a positive integer, so that $\Phi_{m\nu}$ are mutually orthogonal. To obtain the Green's function using Eq. (5.62), these eigenfunctions must be normalized over the region, i.e.,

$$\int_0^a J_\nu^2\left(k_{m\nu}\rho\right) d\rho = \begin{cases} a^2/2, & m = \nu \\ \dfrac{1}{2}\left[a^2 - \left(\nu^2/k_{m\nu}^2\right)\right] J_\nu^2\left(k_{m\nu}a\right), & \text{otherwise} \end{cases} \tag{5.87a}$$

$$\int_0^\alpha \cos^2 \nu\phi \, d\phi = \begin{cases} \dfrac{\pi}{\ell}, & \nu = 0 \\ \dfrac{\pi}{2\ell}, & \text{otherwise} \end{cases} \tag{5.87b}$$

where $\nu = n\ell$. Using the normalized eigenfunctions, we obtain

$$G\left(\rho, \phi; \rho', \phi'\right) = \frac{j2\ell}{\omega\epsilon\pi a^2} - 4j\ell\omega\mu \sum_{n=1}^{\infty}\sum_{m=1}^{\infty} \frac{J_\nu\left(k_{m\nu}\rho\right) J_\nu\left(k_{m\nu}\rho'\right) \cos\nu\phi \cos\nu\phi'}{\epsilon_\nu\pi\left(a^2 - \frac{\nu^2}{k_{m\nu}^2}\right) J_\nu^2\left(k_{m\nu}a\right)\left(k^2 - k_{m\nu}^2\right)} \tag{5.88}$$

where

$$\epsilon_\nu = \begin{cases} 2, & \nu = 0 \\ 1, & \nu \neq 0 \end{cases} \tag{5.89}$$

We have employed the fact that $\omega\mu/k^2 = \dfrac{1}{\omega\epsilon}$ to obtain the first term on the right-hand side of Eq. (5.88). ∎

5.4 Applications I — Quasi-Static Problems

The method of moments has been applied to so many EM problems that covering all of them is practically impossible. We will only consider the relatively easy ones to illustrate the techniques involved. Once the basic approach has been mastered, it will be easy for the reader to extend the idea to attack more complicated problems.

We will apply MOM to a static problem in this section; more involved application will be considered in the sections to follow. We will consider the problem of determining the characteristic impedance Z_o of a strip transmission line [31].

Consider the strip transmission of Fig. 5.8(a). If the line is assumed to be infinitely long, the problem is reduced to a two-dimensional TEM problem of line sources in a plane as in Fig. 5.8(b). Let the potential difference of the strips be $V_d = 2V$ so that strip 1 is maintained at $+1V$ while strip 2 is at $-1V$. Our objective is to find the

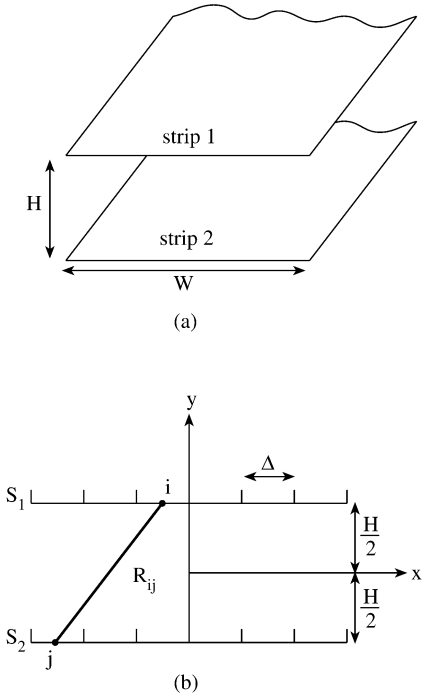

Figure 5.8
(a) The strip transmission line. (b) The two-dimensional view.

surface charge density $\rho(x, y)$ on the strips so that the total charge per unit length on one strip can be found as

$$Q_\ell = \int \rho \, dl \tag{5.90}$$

(Q_ℓ is charge per unit length as distinct from the total charge on the strip because we are treating a three-dimensional problem as a two-dimensional one.) Once Q is known, the capacitance per unit length C_ℓ can be found from

$$C_\ell = \frac{Q_\ell}{V_d} \tag{5.91}$$

Finally, the line characteristic impedance is obtained:

$$Z_o = \frac{(\mu\epsilon)^{1/2}}{C_\ell} = \frac{1}{uC_\ell} \tag{5.92}$$

where $u = 1/\sqrt{\mu\epsilon}$ is the speed of the wave in the (lossless) dielectric medium between the strips. Everything is straightforward once the charge density $\rho(x, y)$ in Eq. (5.90) is known. To find ρ using MOM, we divide each strip into n subareas of

equal width Δ so that subareas in strip 1 are numbered $1, 2, \ldots, n$, while those in strip 2 are numbered $n+1, n+2, n+3, \ldots, 2n$. The potential at an arbitrary field point is

$$V(x, y) = \frac{1}{2\pi\epsilon} \int \rho\left(x', y'\right) \ln \frac{R}{r_o}\, dx' dy' \tag{5.93}$$

where R is the distance between source and field points, i.e.,

$$R = \left[\left(x - x'\right)^2 + \left(y - y'\right)^2\right]^{1/2} \tag{5.94}$$

Since the integral in Eq. (5.93) may be regarded as rectangular subareas in a numerical sense, the potential at the center of a typical subarea S_i is

$$V_i = \frac{1}{2\pi\epsilon} \sum_{j=1}^{2n} \rho_j \int_{S_i} \ln \frac{R_{ij}}{r_o}\, dx'$$

or

$$V_i = \sum_{j=1}^{2n} A_{ij}\rho_j \tag{5.95}$$

where

$$A_{ij} = \frac{1}{2\pi\epsilon} \int_{S_i} \ln \frac{R_{ij}}{r_o}\, dx' \,, \tag{5.96}$$

R_{ij} is the distance between ith and jth subareas, and $A_{ij}\rho_j$ represents the potential at point i due to subarea j. In Eq. (5.95), we have assumed that the charge density ρ is constant within each subarea. For all the subareas $S_i, i = 1, 2, \ldots, 2n$ we have

$$\begin{aligned}
V_1 &= \sum_{j=1}^{2n} \rho_j A_{1j} = 1 \\
V_2 &= \sum_{j=1}^{2n} \rho_j A_{2j} = 1 \\
&\vdots \\
V_n &= \sum_{j=1}^{2n} \rho_j A_{nj} = 1 \\
V_{n+1} &= \sum_{j=1}^{2n} \rho_j A_{n+1,j} = -1 \\
&\vdots \\
V_{2n} &= \sum_{j=1}^{2n} \rho_j A_{2n,j} = -1
\end{aligned}$$

Thus we obtain a set of $2n$ simultaneous equations with $2n$ unknown charge densities ρ_i. In matrix form,

$$\begin{bmatrix} A_{11} & A_{12} & \cdots & A_{1,2n} \\ A_{21} & A_{22} & \cdots & A_{2,2n} \\ \vdots & & & \\ A_{2n,l} & A_{2n,2} & \cdots & A_{2n,2n} \end{bmatrix} \begin{bmatrix} \rho_1 \\ \rho_2 \\ \vdots \\ \rho_{2n} \end{bmatrix} = \begin{bmatrix} 1 \\ 1 \\ \vdots \\ -1 \\ -1 \end{bmatrix}$$

or simply

$$[A][\rho] = [B] \tag{5.97}$$

It can be shown that [32] the elements of matrix [A] expressed in Eq. (5.96) can be reduced to

$$A_{ij} = \begin{cases} \dfrac{\Delta}{2\pi\epsilon} \ln \dfrac{R_{ij}}{r_o}, & i \neq j \\ \dfrac{\Delta}{2\pi\epsilon} \left[\ln \dfrac{\Delta}{r_o} - 1.5 \right], & i = j \end{cases} \tag{5.98}$$

where r_o is a constant scale factor (commonly taken as unity). From Eq. (5.97), we obtain $[\rho]$ either by solving the simultaneous equation or by matrix inversion, i.e.,

$$[\rho] = [A]^{-1}[B] \tag{5.99}$$

Once $[\rho]$ is known, we determine C_ℓ from Eqs. (5.90) and (5.91) as

$$C_\ell = \sum_{j=1}^{n} \rho_j \Delta / V_d \tag{5.100}$$

where $V_d = 2V$. Obtaining Z_o follows from Eqs. (5.92) and (5.100).

Example 5.7

Write a program to find the characteristic impedance Z_o of a strip line with $H = 2\text{m}$, $W = 5\text{m}$, $\epsilon = \epsilon_o$, $\mu_o = \mu_o$, and $V_d = 2V$. □

Solution

The FORTRAN program is shown in Fig. 5.9. With the given data, the program calculates the elements of matrices [A] and [B] and determines $[\rho]$ by matrix inversion. With the computed charge densities the capacitance per unit length is calculated using Eq. (5.100) and the characteristic impedance from Eq. (5.92). Table 5.2 presents the computed values of Z_o for a different number of segments per strip, n. The results agree well with $Z_o = 50\ \Omega$ from Wheeler's curve [33]. ■

```
0001    C ****************************************************************
0002    C     USING MOMENTS METHOD,
0003    C     THIS PROGRAM DETERMINES THE CHARACTERISTIC IMPEDANCE
0004    C     OF A STRIP TRANSMISSION LINE
0005    C     WITH CROSS-SECTION  W X H
0006    C     THE STRIPS MAINTAINED AT 1 VOLT AND - 1 VOLT.
0007    C
0008    C     ONE STRIP IS LOCATED ON THE Y= H/2 PLANE WHILE THE OTHER
0009    C     IS LOCATED ON THE  Y= -H/2  PLANE.
0010    C
0011    C     ALL DIMENSIONS ARE IN S.I. UNITS
0012    C
0013    C     N IS THE NUMBER OF SUBSECTIONS INTO WHICH
              EACH STRIP IS DIVIDED
0014    C****************************************************************
0015
0016          DIMENSION  A(100,100), B(100), X(100), Y(100), RO(100)
0017          DATA  PIE/3.14159/
0018
0019    C     FIRST, SPECIFY THE PARAMETERS
0020
0021          CL=3.E+8  ! SPEED OF LIGHT IN FREE SPACE
0022          ER=1.0
0023          EO=8.8541E-12
0024          H=2.0
0025          W=5.0
0026          N=10
0027          NT=2N
0028          DELTA = W/FLOAT(N)
0029    C
0030    C     SECOND, CALCULATE THE MATCH POINTS
0031    C     AND THE COEFFICIENT MATRIX [A]
0032    C
0033          DO 10 K=1,N
0034          X(K) = DELTA*( FLOAT(K) -0.5 )  ! FOR LOWER STRIP
0035          Y(K) = -H/2.0
0036          X(K+N) = X(K)                   ! FOR UPPER STRIP
0037          Y(K+N) = H/2.0
0038    10    CONTINUE
0039
0040          FACTOR = DELTA/(2.0*PIE*EO)
0041
0042          DO 20 I=1,NT
0043          DO 20 J=1,NT
0044          IF(I-J)  12,11,12
0045
0046    11    A(I,J)= -( ALOG(DELTA) - 1.5)*FACTOR
0047          GO TO 13
0048    12    R=SQRT( (X(I) - X(J))**2 + (Y(I) - Y(J))**2 )
0049          A(I,J)= - ALOG(R)*FACTOR
0050    13    CONTINUE
0051    20    CONTINUE
0052    C
0053    C     NOW DETERMINE THE MATRIX OF CONSTANT VECTOR [B]
0054    C
0055          DO 30 K=1,N
0056          B(K)=1.0
0057    C      B(K+N)= -1.0
0058    30    CONTINUE
0059    C
```

Figure 5.9
FORTRAN program for Example 5.7 ***(Continued).***

```
0060    C     INVERT MATRIX  A(I,J) AND CALCULATE MATRIX RO(N)
0061    C     CONSISTING OF THE UNKNOWN ELEMENTS
0062    C     ALSO CALCULATE THE TOTAL CHARGE Q,
0063    C     THE CAPACITANCE C, AND THE CHARACTERISTIC IMPEDANCE Zo.
0064
0065          NIV=NT
0066          NMAX=100
0067          CALL INVERSE(A,NIV,NMAX) !  APPENDIX D
0068          DO 50 I=1,NT
0069          RO(I)=0.0
0070          DO 40 M=1,NT
0071          RO(I)=RO(I) + A(I,M)*B(M)
0072    40    CONTINUE
0073    50    CONTINUE
0074          SUM=0.0
0075          DO 60 I=1,N
0076          SUM= SUM + RO(I)
0077    60    CONTINUE
0078          Q=SUM*DELTA
0079          VD=2.0
0080          C=ABS(Q)/VD
0081          ZO = SQRT(ER)/CL*C
0082          PRINT *,ZO
0083          WRITE(6,70) ZO
0084    70    FORMAT(2X,'ZO=',E14.6,/)
0085          STOP
0086          END
```

Figure 5.9
(Cont.) **FORTRAN program for Example 5.7.**

Table 5.2 Characteristic Impedance of a Strip Transmission Line

n	Z_o(in Ω)
3	53.02
7	51.07
11	50.49
18	50.39
39	49.71
59	49.61

5.5 Applications II — Scattering Problems

The purpose of this section is to illustrate, with two examples, how the method of moments can be applied to solve electromagnetic scattering problems. The first example is on scattering of a plane wave by a perfectly conducting cylinder [3], while the second is on scattering of a plane wave by an arbitrary array of parallel wires [34].

5.5.1 Scattering by Conducting Cylinder

Consider an infinitely long, perfectly conducting cylinder located at a far distance from a radiating source. Assuming a time-harmonic field with time factor $e^{j\omega t}$, Maxwell's equations can be written in phasor form as

$$\nabla \cdot \mathbf{E}_s = 0 \tag{5.101a}$$

$$\nabla \cdot \mathbf{H}_s = 0 \tag{5.101b}$$

$$\nabla \times \mathbf{E}_s = -j\omega\mu\mathbf{H}_s \tag{5.101c}$$

$$\nabla \times \mathbf{H}_s = \mathbf{J}_s + j\omega\epsilon\mathbf{E}_s \tag{5.101d}$$

where the subscript s denotes phasor or complex quantities. Henceforth, we will drop subscript s for simplicity and use the same symbols for the frequency-domain quantities and time-domain quantities. It is assumed that the reader can differentiate between the two quantities. Taking the curl of Eq. (5.101c) and applying Eq. (5.101d), we obtain

$$\nabla \times \nabla \times \mathbf{E} = -j\omega\mu\nabla \times \mathbf{H} = -j\omega\mu(\mathbf{J} + j\omega\epsilon\mathbf{E}) \tag{5.102}$$

Introducing the vector identity

$$\nabla \times \nabla \times \mathbf{A} = \nabla(\nabla \cdot \mathbf{A}) - \nabla^2\mathbf{A}$$

into Eq. (5.102) gives

$$\nabla(\nabla \cdot \mathbf{E}) - \nabla^2\mathbf{E} = -j\omega\mu(\mathbf{J} + j\omega\epsilon\mathbf{E})$$

In view of Eq. (5.101a), $\nabla(\nabla \cdot \mathbf{E}) = 0$ so that

$$\nabla^2\mathbf{E} + k^2\mathbf{E} = j\omega\mu\mathbf{J} \tag{5.103}$$

where $k = \omega(\mu\epsilon)^{1/2} = 2\pi/\lambda$ is the wave number and λ is the wavelength. Equation (5.103) is the vector form of the Helmholtz wave equation. If we assume a TM wave ($H_z = 0$) with $\mathbf{E} = \mathbf{E}_z(x, y)\mathbf{a}_z$, the vector equation (5.103) becomes a scalar equation, namely,

$$\nabla^2 E_z + k^2 E_z = j\omega\mu J_z \tag{5.104}$$

where $\mathbf{J} = J_z\mathbf{a}_z$ is the source current density. The integral solution to Eq. (5.104) is

$$E_z(x, y) = E_z(\rho) = -\frac{k\eta_o}{4}\int_S J_z\left(\rho'\right) H_0^{(2)}\left(k\left|\rho - \rho'\right|\right) dS' \tag{5.105}$$

where $\rho = x\mathbf{a}_x + y\mathbf{a}_y$ is the field point, $\rho' = x'\mathbf{a}_x + y'\mathbf{a}_y$ is the source point, $\eta_o = (\mu_o/\epsilon_o)^{1/2} \simeq 377\,\Omega$ is the intrinsic impedance of free space, and $H_0^{(2)} =$ Hankel function of the second kind of zero order since an outward-traveling wave is assumed and there is no ϕ dependence. The integration in Eq. (5.105) is over the cross section of the cylinder shown in Fig. 5.10.

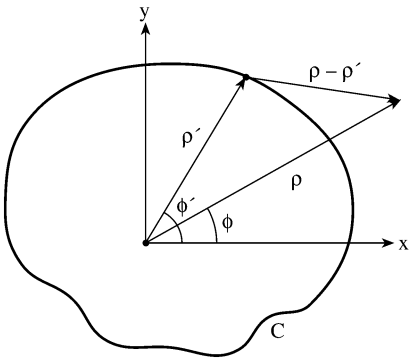

Figure 5.10
Cross section of the cylinder.

If field E_z^i is incident on a perfectly conducting cylinder, it induces surface current J_z on the conducting cylinder, which in turn produces a scattered field E_z^s. The scattered field E_z^s due to J_z is expressed by Eq. (5.105). On the boundary C, the tangential component of the total field must vanish. Thus

$$E_z^i + E_z^s = 0 \text{ on } C \tag{5.106}$$

Substitution of Eq. (5.105) into Eq. (5.106) yields

$$E_z^i(\rho) = \frac{k\eta_o}{4} \int_C J_z\left(\rho'\right) H_0^{(2)}\left(k\left|\rho - \rho'\right|\right) dl' \tag{5.107}$$

In the integral equation (5.107), the induced surface current density J_z is the only unknown. We determine J_z using the moment method.

We divide the boundary C into N segments and apply the point matching technique. On a segment ΔC_n, Eq. (5.107) becomes

$$E_z^i\left(\rho_n\right) = \frac{k\eta_o}{4} \sum_{m=1}^{N} J_z\left(\rho_m\right) H_0^{(2)}\left(k\left|\rho_n - \rho_m\right|\right) \Delta C_m \tag{5.108}$$

where the integration in Eq. (5.107) has been replaced by summation. On applying Eq. (5.108) to all segments, a system of simultaneous equations results. The system of equations can be cast in matrix form as

$$\begin{bmatrix} E_z^i\left(\rho_1\right) \\ E_z^i\left(\rho_2\right) \\ \vdots \\ E_z^i\left(\rho_N\right) \end{bmatrix} = \begin{bmatrix} A_{11} & A_{12} & \ldots & A_{1N} \\ A_{21} & A_{22} & \ldots & A_{2N} \\ \vdots & & \vdots & \\ A_{N1} & A_{N2} & \ldots & A_{NN} \end{bmatrix} \begin{bmatrix} J_z\left(\rho_1\right) \\ J_z\left(\rho_2\right) \\ \vdots \\ J_z\left(\rho_N\right) \end{bmatrix} \tag{5.109a}$$

or

$$[E] = [A][J] \tag{5.109b}$$

Hence

$$[J] = [A]^{-1}[E] \tag{5.110}$$

To determine the exact values of elements of matrix [A] may be difficult. Approximately [6],

$$A_{mn} \simeq \begin{cases} \dfrac{\eta_o k}{4} \Delta C_n H_0^{(2)} \left\{ k \left[(x_n - x_m)^2 + (y_n - y_m)^2 \right]^{(1/2)} \right\}, & m \neq n \\ \dfrac{\eta_o k}{4} \left[1 - j \dfrac{2}{\pi} \log_{10} \left(\dfrac{\gamma k \Delta C_n}{4e} \right) \right], & m = n \end{cases} \tag{5.111}$$

where (x_n, y_n) is the midpoint of ΔC_n, $e = 2.718\ldots$, and $\gamma = 1.781\ldots$. Thus for a given cross section and specified incident field E_z^i, the induced surface current density J_z can be found from Eq. (5.110). To be specific, assume the propagation vector $\mathbf{k}$ is directed as shown in Fig. 5.11 so that

$$E_z^i = E_o e^{j\mathbf{k}\cdot\mathbf{r}}$$

where $\mathbf{r} = x\mathbf{a}_x + y\mathbf{a}_y$, $\mathbf{k} = k(\cos\phi_i \mathbf{a}_x + \sin\phi_i \mathbf{a}_y)$, $k = 2\pi/\lambda$, and ϕ_i is the incidence angle. Taking $E_o = 1$ so that $|E_z^i| = 1$,

$$E_z^i = e^{jk(x\cos\phi_i + y\sin\phi_i)} \tag{5.112}$$

Given any C (dictated by the cross section of the cylinder), we can substitute Eqs. (5.111) and (5.112) into Eq. (5.109) and determine $[J]$ from Eq. (5.110). Once J_z, the induced current density, is known, we calculate the *scattering cross section* σ defined by

$$\begin{aligned} \sigma(\phi, \phi_i) &= 2\pi\rho \left| \frac{E_z^s(\phi)}{E_z^s(\phi_i)} \right|^2 \\ &= \frac{k\eta_o^2}{4} \left| \int_C J_z(x', y') e^{jk(x'\cos\phi + y'\sin\phi)} dl' \right|^2 \end{aligned} \tag{5.113}$$

where ϕ is the angle at the observation point, the point at which σ is evaluated. In matrix form,

$$\sigma(\phi_i, \phi) = \frac{k\eta^2}{4} \left| \left[V_n^s \right] [Z_{nm}]^{-1} \left[V_m^i \right] \right|^2 \tag{5.114}$$

where

$$V_m^i = \Delta C_m e^{jk(x_m\cos\phi_i + y_m\cos\phi_i)}, \tag{5.115a}$$

$$V_n^s = \Delta C_n e^{jk(x_n\cos\phi + y_n\cos\phi)}, \tag{5.115b}$$

and

$$Z_{mn} = \Delta C_m A_{mn} \tag{5.115c}$$

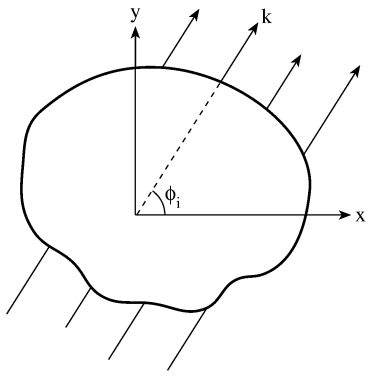

Figure 5.11
Typical propagation of vector k.

5.5.2 Scattering by an Arbitrary Array of Parallel Wires

This problem is of more general nature than the one just described. As a matter of fact, any infinitely long, perfectly conducting, thin metal can be modeled as an array of parallel wires. It will be shown that the scattering pattern due to an arbitrary array of line sources approaches that of a solid conducting cylinder of the same cross-sectional geometry if a sufficiently large number of wires are present and they are arrayed on a closed curve. Hence the problem of scattering by a conducting cylinder presented above can also be modeled with the techniques to be described here (see Problems 5.17 and 5.19).

Consider an arbitrary array of N parallel, infinitely long wires placed parallel to the z-axis [34]. Three of such wires are illustrated in Fig. 5.12. Let a harmonic TM wave be incident on the wires. Assuming a time factor $e^{j\omega t}$, the incident wave in phasor form is given by

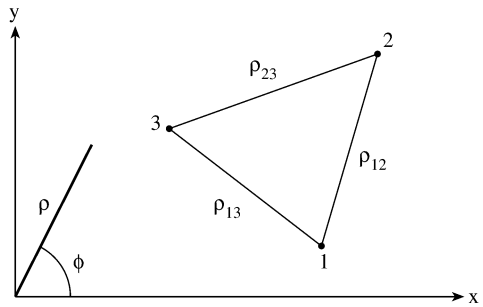

Figure 5.12
An array of three wires parallel to the z-axis.

$$E_z^i = E_i(x, y)e^{-jhz} \tag{5.116}$$

where

$$E_i(x, y) = E_o e^{-jk(x \sin\theta_i \cos\phi_i + y \sin\theta_i \sin\phi_i)} \tag{5.117a}$$

$$h = k \cos\theta_i \ , \tag{5.117b}$$

$$k = \frac{2\pi}{\lambda} = \omega(\mu\epsilon)^{1/2} \ , \tag{5.117c}$$

and θ_i and ϕ_i define the axis of propagation as illustrated in Fig. 5.13. The incident wave induces current on the surface of wire n. The induced current density has only z component.

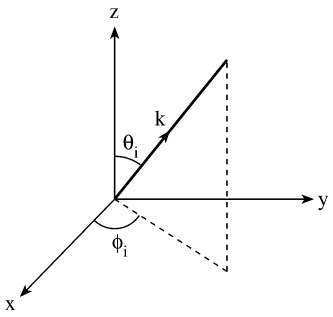

Figure 5.13
Propagation vector k.

It can be shown that the field due to a harmonic current I_n uniformly distributed on a circular cylinder of radius a_n has a z component given by

$$E_n = -I_n' H_0^{(2)}(g\rho_n)\, e^{-jhz}, \quad \rho_n > a_n \tag{5.118}$$

where

$$I_n' = \frac{\omega\mu g^2}{4k^2} I_n J_0(g a_n) \ , \tag{5.119}$$

$$g^2 + h^2 = k^2 \ , \tag{5.120}$$

J_0 is Bessel function of order zero, and H_0 is Hankel function of the second kind of order zero. By induction theorem, if I_n is regarded as the induced current, Eq. (5.118) may be considered as the scattered field, i.e.,

$$E_z^s = -\sum_{n=1}^{N} I_n' H_0^{(2)}(g\rho_n)\, e^{-jhz} \tag{5.121}$$

where the summation is taken over all the N wires. On the surface of each wire (assumed perfectly conducting),

$$E_z^i + E_z^s = 0$$

or

$$E_z^i = -E_z^s, \quad \rho = \rho_n \tag{5.122}$$

Substitution of Eqs. (5.116) and (5.121) into Eq. (5.122) leads to

$$\sum_{n=1}^{N} I_n' H_0^{(2)}(g\rho_{mn}) = E_i(x_m, y_m) \tag{5.123}$$

where

$$\rho_{mn} = \begin{cases} \sqrt{(x_m - x_n)^2 + (y_m - y_n)^2} & , m \neq n \\ a_m & , m = n \end{cases} \tag{5.124}$$

and a_m is the radius of the mth wire. In matrix form, Eq. (5.123) can be written as

$$[A][I] = [B]$$

or

$$[I] = [A]^{-1}[B] \tag{5.125}$$

where

$$I_n = I_n' , \tag{5.126a}$$

$$A_{mn} = H_0^{(2)}(g\rho_{mn}) , \tag{5.126b}$$

$$B_m = E_o e^{-jk(x_m \sin\theta_i \cos\phi_i + y_m \sin\theta_i \sin\phi_i)} \tag{5.126c}$$

Once I_n' is calculated from Eq. (5.125), the scattered field can be obtained as

$$E_z^s = -\sum_{n=1}^{N} I_n' H_0^{(2)}(g\rho_n)\, e^{-jhz} \tag{5.127}$$

Finally, we may calculate the "distant scattering pattern," defined as

$$E(\phi) = \sum_{n=1}^{N} I_n' e^{jg(x_n \cos\phi + y_n \sin\phi)} \tag{5.128}$$

The following example, taken from Richmond's work [34], will be used to illustrate the techniques discussed in the latter half of this section.

Example 5.8

Consider the two arrays shown in Fig. 5.14. For Fig. 5.14(a), take

$$\begin{aligned} \text{no. of wires, } & N = 15 \\ \text{wire radius, } & ka = 0.05 \\ \text{wire spacing, } & ks = 1.0 \\ & \theta_o = 90^\circ,\ \phi_o = 40^\circ,\ 270^\circ < \phi < 90^\circ \end{aligned}$$

and for Fig. 5.14(b), take

$$\begin{aligned} \text{no. of wires,} \quad & N = 30 \\ \text{wire radius,} \quad & ka = 0.05 \\ \text{cylinder radius,} \quad & R = 1.12\ \lambda \\ \theta_o = 90^\circ, \quad & \phi_o = 0,\ 0 < \phi < 180^\circ \end{aligned}$$

For the two arrays, calculate and plot the scattering pattern as a function of ϕ. □

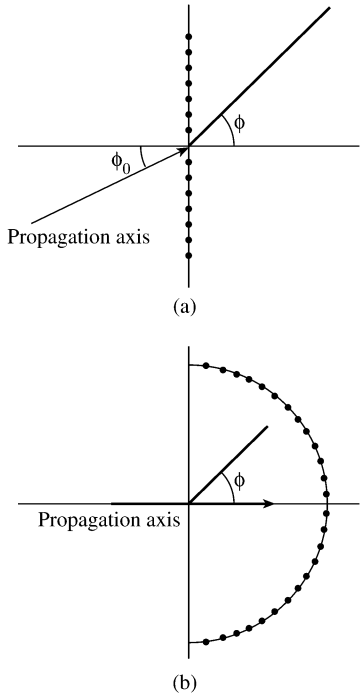

Figure 5.14
For Example 5.8: (a) A plane array of 15 parallel wires, (b) a semicircular array of 30 parallel wires.

Solution

The FORTRAN code for calculating the scattering pattern $E(\phi)$ based on Eq. (5.128) is shown in Fig. 5.15. The same program can be used for the two arrays in Fig. 5.14, except that the input data on N, ka, ks and the locations $(x_n, y_n), n = 1, 2, \ldots, N$ of the wires are different. The program essentially calculates I_n required

```
0001    C ======================================================
0002    C   THIS PROGRAM CALCULATES THE SCATTERING PATTERN OF AN
0003    C   ARRAY OF PARALLEL WIRES
0004    C   REFERENCE - RICHMOND'S WORK [8]
0005    C ======================================================
0006
0007        PARAMETER (IDM=50)
0008        DIMENSION X(IDM),Y(IDM),RHO(IDM,IDM),E(IDM)
0009        REAL LAMBDA,K
0010        COMPLEX J,HO,SUM,A(IDM,IDM),B(IDM),I(IDM)
0011        DATA  PIE,LAMBDA/3.14159,1.0/
0012
0013        J=(0.0,1.0)
0014    C
0015    C   SPECIFY NECESSARY DATA AND CALCULATE
            RELEVANT PARAMETERS
0016    C
0017        NN = 30
0018        THETA0 = PIE/2.0
0019        PHI0 = 0.0
0020        E0 = 1.0
0021        R = 1.125*LAMBDA
0022        K = 2.0*PIE/LAMBDA
0023        AA = 0.05/K
0024        S = 1.0/K
0025        H = K*COS(THETA0)
0026        G = SQRT( K**2 - H**2 )
0027    C
0028    C   DEFINE WIRE LOCATIONS AND CALCULATE RHO
0029    C
0030        DO 10 N=1,NN
0031        PHI = PIE*( FLOAT(N-1)/FLOAT(NN-1) ) - PIE/2.0
0032        X(N) = R*COS(PHI)
0033        Y(N) = R*SIN(PHI)
0034    10  CONTINUE
0035        DO 40 M=1,NN
0036        DO 40 N=1,NN
0037        IF(M-N) 20,30,20
0038    20  RHO(M,N) = SQRT( (X(M) - X(N))**2 + (Y(M) - Y(N))**2 )
0039        GO TO 40
0040    30  RHO(M,N) = AA
0041    40  CONTINUE
0042    C
0043    C CONSTRUCT MATRIX [A]
0044    C
0045        DO 50 M=1,NN
0046        DO 50 N=1,NN
0047        ARGU = G*RHO(M,N)
0048        CALL HANKEL(ARGU,HO)
0049        A(M,N) = HO
0050    50  CONTINUE
0051    C
0052    C CONSTRUCT MATRIX [B]
0053    C
0054        DO 60 M=1,NN
0055        ALPHA = X(M)*SIN(THETA0)*COS(PHI0)
0056       1       +  Y(M)*SIN(THETA0)*SIN(PHI0)
0057        B(M) = E0*CEXP( -J*K*ALPHA )
0058    60  CONTINUE
0059    C
```

Figure 5.15

Computer program for Example 5.8 ***(Continued).***

```
0060    C SOLVE FOR MATRIX [I] CONSISTING OF "MODIFIED CURRENT"OR
0061    C CURRENT COEFFICIENTS
0062    C
0063        CALL INVERSE(A,NN,IDM)
0064        DO 70 N=1,NN
0065        I(N) = (0.0,0.0)
0066        DO 70 M=1,NN
0067        I(N) = I(N) + A(N,M)*B(M)
0068    70  CONTINUE
0069    C
0070    C FINALLY, CALCULATE THE SCATTERING PATTERN E(PHI)
0071    C
0072        DPHI = 5.0
0073        DO 90 L=1,37
0074        PHI = DPHI*FLOAT(L-1)
0075        SUM = (0.0,0.0)
0076        DO 80 N=1,NN
0077        ALP = X(N)*COSD(PHI) + Y(N)*SIND(PHI)
0078        SUM = SUM + I(N)*CEXP( J*G*ALP )
0079    80  CONTINUE
0080        E(L) = CABS(SUM)
0081        WRITE(6,100) PHI,E(L)
0082    90  CONTINUE
0083    100 FORMAT(2X,'PHI=',F8.2,3X,'E(PHI)=',F12.6,/)
0084        CALL PLOT(E,37,0.0,DPHI,1)
0085        STOP
0086        END

0001    C*************************************************************
0002    C THIS PROGRAM EVALUATES HANKEL FUNCTION OF THE SECOND KIND
0003    C AND ORDER ZERO USING NEWTON-COTES RULE (N=5)
0004    C*************************************************************
0005    C
0006    C INITIALIZATION OF VARIABLES
0007    C
0008            SUBROUTINE HANKEL(X,H)
0009            DIMENSION O1(150),C(10),A1(10),A2(100),O2(150)
0010            DATA  ( C(I), I=1,6 )/19.0,75.0,50.0,50.0,75.0,19.0/
0011            COMPLEX H
0012            A=0.
0013            B=3.141592654
0014            M=30.
0015            H1=(B-A)/M
0016            H2=H1/2
0017            N=5
0018            NX=288
0019            E=.577216
0020    C
0021    C SET VALUES OF ANGLES
0022    C
0023            DO 5 I=1,M+1
0024            O1(I)=(I-1)*H1
0025            O2(I)=(I-1)*H2
0026     5      CONTINUE
0027    C
0028    C COMPUTE VALUES OF XJO &YO
0029    C
0030            L=M/N
0031            SUM1=0.
0032            SUM3=0.
0033            DO 500 I=1,L
0034            SUM2=0.
```

Figure 5.15

(Cont.) **Computer program for Example 5.8** ***(Continued).***

```
0035            SUM4=0.
0036      C
0037      C SET UP COMPUTATIONS OF AIS
0038      C
0039            DO 100 II=1,N+1
0040            J=(I-1)*N+II
0041            SUM2=SUM2+C(II)*COS(X*COS(O1(J)))
0042            IF(J.EQ.1)O2(J)=.00405
0043            SUM4=SUM4+C(II)*COS(X*COS(O2(J)))*(E+
0044           2 ALOG(2*X*(SIN(O2(J)))**2))
0045       100  CONTINUE
0046      C
0047      C COMPUTE THE SUM A1S
0048      C
0049            A1(I)=SUM2
0050            A2(I)=SUM4
0051            SUM1=SUM1+A1(I)
0052            SUM3=SUM3+A2(I)
0053       500  CONTINUE
0054      C
0055      C COMPUTE HO(X)=XJO(X)+I*YO(X)
0056      C
0057            XJO=(N*H1*SUM1)/(NX*B)
0058            YO=(N*H2*4*SUM3)/(NX*B**2)
0059            H=CMPLX( XJO,-YO )
0060            RETURN
0061            END
```

Figure 5.15
(Cont.) **Computer program for Example 5.8.**

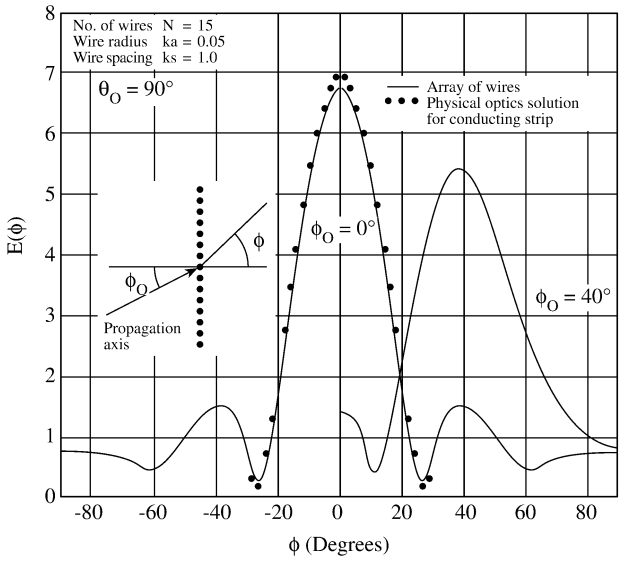

Figure 5.16
Scattering pattern for the plane array of Fig. 5.14(a).

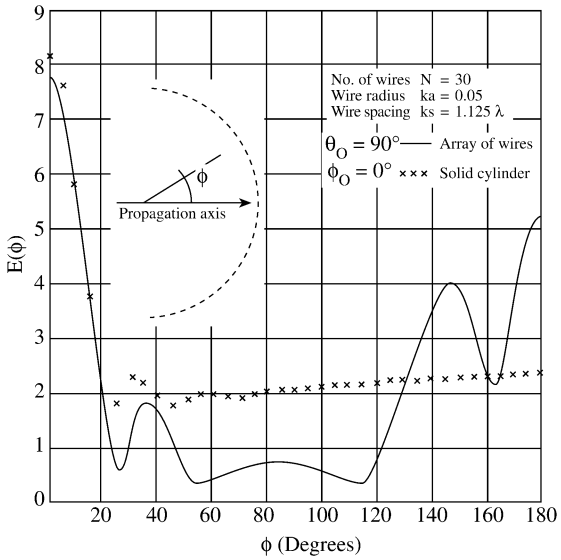

Figure 5.17
Scattering pattern for the semicircular array of Fig. 5.14(b).

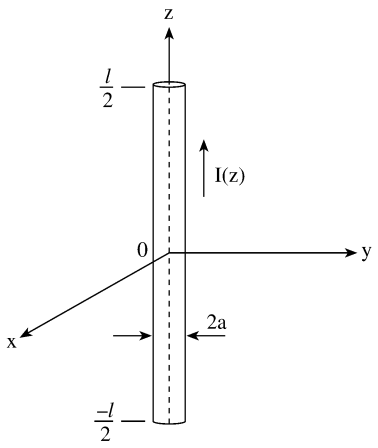

Figure 5.18
Cylindrical antenna of length l and radius a.

in Eq. (5.128) using Eqs. (5.125) and (5.126). The plots of $E(\phi)$ against ϕ are portrayed in Figs. 5.16 and 5.17 for the arrays in Fig. 5.14(a) and 5.14(b), respectively. ∎

5.6 Applications III — Radiation Problems

In this section, we consider the application of MOM to wires or cylindrical antennas. The distinction between scatterers considered in the previous section and antennas to be treated here is primarily that of the location of the source. An object acts as a scatterer if it is far from the source; it acts as an antenna if the source is on it [3].

Consider a perfectly conducting cylindrical antenna of radius a, extending from $z = -\ell/2$ to $z = \ell/2$ as shown in Fig. 5.18. Let the antenna be situated in a lossless homogeneous dielectric medium ($\sigma = 0$). Assuming a z-directed current on the cylinder ($\mathbf{J} = J_z a_z$), only axial electric field E_z is produced due to axial symmetry. The electric field can be expressed in terms of the retarded potentials of Eq. (1.38) as

$$E_z = -j\omega A_z - \frac{\partial V}{\partial z} \tag{5.129}$$

Applying the Lorentz condition of Eq. (1.41), namely,

$$\frac{\partial A_z}{\partial_z} = -j\omega\mu\epsilon V \ , \tag{5.130}$$

Eq. (5.129) becomes

$$E_z = -j\omega\left(1 + \frac{1}{k^2}\frac{\partial^2}{\partial z^2}\right) A_z \tag{5.131}$$

where $k = \omega(\mu\epsilon)^{1/2} = 2\pi/\lambda$, ω is the angular frequency of the suppressed harmonic time variation $e^{j\omega t}$. From Eq. (1.44)

$$A_z = \mu \int_{-\ell/2}^{\ell/2} I\left(z'\right) G\left(x, y, z; x', y', z'\right) dz' \tag{5.132}$$

where $G(x, y, z; x', y', z')$ is the free space Greens' function, i.e.,

$$G\left(x, y, z; x', y', z'\right) = \frac{e^{-jkR}}{4\pi R} \tag{5.133}$$

and R is the distance between observation point (x, y, z) and source point (x', y', z') or

$$R = \left[\left(x - x'\right)^2 + \left(y - y'\right)^2 + \left(z - z'\right)^2\right]^{1/2} \tag{5.134}$$

Combining Eqs. (5.131) and (5.132) gives

$$E_z = -j\omega\mu \left(1 + \frac{1}{k^2}\frac{d^2}{dz^2}\right) \int_{-\ell/2}^{\ell/2} I\left(z'\right) G\left(x, y, z; x', y', z'\right) dz' \tag{5.135}$$

This integro-differential equation is not convenient for numerical analysis because it requires evaluation of the second derivative with respect to z of the integral. We will now consider two types of modification of Eq. (5.135) leading to Hallen's (magnetic vector potential) and Pocklington's (electric field) integral equations. Either of these integral equations can be used to determine the current distribution on a cylindrical antenna or scatterer and subsequently calculate all other quantities of interest.

5.6.1 Hallen's Integral Equation

We can rewrite Eq. (5.135) in a compact form as

$$\left(\frac{d^2}{dz^2} + k^2\right) F(z) = k^2 S(z), \quad -\ell/2 < z < \ell/2 \tag{5.136}$$

where

$$F(z) = \int_{-\ell/2}^{\ell/2} I\left(z'\right) G\left(z, z'\right) dz' \,, \tag{5.137a}$$

$$S(z) = -\frac{E_z}{j\omega\mu} \tag{5.137b}$$

Equation (5.136) is a second-order linear ordinary differential equation. The general solution to the homogeneous equation

$$\left(\frac{d^2}{dz^2} + k^2\right) F(z) = 0 \,,$$

which is consistent with the boundary condition that the current must be zero at the wire ends ($z = \pm\ell/2$), is

$$F_h(z) = c_1 \cos kz + c_2 \sin kz \tag{5.138}$$

where c_1 and c_2 are integration constants. The particular solution of Eq. (5.136) can be obtained, for example, by the Lagrange method of varying constants [35] as

$$F_p(z) = k \int_{-\ell/2}^{\ell/2} S\left(z'\right) \sin k\left|z - z'\right| dz' \tag{5.139}$$

Thus from Eqs. (5.137) to (5.139), the solution to Eq. (5.136) is

$$\int_{-\ell/2}^{\ell/2} I\left(z'\right) G\left(z, z'\right) dz' = c_1 \cos kz + c_2 \sin kz - \frac{j}{\eta} \int_{-\ell/2}^{\ell/2} E_z\left(z'\right) \sin k\left|z - z'\right| dz' \tag{5.140}$$

where $\eta = \sqrt{\mu/\epsilon}$ is the intrinsic impedance of the surrounding medium. Equation (5.140) is referred to as *Hallen's integral equation* [36] for a perfectly conducting cylindrical antenna or scatterer. The equation has been generalized by Mei [37] to perfectly conducting wires of arbitrary shape. Hallen's IE is computationally convenient since its kernel contains only ℓ/r terms. Its major advantage is the ease with which a converged solution may be obtained, while its major drawback lies in the additional work required in finding the integration constants c_1 and c_2 [35, 38].

5.6.2 Pocklington's Integral Equation

We can also rewrite Eq. (5.135) by introducing the operator in parentheses under the integral sign so that

$$\int_{-\ell/2}^{\ell/2} I\left(z'\right)\left(\frac{\partial^2}{\partial z^2}+k^2\right) G\left(z,z'\right) dz' = j\omega\epsilon E_z \tag{5.141}$$

This is known as *Pocklington's integral equation* [39]. Note that Pocklington's IE has E_z, which represents the field from the source on the right-hand side. Both Pocklington's and Hallen's IEs can be used to treat wire antennas. The third type of IE derivable from Eq. (5.135) is the Schelkunoff's IE, found in [35].

5.6.3 Expansion and Weighting Functions

Having derived suitable integral equations, we can now find solutions for a variety of wire antennas or scatterers. This usually entails reducing the integral equations to a set of simultaneous linear equations using the method of moments. The unknown current $I(z)$ along the wire is approximated by a finite set $u_n(z)$ of basis (or expansion) functions with unknown amplitudes as discussed in the last chapter. That is, we let

$$I(z) = \sum_{n=1}^{N} I_n u_n(z) \ , \tag{5.142}$$

where N is the number of basis functions needed to cover the wire and the expansion coefficients I_n are to be determined. The functions u_n are chosen to be linearly independent. The basis functions commonly used in solving antenna or scattering problems are of two types: entire domain functions and subdomain functions. The entire domain basis functions exist over the full domain $-\ell/2 < z < \ell/2$. Typical examples are [8, 40]:

(1) Fourier:

$$u_n(z) = \cos(n-1)v/2 \ , \tag{5.143a}$$

(2) Chebychev:

$$u_n(z) = T_{2n-2}(v) \ , \tag{5.143b}$$

(3) Mauclaurin:

$$u_n(z) = v^{2n-2}\,, \tag{5.143c}$$

(4) Legendre:

$$u_n(z) = P_{2n-2}(v)\,, \tag{5.143d}$$

(5) Hermite:

$$u_n(z) = H_{2n-2}(v)\,, \tag{5.143e}$$

where $v = 2z/\ell$ and $n = 1, 2, \ldots, N$. The subdomain basis functions exist only on one of the N nonoverlapping segments into which the domain is divided. Typical examples are [41, 42]:

(1) piecewise constant (pulse) function:

$$u_n(z) = \begin{cases} 1, & z_{n-1/2} < z < z_{n+1/2} \\ 0, & \text{otherwise,} \end{cases} \tag{5.144a}$$

(2) piecewise linear (triangular) function:

$$u_n(z) = \begin{cases} \dfrac{\Delta - |z - z_n|}{\Delta}, & z_{n-1} < z < z_{n+1} \\ 0, & \text{otherwise,} \end{cases} \tag{5.144b}$$

(3) piecewise sinusoidal function:

$$u_n(z) = \begin{cases} \dfrac{\sin k\,(z - |z - z_n|}{\sin k\Delta}, & z_{n-1} < z < z_{n+1} \\ 0, & \text{otherwise,} \end{cases} \tag{5.144c}$$

where $\Delta = \ell/N$, assuming equal subintervals although this is unnecessary. Figure 5.19 illustrates these subdomain functions. The entire domain basis functions are of limited applications since they require a prior knowledge of the nature of the function to be represented. The subdomain functions are the most commonly used, particularly in developing general-purpose user-oriented computer codes for treating wire problems. For this reason, we will focus on using subdomain functions as basis functions.

Substitution of the approximate representation of current $I(z)$ in Eq. (5.142) into Pocklington's IE of Eq. (5.141) gives

$$\int_{-\ell/2}^{\ell/2} \sum_{n=1}^{N} I_n u_n\left(z'\right) K\left(z_m, z'\right) dz' \simeq E_z\left(z_m\right) \tag{5.145}$$

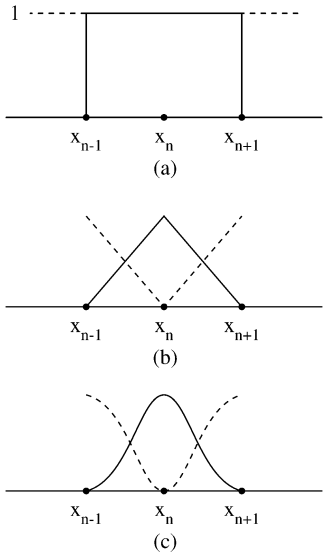

Figure 5.19

Typical subdomain weighting functions: (a) Piecewise uniform function, (b) piecewise linear function, (c) piecewise sinusoidal function.

where

$$K\left(z_m, z'\right) = \frac{1}{j\omega\epsilon}\left(\frac{\partial^2}{\partial z^2} + k^2\right) G\left(z_m, z'\right)$$

is the kernel $z = z_m$ on segment m is the point on the wire at which the IE is being enforced. Equation (5.145) may be written as

$$\sum_{n=1}^{N} I_n \int_{\Delta z_n} K\left(z_m, z'\right) u_n\left(z'\right) dz' \simeq E_z\left(z_m\right)$$

or

$$\sum_{n=1}^{N} I_n g_m = E_z\left(z_m\right) \tag{5.146}$$

where

$$g_m = \int_{\Delta z'_n} K\left(z_m, z'\right) u_n\left(z'\right) dz' \tag{5.147}$$

In order to solve for the unknown current amplitudes I_n $(n = 1, 2, \ldots, N)$, N equations need to be derived from Eq. (5.146). We achieve this by multiplying Eq. (5.146) by weighting (or testing) functions w_n $(n = 1, 2, \ldots, n)$ and integrating

over the wire length. In other words, we let Eq. (5.146) be satisfied in an average sense over the entire domain. This leads to forming the inner product between each of the weighting functions and g_m so that Eq. (5.146) is reduced to

$$\sum_{n=1}^{N} I_n \langle \omega_n, g_m \rangle = \langle \omega_n, E_z \rangle, \quad m = 1, 2, \ldots, N \tag{5.148}$$

Thus we have a set of N simultaneous equations which can be written in matrix form as

$$\begin{bmatrix} \langle \omega_1, g_1 \rangle & \ldots & \langle \omega_1, g_N \rangle \\ \langle \omega_2, g_1 \rangle & \ldots & \langle \omega_2, g_N \rangle \\ \vdots & & \vdots \\ \langle \omega_N, g_1 \rangle & \ldots & \langle \omega_N, g_N \rangle \end{bmatrix} \begin{bmatrix} I_1 \\ I_2 \\ \vdots \\ I_N \end{bmatrix} = \begin{bmatrix} \langle \omega_1, E_{z1} \rangle \\ \langle \omega_2, E_{z2} \rangle \\ \vdots \\ \langle \omega_N, E_{zN} \rangle \end{bmatrix}$$

or

$$[Z][I] = [V] \tag{5.149}$$

where $z_{mn} = \langle \omega_n, g_m \rangle$ and $V_m = \langle \omega_m, E_z \rangle$. The desired solution for the current is then obtained by solving the simultaneous equations (5.149) or by matrix inversion, i.e.,

$$[I] = [Z]^{-1}[V] \tag{5.150}$$

Because of the similarity of Eq. (5.149) to the network equations, the matrices $[Z]$, $[V]$, and $[I]$ are referred to as *generalized* impedance, voltage, and current matrices, respectively [6]. Once the current distribution $I(z')$ is determined from Eq. (5.149) or (5.150), parameters of practical interest such as input impedance and radiation patterns are readily obtained.

The weighting functions $\{w_n\}$ must be chosen so that each Eq. (5.148) is linearly independent and computation of the necessary numerical integration is minimized. Evaluation of the integrals in Eq. (5.149) is often the most time-consuming portion of scattering or radiation problems. Sometimes we select similar types of functions for both weighting and expansion. As discussed in the previous chapter, choosing $w_n = u_n$ leads to Galerkin's method, while choosing $w_n = \delta(z - z_n)$ results in point matching (or colocation) method. The point matching method is simpler than Galerkin's method and is sufficiently adequate for many EM problems. However, it tends to be a slower converging method. The general rules that should be followed in selecting the weighting functions are addressed in [43]. The following examples are taken from [41], [44]–[46].

Example 5.9

Solve the Hallen's integral equation

$$\int_{-\ell/2}^{\ell/2} I\left(z'\right) G\left(z, z'\right) dz' = -\frac{j}{\eta_o}(A \cos kz + B \sin k|z|)$$

where $k = 2\pi/\lambda$ is the phase constant and $\eta_o = 377\ \Omega$ is the intrinsic impedance of free space. Consider a straight wire dipole with length $L = 0.5\ \lambda$ and radius $a = 0.005\ \lambda$. □

Solution
The integral equation has the form

$$\int_{-\ell/2}^{\ell/2} I\left(z'\right) K\left(z, z'\right) dz' = D(z) \tag{5.151}$$

which is a Fredholm integral equation of the first kind. In Eq. (5.151),

$$K\left(z, z'\right) = G\left(z, z'\right) = \frac{e^{-jkR}}{4\pi R}\ , \tag{5.152a}$$

$$R = \sqrt{a^2 + (z - z')^2}\ , \tag{5.152b}$$

and

$$D(z) = -\frac{j}{\eta_o}[A\cos(kz) + B\sin(k|z|)] \tag{5.152c}$$

If the terminal voltage of the wire antenna is V_T, the constant $B = V_T/2$. The absolute value in $\sin k|z|$ expresses the assumption of antenna symmetry, i.e., $I(-z') = I(z')$. Thus

$$\int_{-\ell/2}^{\ell/2} I\left(z'\right) \frac{e^{-jkR}}{4\pi R}\, dz' = -\frac{j}{\eta_o}\left[A\cos kz + \frac{V_T}{2}\sin k|z|\right] \tag{5.153}$$

If we let

$$I(z) = \sum_{n=1}^{N} I_n u_n(z)\ , \tag{5.154}$$

Eq. (5.153) will contain N unknown variables I_n and the unknown constant A. To determine the $N + 1$ unknowns, we divide the wire into N segments. For the sake of simplicity, we choose segments of equal lengths $\Delta z = \ell/N$ and select $N + 1$ matching points such as:

$$z = -\ell/2, -\ell/2 + \Delta z, \ldots,\ 0, \ldots, \ell/2 - \Delta z, \ell/2$$

At each match point $z = z_m$,

$$\int_{-\ell/2}^{\ell/2} \sum_{n=1}^{N} I_n u_n\left(z'\right) K\left(z_m, z'\right)\, dz' = D\left(z_m\right) \tag{5.155}$$

Taking the inner products (moments) by multiplying either side with a weighting function $w_m(z)$ and integrating both sides,

$$\int_{-\ell/2}^{\ell/2} \int_{-\ell/2}^{\ell/2} \sum_{n=1}^{N} I_n u_n \left(z'\right) K \left(z_m, z'\right) \, dz' w_m(z) dz$$
$$= \int_{-\ell/2}^{\ell/2} D \left(z_m\right) w_m(z) \, dz \tag{5.156}$$

By reversing the order of the summation and integration,

$$\sum_{n=1}^{N} I_n \int_{-\ell/2}^{\ell/2} u_n \left(z'\right) \int_{-\ell/2}^{\ell/2} K \left(z_m, z'\right) w_m(z) \, dz dz'$$
$$= \int_{-\ell/2}^{\ell/2} D \left(z_m\right) w_m(z) \, dz \tag{5.157}$$

The integration on either side of Eq. (5.157) can be carried out numerically or analytically if possible. If we use the point matching method by selecting the weighting function as delta function, then

$$w_m(z) = \delta \left(z - z_m\right)$$

Since the integral of any function multiplied by $\delta(z - z_m)$ gives the value of the function at $z = z_m$, Eq. (5.157) becomes

$$\sum_{n=1}^{N} I_n \int_{-\ell/2}^{\ell/2} u_n \left(z'\right) K \left(z_m, z'\right) dz' = D \left(z_m\right) \ , \tag{5.158}$$

where $m = 1, 2, \ldots, N + 1$. Also, if we choose pulse function as the basis or expansion function,

$$u_n(z) = \begin{cases} 1, & z_n - \Delta z/2 < z < z_n + \Delta z/2 \\ 0, & \text{elsewhere,} \end{cases}$$

and Eq. (5.158) yields

$$\sum_{n=1}^{N} I_n \int_{z_n - \Delta z/2}^{z_n + \Delta z/2} K \left(z_m, z'\right) dz' = D \left(z_m\right) \tag{5.159}$$

Substitution of Eq. (5.152) into Eq. (5.159) gives

$$\sum_{n=1}^{N} I_n \int_{z_n - \Delta z/2}^{z_n + \Delta z/2} \frac{e^{jkR_m}}{4\pi R_m} \, dz' = -\frac{j}{\eta_o} \left[A \cos k z_m + \frac{V_T}{2} \sin k \left| z_m \right| \right] \tag{5.160}$$

where $m = 1, 2, \ldots, N+1$ and $R_m = [a^2 + (z_m - z')^2]^{1/2}$. Thus we have a set of $N+1$ simultaneous equations, which can be cast in matrix form as

$$\begin{bmatrix} F_{11} & F_{12} & \ldots & F_{1,N} & \dfrac{j}{\eta}\cos(kz_1) \\ F_{21} & F_{22} & \ldots & F_{2,N} & \dfrac{j}{\eta}\cos(kz_2) \\ \vdots & & & & \vdots \\ F_{N+1,1} & F_{N+1,2} & \ldots & F_{N+1,N} & \dfrac{j}{\eta}\cos(kz_{N+1}) \end{bmatrix} \begin{bmatrix} I_1 \\ I_2 \\ \vdots \\ A \end{bmatrix}$$

$$= \begin{bmatrix} -\dfrac{j}{2\eta}V_T \sin k|z_1| \\ -\dfrac{j}{2\eta}V_T \sin k|z_2| \\ \vdots \\ -\dfrac{j}{2\eta}V_T \sin k|z_{N+1}| \end{bmatrix} \tag{5.161a}$$

or

$$[F][X] = [Q] \tag{5.161b}$$

where

$$F_{mn} = \int_{z_n - \Delta z/2}^{z_n + \Delta z/2} \frac{e^{-jkR_m}}{4\pi R_m}\, dz' \tag{5.162}$$

The $N+1$ unknowns are determined by solving Eq. (5.161) in the usual manner. To evaluate F_{mn} analytically rather than numerically, let the integrand in Eq. (5.162) be separated into its real (RE) and imaginary (IM) parts,

$$\begin{aligned} \frac{e^{-jkR_m}}{R_m} &= \mathrm{RE} + j\,\mathrm{IM} \\ &= \frac{\cos kR_m}{R_m} - j\frac{\sin kR_m}{R_m} \end{aligned} \tag{5.163}$$

IM as a function of z' is a smooth curve so that

$$\begin{aligned} \int_{z_n - \Delta z/2}^{z_n + \Delta z/2} \mathrm{IM}\left(z'\right) dz' &= -\int_{z_n - \Delta z/2}^{z_n + \Delta z/2} \frac{\sin k\left[a^2 + \left(z_m - z'\right)^2\right]^{1/2}}{\left[a^2 + (z_m - z')^2\right]^{1/2}}\, dz' \\ &\simeq -\frac{\Delta z \sin k\left[a^2 + (z_m - z_n)^2\right]^{1/2}}{\left[a^2 + (z_m - z_n)^2\right]^{1/2}} \end{aligned} \tag{5.164}$$

The approximation is accurate as long as $\Delta z < 0.05\ \lambda$. On the other hand, RE changes rapidly as $z' \to z_m$ due to R_m. Hence

$$\begin{aligned}\int_{z_n-\Delta z/2}^{z_n+\Delta z/2} \mathrm{RE}\left(z'\right)\, dz' &= -\int_{z_n-\Delta z/2}^{z_n+\Delta z/2} \frac{\cos k\left[a^2+\left(z_m-z'\right)^2\right]^{1/2}}{\left[a^2+(z_m-z')^2\right]^{1/2}}\, dz' \\ &\simeq \cos k\left[a^2+(z_m-z_n)^2\right]^{1/2} \int_{z_n-\Delta z/2}^{z_n+\Delta z/2} \frac{dz'}{\left[a^2+(z_m-z')^2\right]^{1/2}} \\ &= \cos k\left[a^2+(z_m-z_n)^2\right]^{1/2} \\ &\quad \ln\left[\frac{z_m+\Delta z/2-z_n+\left[a^2+(z_m-z_n+\Delta z/2)^2\right]^{1/2}}{z_m-\Delta z/2-z_n+\left[a^2+(z_m-z_n-\Delta z/2)^2\right]^{1/2}}\right] \end{aligned} \tag{5.165}$$

Thus

$$\begin{aligned} F_{mn} \simeq{}& \frac{1}{4\pi}\cos k\left[a^2+(z_m-z_n)^2\right]^{1/2} \\ &\times \ln\left[\frac{z_m+\Delta z/2-z_n+\left[a^2+(z_m-z_n+\Delta z/2)^2\right]^{1/2}}{z_m-\Delta z/2-z_n+\left[a^2+(z_m-z_n-\Delta z/2)^2\right]^{1/2}}\right] \\ &- \frac{j\Delta z \sin k\left[a^2+(z_m-z_n)^2\right]^{1/2}}{4\pi\left[a^2+(z_m-z_n)^2\right]^{1/2}} \end{aligned} \tag{5.166}$$

A typical example of the current distribution obtained for $\ell = \lambda$, $a = 0.01\ \lambda$ is shown in Fig. 5.20, where the sinusoidal distribution commonly assumed for wire antennas is also shown for comparison. Notice the remarkable difference between the two near the dipole center. ∎

Example 5.10

Consider a perfectly conducting scatterer or antenna of cylindrical cross section shown in Fig. 5.21. Determine the axial current $I(z)$ on the structure by solving the electric field integral equation (EFIE)

$$\frac{j\eta}{4k\pi}\left(\frac{d^2}{dz^2}+k^2\right)\int_{-h}^{h} I\left(z'\right) G\left(z,z'\right) dz' = E_z^i(z) \tag{5.167}$$

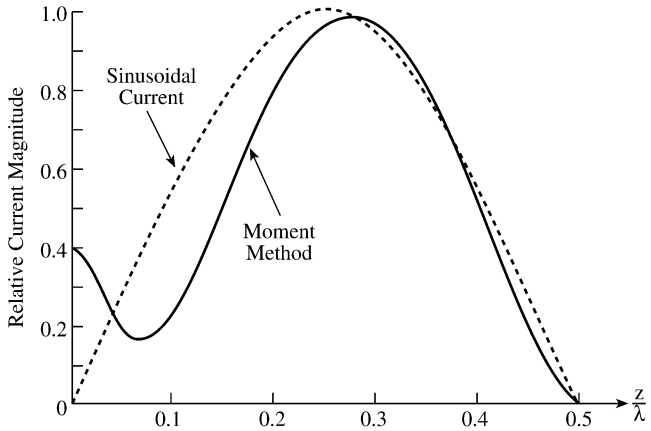

Figure 5.20
Current distribution of straight center-fed dipole.

where

$$G\left(z, z'\right) = \frac{1}{2\pi} \int_0^{2\pi} \frac{e^{-jkR}}{R}\, d\phi' \,,$$

$$R = \left[\left(z - z'\right)^2 + 4a^2 \sin^2 \frac{\phi'}{2}\right]^{1/2} \,,$$

$$\eta = \sqrt{\frac{\mu}{\epsilon}}, \quad \text{and} \quad k = \frac{2\pi}{\lambda} \quad \square$$

Solution
If the radius $a << \lambda$ (the wavelength) and $a << 2h$ (the length of the wire), the structure can be regarded as a "thin-wire" antenna or scatterer. As a scatterer, we may consider a plane wave excitation

$$E_z^i(z) = E_o \sin\theta e^{jkz\cos\theta} \tag{5.168a}$$

where θ is the angle of incidence. As an antenna, we may assume a delta-gap generator

$$E_z^i = V\delta\left(z - z_g\right) \tag{5.168b}$$

where V is the generator voltage and $z = z_g$ is the location of the generator.

In order to apply the method of moments to the given integral equation (5.167), we expand the currents in terms of pulse basis function as

$$I(z) = \sum_{n=1}^{N} I_n u_n(z) \tag{5.169}$$

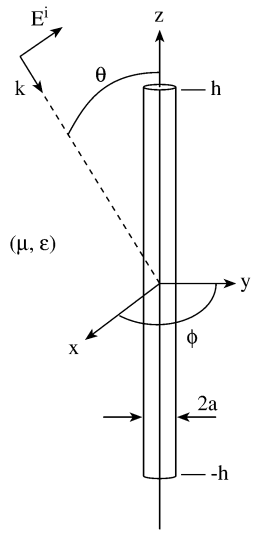

Figure 5.21
Cylindrical scatterer or antenna.

where

$$u_n(z) = \begin{cases} 1, & z_{n-1/2} < z < z_{n+1/2} \\ 0, & \text{elsewhere} \end{cases}$$

Substituting Eq. (5.169) into Eq. (5.167) and weighting the result with triangular functions

$$w_m(z) = \begin{cases} \dfrac{z - z_{m-1}}{\Delta}, & z_{m-1} < z < z_m \\ -\dfrac{z - z_{m+1}}{\Delta}, & z_{m-1} < z < z_{m+1} \\ 0, & \text{elsewhere,} \end{cases} \tag{5.170}$$

where $\Delta = 2h/N$, leads to

$$\sum_{n=1}^{N} Z_{mn} I_n = V_m, \quad m = 1, 2, \ldots, N \tag{5.171}$$

Figure 5.22 illustrates $u_n(z)$ and $w_m(z)$. Equation (5.171) can be cast in matrix form as

$$[Z][I] = [V] \tag{5.172}$$

where $[I]$ can be solved using any standard method. For the impedance matrix $[Z]$, the elements are given by

$$Z_{mn} = \frac{j\eta}{4\pi k}\frac{2}{\Delta}\left[\frac{1}{2}G_{m-1,n} - \left(1 - \frac{k^2\Delta^2}{2}\right)G_{m,n} + \frac{1}{2}G_{m+1,n}\right] \tag{5.173}$$

where

$$G_{m,n} = \int_{z_n-\Delta/2}^{z_n+\Delta/2} G\left(z_m, z'\right) dz' \tag{5.174}$$

To obtain Eq. (5.173), we have used the approximation

$$\int_{z_{m-1}}^{z_{m+1}} w_m(z) f(z)\, dz = \Delta f\left(z_m\right)$$

For the plane wave excitation, the elements of the forcing vector [V] are

$$V_m = \Delta E_0 e^{jkz_m \cos\theta} \tag{5.175a}$$

For delta-gap generator,

$$V_m = V \delta_{mg} \tag{5.175b}$$

where g is the index of the feed zone pulse.

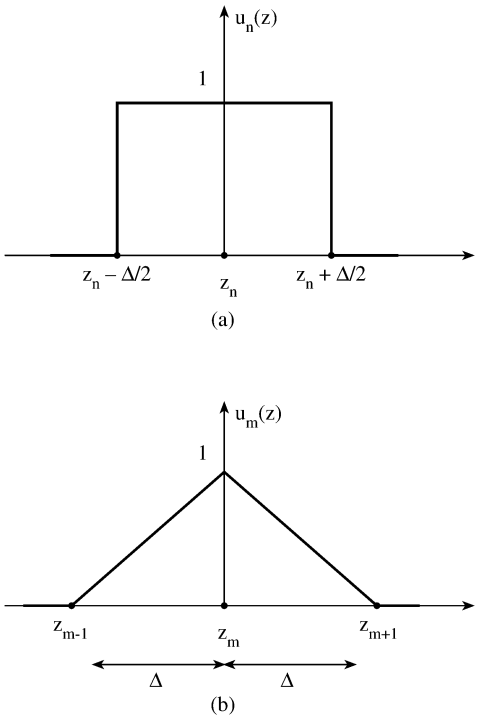

Figure 5.22
For Example 5.10: (a) Pulse basis function, (b) triangular weighting function.

Solving Eq. (5.172) requires that we incorporate a method to perform numerically the double integration in Eq. (5.174). The kernel $G(z, z')$ exhibits a logarithmic singularity as $|z - z'| \to 0$, and therefore care must be exercised. To circumvent the difficulty, we let

$$G\left(z, z'\right) = \frac{1}{2\pi} \int_0^{2\pi} \frac{e^{-jkR}}{R}\, d\phi' = G_o\left(z, z'\right) + G_1\left(z, z'\right) \tag{5.176}$$

where

$$G_o\left(z, z'\right) = \frac{1}{2\pi} \int_0^{2\pi} \frac{d\phi'}{R} \tag{5.177}$$

and

$$G_1\left(z, z'\right) = \frac{1}{2\pi} \int_0^{2\pi} \frac{e^{-jkR} - 1}{R}\, d\phi' \tag{5.178}$$

We note that

$$G_o\left(z, z'\right) \xrightarrow{\left(\frac{z-z'}{2a}\right) \to 0} -\frac{1}{\pi a} \ln \frac{\left|z - z'\right|}{8a}$$

and hence we replace $G_o(z, z')$ by

$$\left[G_o\left(z, z'\right) + \frac{1}{\pi a} \ln \frac{\left|z - z'\right|}{8a}\right] - \frac{1}{\pi a} \ln \frac{\left|z - z'\right|}{8a} \tag{5.179}$$

The term $G_1(z, z')$ is nonsingular, while the singularity of $G_o(z, z')$ can be avoided by using Eq. (5.179). Thus the double integral involved in evaluating Z_{mn} is easily done numerically. It is interesting to note that Z_{mn} would remain the same if we had chosen the triangular basis function and pulse weighting function [46]. ∎

5.7 Applications IV — EM Absorption in the Human Body

The interest in hyperthermia (or electromagnetic heating of deep-seated tumors) and in the assessment of possible health hazards due to EM radiation have prompted the development of analytical and numerical techniques for evaluating EM power deposition in the interior of the human body or a biological system [47]. The overall need is to provide a scientific basis for the establishment of an EM radiation safety standard. Since human experimentation is not possible, irradiation experiments must be performed on animals. Theoretical models are required to interpret and confirm the experiment, develop an extrapolation process, and thereby develop a radiation safety standard for man [48].

The mathematical complexity of the problem has led researchers to investigate simple models of tissue structures such as plane slab, dielectric cylinder homogeneous and layered spheres, and prolate spheroid. A review of these earlier efforts is given in [49, 50]. Although spherical models are still being used to study the power deposition characteristics of the head of man and animals, realistic block model composed of cubical cells is being used to simulate the whole body.

The key issue in this bioelectromagnetic effort is how much EM energy is absorbed by a biological body and where is it deposited. This is usually quantified in terms of the specific absorption rate (SAR), which is the mass normalized rate of energy absorbed by the body. At a specific location, SAR may be defined by

$$\text{SAR} = \frac{\sigma}{\rho}|E|^2 \tag{5.180}$$

where σ = tissue conductivity, ρ = tissue mass density, E = RMS value of the internal field strength. Thus the localized SAR is directly related to the internal electric field and the major effort involves the determination of the electric field distribution within the biological body. The method of moments has been extensively utilized to calculate localized SARs in block model representation of humans and animals.

As mentioned in Section 5.1, an application of MOM to EM problems usually involves four steps:

- deriving the appropriate IE,
- transforming the IE into a matrix equation (discretization),
- evaluating the matrix elements, and
- solving the resulting set of simultaneous equations.

We will apply these steps for calculating the electric field induced in an arbitrary human body or a biological system illuminated by an incident EM wave.

5.7.1 Derivation of Integral Equations

In general, the induced electric field inside a biological body was found to be quite complicated even for the simple case of assuming the plane wave as the incident field. The complexity is due to the irregularity of the body geometry, and the fact that the body is finitely conducting. To handle the complexity, the so-called *tensor integral-equation* (TIE) was developed by Livesay and Chen [51]. Only the essential steps will be provided here; the interested reader is referred to [51]–[53].

Consider a biological body of an arbitrary shape, with constitutive parameters ϵ, μ, σ illuminated by an incident (or impressed) plane EM wave as shown in Fig. 5.23. The induced current in the body gives rise to a scattered field $\mathbf{E}^s$, which may be accounted for by replacing the body with an equivalent free-space current density $\mathbf{J}_{eq}$ given by

$$\mathbf{J}_{eq}(\mathbf{r}) = \big(\sigma(\mathbf{r}) + j\omega[\epsilon(\mathbf{r}) - \epsilon_o]\big)\mathbf{E}(\mathbf{r}) = \tau(\mathbf{r})\mathbf{E}(\mathbf{r}) \tag{5.181}$$

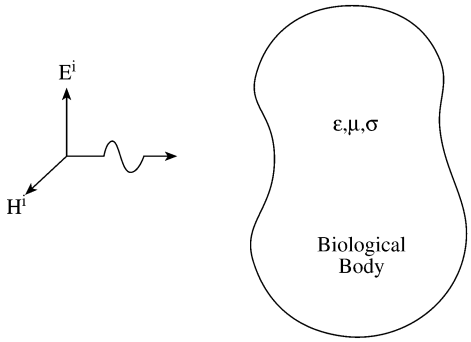

Figure 5.23
A biological body illuminated by a plane EM wave.

where a time factor $e^{j\omega t}$ is assumed. The first term in Eq. (5.181) is the conduction current density, while the second term is the polarization current density. With the equivalent current density $\mathbf{J}_{eq}$, we can obtain the scattered fields $\mathbf{E}^s$ and $\mathbf{H}^s$ by solving Maxwell's equations

$$\nabla \times \mathbf{E}^s = -\mathbf{J}_{eq} - j\omega \mathbf{H}^s \tag{5.182a}$$

$$\nabla \times \mathbf{H}^s = j\omega \mathbf{E}^s \tag{5.182b}$$

where $\mathbf{E}^s$, $\mathbf{H}^s$, and $\mathbf{J}_{eq}$ are all in phasor (complex) form. Elimination of $\mathbf{E}^s$ or $\mathbf{H}^s$ in Eq. (5.182) leads to

$$\nabla \times \nabla \times \mathbf{E}^s - k_o^2 \mathbf{E}^s = -j\omega\mu_o \mathbf{J}_{eq} \tag{5.183a}$$

$$\nabla \times \nabla \times \mathbf{H}^s - k_o^2 \mathbf{H}^s = \nabla \times \mathbf{J}_{eq} \tag{5.183b}$$

where $k_o^2 = \omega^2 \mu_o \epsilon_o$. The solutions to Eq. (5.183) are

$$\mathbf{E}^s = -j\omega \left[1 + \frac{1}{k_o^2} \nabla\nabla\cdot \right] \mathbf{A} \tag{5.184a}$$

$$\mathbf{H}^s = \frac{1}{\mu_o} \nabla \times \mathbf{A} \tag{5.184b}$$

where

$$\mathbf{A} = \mu_o \int_v G_o\left(\mathbf{r}, \mathbf{r}'\right) \mathbf{J}_{eq}\left(\mathbf{r}'\right)\, dv' \tag{5.185}$$

and

$$G_o\left(\mathbf{r}, \mathbf{r}'\right) = \frac{e^{-jk_o(\mathbf{r}-\mathbf{r}')}}{4\pi\,|\mathbf{r}-\mathbf{r}'|} \tag{5.186}$$

is the free-space scalar Green's function. By the operator $\nabla\nabla\cdot$, we mean that $\nabla\nabla\cdot\mathbf{A} = \nabla(\nabla\cdot\mathbf{A})$. It is evident from Eqs. (5.184) to (5.186) that $\mathbf{E}^s$ and $\mathbf{H}^s$ depend on $\mathbf{J}_{eq}$.

Suppose $\mathbf{J}_{eq}$ is an infinitesimal, elementary source at $\mathbf{r}'$ pointed in the x direction so that

$$\mathbf{J}_{eq} = \delta\left(\mathbf{r} - \mathbf{r}'\right)\mathbf{a}_x \ , \tag{5.187}$$

the corresponding vector potential is obtained from Eq. (5.185) as

$$\mathbf{A} = \mu_o G_o\left(\mathbf{r}, \mathbf{r}'\right)\mathbf{a}_x \tag{5.188}$$

If $\mathbf{G}_{ox}(\mathbf{r}, \mathbf{r}')$ is the electric field produced by the elementary source, then $\mathbf{G}_{ox}(\mathbf{r}, \mathbf{r}')$ must satisfy

$$\nabla \times \nabla \times \mathbf{G}_{ox}\left(\mathbf{r}, \mathbf{r}'\right) - k_o^2 \mathbf{G}_{ox}\left(\mathbf{r}, \mathbf{r}'\right) = -j\omega\mu_o \delta\left(\mathbf{r}, \mathbf{r}'\right) \tag{5.189}$$

with solution

$$\mathbf{G}_{ox}\left(\mathbf{r}, \mathbf{r}'\right) = -j\omega\mu_o\left(1 + \frac{1}{k^2}\nabla\nabla\cdot\right) G_o\left(\mathbf{r}, \mathbf{r}'\right) \tag{5.190}$$

$\mathbf{G}_{ox}(\mathbf{r}, \mathbf{r}')$ is referred to as a free-space vector Green's function with a source pointed in the x direction. We could also have $\mathbf{G}_{oy}(\mathbf{r}, \mathbf{r}')$ and $\mathbf{G}_{oz}(\mathbf{r}, \mathbf{r}')$ corresponding to infinitesimal, elementary sources pointed in the y and z direction, respectively. We now introduce a dyadic function[2] which can store the three vector Green functions $\mathbf{G}_{ox}(\mathbf{r}, \mathbf{r}')$, $\mathbf{G}_{oy}(\mathbf{r}, \mathbf{r}')$, and $\mathbf{G}_{oz}(\mathbf{r}, \mathbf{r}')$, i.e.,

$$\mathbf{G}_o\left(\mathbf{r}, \mathbf{r}'\right) = \mathbf{G}_{ox}\left(\mathbf{r}, \mathbf{r}'\right)\mathbf{a}_x + \mathbf{G}_{oy}\left(\mathbf{r}, \mathbf{r}'\right)\mathbf{a}_y + \mathbf{G}_{oz}\left(\mathbf{r}, \mathbf{r}'\right)\mathbf{a}_z \tag{5.191}$$

This is called free-space dyadic Green's function [53]. It is a solution to the dyadic differential equation

$$\nabla \times \nabla \times \mathbf{G}_o\left(\mathbf{r}, \mathbf{r}'\right) - k_o^2 \mathbf{G}_o\left(\mathbf{r}, \mathbf{r}'\right) = \widetilde{I}\delta\left(\mathbf{r} - \mathbf{r}'\right) \tag{5.192}$$

where $\widetilde{I}$ denotes the unit dyad (or idem factor) defined by

$$\widetilde{I} = \mathbf{a}_x\mathbf{a}_x + \mathbf{a}_y\mathbf{a}_y + \mathbf{a}_z\mathbf{a}_z \tag{5.193}$$

The physical meaning of $\mathbf{G}_o(\mathbf{r}, \mathbf{r}')$ is rather obvious. $\mathbf{G}_o(\mathbf{r}, \mathbf{r}')$ is the electric field at a field point $\mathbf{r}$ due to an infinitesimal source at $\mathbf{r}'$.

From Eqs. (5.183a) and (5.192), the solution of $\mathbf{E}$ is

$$\mathbf{E}^s(\mathbf{r}) = -j\omega\mu_o \int \mathbf{G}_o\left(\mathbf{r}, \mathbf{r}'\right) \cdot \mathbf{J}_{eq}\left(\mathbf{r}'\right)\, dv' \tag{5.194}$$

Since $\mathbf{G}_o(\mathbf{r}, \mathbf{r}')$ has a singularity of the order $|\mathbf{r} - \mathbf{r}'|^3$, the integral in Eq. (5.194) diverges if the field point $\mathbf{r}$ is inside the volume v of the body (or source region).

[2] A dyad is a group of two or a pair of quantities. A dyadic function, denoted by $\widetilde{D}$, is formed by two functions, i.e., $\widetilde{D} = \mathbf{AB}$. See Tai [53] or Balanis [28] for an exposition on dyadic functions.

This difficulty is overcome by excluding a small volume surrounding the field point first and then letting the small volume approach zero. The process entails defining the principal value (PV) and adding a correction term needed to yield the correct solution. Thus

$$\mathbf{E}^s(\mathbf{r}) = PV \int_v \mathbf{J}_{eq}(\mathbf{r}) \cdot \mathbf{G}\left(\mathbf{r}, \mathbf{r}'\right)\, dv' + \left[\mathbf{E}^s(\mathbf{r})\right]_{\text{correction}} \tag{5.195}$$

The correction term has been evaluated [51, 52] to be $-\mathbf{J}_{eq}/j3\omega\epsilon_o$ so that

$$\mathbf{E}^s(\mathbf{r}) = PV \int_v \mathbf{J}_{eq}(\mathbf{r}) \cdot \mathbf{G}\left(\mathbf{r}, \mathbf{r}'\right)\, dv' - \frac{\mathbf{J}_{eq}(\mathbf{r})}{j3\omega\epsilon_o} \tag{5.196}$$

The total electric field inside the body is the sum of the incident field $\mathbf{E}^i$ and scattered field $\mathbf{E}^s$, i.e.,

$$\mathbf{E}(\mathbf{r}) = \mathbf{E}^i(\mathbf{r}) + \mathbf{E}^s(\mathbf{r}) \tag{5.197}$$

Combining Eqs. (5.181), (5.196), and (5.197) gives the desired tensor integral equation for $\mathbf{E}(\mathbf{r})$:

$$\left[1 + \frac{\tau(\mathbf{r})}{3j\omega\epsilon_o}\right]\mathbf{E}(\mathbf{r}) - PV \int_v \tau\left(\mathbf{r}'\right)\mathbf{E}(\mathbf{r}) \cdot \mathbf{G}\left(\mathbf{r}, \mathbf{r}'\right)\, dv' = \mathbf{E}^i(\mathbf{r}) \tag{5.198}$$

In Eq. (5.198), $\tau(\mathbf{r}) = \sigma(\mathbf{r}) + j\omega[\epsilon(\mathbf{r}) - \epsilon_o]$ and the incident electric field $\mathbf{E}^i$ are known quantities; the total electric field $\mathbf{E}$ inside the body is unknown and is to be determined by MOM.

5.7.2 Transformation to Matrix Equation (Discretization)

The inner product $\mathbf{E}(\mathbf{r}) \cdot \mathbf{G}(\mathbf{r}, \mathbf{r}')$ in Eq. (5.198) may be represented as

$$\mathbf{E}(\mathbf{r}) \cdot \mathbf{G}\left(\mathbf{r}, \mathbf{r}'\right) = \begin{bmatrix} \mathbf{G}_{xx}\left(\mathbf{r}, \mathbf{r}'\right) & \mathbf{G}_{xy}\left(\mathbf{r}, \mathbf{r}'\right) & \mathbf{G}_{xz}\left(\mathbf{r}, \mathbf{r}'\right) \\ \mathbf{G}_{yx}\left(\mathbf{r}, \mathbf{r}'\right) & \mathbf{G}_{yy}\left(\mathbf{r}, \mathbf{r}'\right) & \mathbf{G}_{yz}\left(\mathbf{r}, \mathbf{r}'\right) \\ \mathbf{G}_{zx}\left(\mathbf{r}, \mathbf{r}'\right) & \mathbf{G}_{zy}\left(\mathbf{r}, \mathbf{r}'\right) & \mathbf{G}_{zz}\left(\mathbf{r}, \mathbf{r}'\right) \end{bmatrix} \begin{bmatrix} E_x\left(\mathbf{r}'\right) \\ E_y\left(\mathbf{r}'\right) \\ E_z\left(\mathbf{r}'\right) \end{bmatrix} \tag{5.199}$$

showing that $\mathbf{G}(\mathbf{r}, \mathbf{r}')$ is a symmetric dyad. If we let

$$x_1 = x, \quad x_2 = y, \quad x_3 = z\,,$$

then $G_{x_p x_q}(\mathbf{r}, \mathbf{r}')$ can be written as

$$G_{x_p x_q}\left(\mathbf{r}, \mathbf{r}'\right) = -j\omega\mu_o\left[\delta_{pq} + \frac{1}{k_o^2}\frac{\partial^2}{\partial x_q \partial x_p}\right] G_o\left(\mathbf{r}, \mathbf{r}'\right), \quad p, q = 1, 2, 3 \tag{5.200}$$

We now apply MOM to transform Eq. (5.198) into a matrix equation. We partition the body into N subvolumes or cells, each denoted by v_m ($m = 1, 2, \ldots, N$), and

assume that $\mathbf{E}(\mathbf{r})$ and $\tau(\mathbf{r})$ are constant within each cell. If $\mathbf{r}_m$ is the center of the mth cell, requiring that each scalar component of Eq. (5.198) be satisfied at $\mathbf{r}_m$ this leads to

$$\left[1+\frac{\tau(\mathbf{r})}{3j\omega\epsilon_o}\right]E_{x_p}(\mathbf{r}_m)-\sum_{q=1}^{3}\left[\sum_{q=1}^{3}\tau(\mathbf{r}_n)\,PV\int_{v_m}G_{x_px_q}\left(\mathbf{r}_m,\mathbf{r}'\right)dv'\right]E_{x_q}(\mathbf{r}_n)$$
$$=E^i_{x_p}(\mathbf{r}_m) \tag{5.201}$$

If we let $[G_{x_px_q}]$ be an $N\times N$ matrix with elements

$$G^{mn}_{x_px_q}=\tau(\mathbf{r}_n)\,PV\int_{v_n}G_{x_px_q}\left(\mathbf{r}_m,\mathbf{r}'\right)dv'-\delta_{pq}\delta_{mn}\left[1+\frac{\tau(\mathbf{r})}{3j\omega\epsilon_o}\right], \tag{5.202}$$

where $m,n=1,2,\ldots,N,\ \ p,q=1,2,3$, and let $[E_{x_p}]$ and $[E^i_{x_p}]$ be column matrices with elements

$$E_{x_p}=\begin{bmatrix}E_{x_p}(\mathbf{r}_1)\\ \vdots\\ E_{x_p}(\mathbf{r}_N)\end{bmatrix},\quad E^i_{x_p}=\begin{bmatrix}E^i_{x_p}(\mathbf{r}_1)\\ \vdots\\ E^i_{x_p}(\mathbf{r}_N)\end{bmatrix}, \tag{5.203}$$

then from Eqs. (5.198) and (5.201), we obtain $3N$ simultaneous equations for E_x, E_y and E_z at the centers of N cells by the point matching technique. These simultaneous equations can be written in matrix form as

$$\begin{bmatrix}[G_{xx}] & [G_{xy}] & [G_{xz}]\\ \hline [G_{yx}] & [G_{yy}] & [G_{yz}]\\ \hline [G_{zx}] & [G_{zy}] & [G_{zz}]\end{bmatrix}\begin{bmatrix}[E_x]\\ \hline [E_y]\\ \hline [E_z]\end{bmatrix}=-\begin{bmatrix}[E^i_x]\\ \hline [E^i_y]\\ \hline [E^i_z]\end{bmatrix} \tag{5.204a}$$

or simply

$$[G][E]=-[E^i] \tag{5.204b}$$

where $[G]$ is $3N\times 3N$ matrix and $[E]$ and $[E^i]$ are $3N$ column matrices.

5.7.3 Evaluation of Matrix Elements

Although the matrix $[E^i]$ in Eq. (5.204) is known, while the matrix $[E]$ is to be determined, the elements of the matrix [G], defined in Eq. (5.202), are yet to be calculated. For the off-diagonal elements of $[G_{x_px_q}]$, $\mathbf{r}_m$ is not in the nth cell ($\mathbf{r}_m$ is not in v_n) so that $G_{x_px_q}(\mathbf{r}_m,\mathbf{r}')$ is continuous in v_n and the principal value operation can be dropped. Equation (5.202) becomes

$$G^{mn}_{x_px_q}=\tau(\mathbf{r}_n)\int_{v_n}G_{x_px_q}\left(\mathbf{r}_m,\mathbf{r}'\right)dv',\quad m\neq n \tag{5.205}$$

As a first approximation,

$$G^{mn}_{x_p x_q} = \tau\left(\mathbf{r}_n\right) G_{x_p x_q}\left(\mathbf{r}_m, \mathbf{r}'\right) \Delta v_n, \quad m \neq n \tag{5.206}$$

where Δv_n is the volume of cell v_n. Incorporating Eqs. (5.190) and (5.200) into Eq. (5.206) yields

$$G^{mn}_{x_p x_q} = \frac{-j\omega\mu k_o \Delta v_n \tau\left(\mathbf{r}_n\right) \exp(-j\alpha_{mn})}{4\pi\alpha^3_{mn}} \Big[\left(\alpha_{mn} - 1 - j\alpha_{mn}\right) \delta_{pq} + \cos\theta^{mn}_{x_p} \cos\theta^{mn}_{x_q} \left(3 - \alpha^2_{mn} + 3j\alpha_{mn}\right)\Big], \quad m \neq n \tag{5.207}$$

where

$$\alpha_{mn} = k_o R_{mn}, \quad R_{mn} = \left|\mathbf{r}_m - \mathbf{r}_n\right| ,$$
$$\cos\theta^{mn}_{x_p} = \frac{x^m_p - x^n_p}{R_{mn}}, \quad \cos\theta^{mn}_{x_q} = \frac{x^m_q - x^n_q}{R_{mn}} ,$$
$$\mathbf{r}_m = \left(x^m_1, x^m_2, x^m_3\right), \quad \mathbf{r}_n = \left(x^n_1, x^n_2, x^n_3\right)$$

The approximation in Eq. (5.207) yields adequate results provided N is large. If greater accuracy is desired, the integral in Eq. (5.205) must be evaluated numerically.

For the diagonal terms ($m = n$), Eq. (5.202) becomes

$$G^{nn}_{x_p x_q} = \tau\left(\mathbf{r}_n\right) PV \int_{v_n} G_{x_p x_q}\left(\mathbf{r}_n, \mathbf{r}'\right) dv' - \delta_{pq}\left[1 + \frac{\tau(\mathbf{r})}{3j\omega\epsilon_o}\right] \tag{5.208}$$

To evaluate this integral, we approximate cell v_n by an equivolumic sphere of radius a_n centered at $\mathbf{r}_n$, i.e.,

$$\Delta v = \frac{4}{3}\pi a^3_n$$

or

$$a_n = \left(\frac{3\Delta v}{4\pi}\right)^{1/3} \tag{5.209}$$

After a lengthy calculation, we obtain [51]

$$G^{nn}_{x_p x_q} = \delta_{pq}\Big[\frac{-2j\omega\mu_o\tau\left(r_n\right)}{3k^3_o}\left(\exp\left(-jk_o a_n\right)\left(1 + jk_o a_n\right) - 1\right) - \left(1 + \frac{\tau\left(r_n\right)}{3j\omega\epsilon_o}\right)\Big], \quad m = n \tag{5.210}$$

In case the shape of cell v_n differs considerably from that of a sphere, the approximation in Eq. (5.210) may yield poor results. To have a greater accuracy, a small cube, cylinder, or sphere is created around $\mathbf{r}_n$ to evaluate the correction term, and the integration through the remainder of v_n is performed numerically.

5.7.4 Solution of the Matrix Equation

Once the elements of matrix $[G]$ are evaluated, we are ready to solve Eq. (5.204), namely,

$$[G][E] = -[E^i] \tag{5.204}$$

With the known incident electric field represented by $[E^i]$, the total induced electric field represented by $[E]$ can be obtained from Eq. (5.204) by inverting $[G]$ or by employing a Gauss–Jordan elimination method. If matrix inversion is used, the total induced electric field inside the biological body is obtained from

$$[E] = -[G]^{-1}[E^i] \tag{5.211}$$

Guru and Chen [55] have developed computer programs that yield accurate results on the induced electric field and the absorption power density in various biological bodies irradiated by various EM waves. The validity and accuracy of their numerical results were verified by experiments.

In the following examples, we illustrate the accuracy of the numerical procedure with one simple elementary shape and one advanced shape of biological bodies. The examples are taken from the works of Chen and others [52], [56]–[58].

Example 5.11

Determine the distribution of the energy absorption rate or EM heating induced by plane EM waves of 918 MHz in spherical models of animal brain having radius 3 cm. Assume the $\mathbf{E}^i$ field expressed as

$$\mathbf{E}^i = E_o e^{-jk_o z}\mathbf{a}_x = \mathbf{a}_x E_o\,(\cos k_o z - j \sin k_o z)\ \text{V/m} \tag{5.212}$$

where $k_o = 2\pi/\lambda = 2\pi f/c$, $E_o = \sqrt{2\eta_o P_i}$, P_i is the incident power in mW/cm^2 and $\eta_o = 377\ \Omega$ is the intrinsic impedance of free space. Take $P_i = 1$ mW/cm^2 ($E_o = 86.83$ V/m), $\epsilon_r = 35$, $\sigma = 0.7$ mhos/m. □

Solution

In order to apply MOM, we first approximate the spherical model by a "cubic sphere." Figure 5.24 portrays an example in which one eighth of a sphere is approximated by 40 or 73 cubic cells. The center of each cell, for the case of 40 cells, is determined from Fig. 5.25. $\mathbf{E}^i$ at the center of each cell can be calculated using Eq. (5.212). With the computed $\mathbf{E}^i$ and the elements of the matrix $[G_{x_p x_q}]$ calculated using Eqs. (5.207) and (5.210), the induced electric field $\mathbf{E}$ in each cell is computed from Eq. (5.211). Once $\mathbf{E}$ is obtained, the absorption rate of the EM energy is determined using

$$P = \frac{\sigma}{2}|\mathbf{E}|^2 \tag{5.213}$$

The average heating is obtained by averaging P in the brain. The curve showing relative heating as a function of location is obtained by normalizing the distribution of P with respect to the maximum value of P at a certain location in the brain.

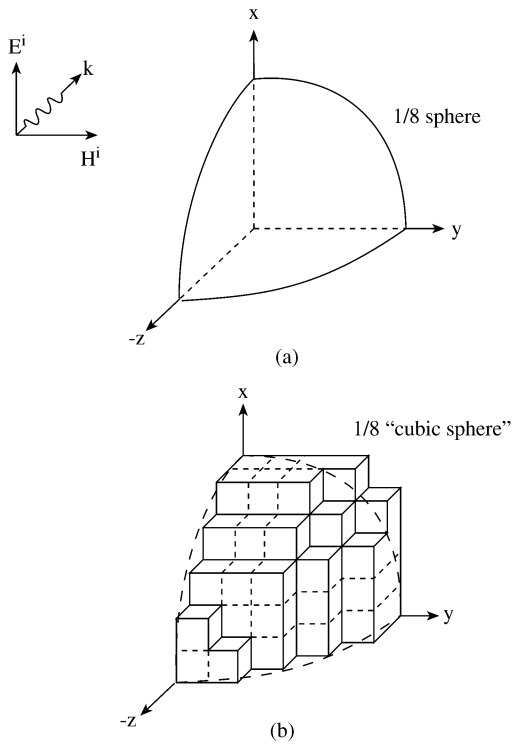

Figure 5.24

For Example 5.11: (a) One eighth of a sphere, (b) a "cubic sphere" constructed from 73 cubic cells.

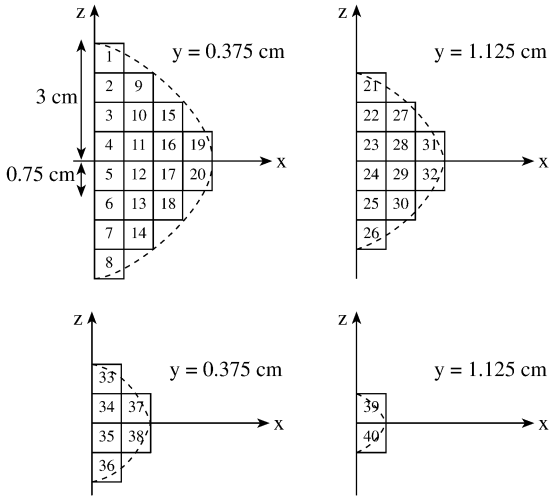

Figure 5.25

Geometry and dimensions of one half of the spherical model of the brain constructed from 40 cells. The cell numbering is used in the program of Fig. 5.26.

The computer program for the computation is shown in Fig. 5.26. It is a modified version of the one developed by Jongakiem [58]. The numerical results are shown in Fig. 5.27(a), where relative heating along the x-, y-, and z-axes in the brain is plotted. The three curves identified by X, Y, and Z correspond with the distributions of the relative heating along x-, y-, and z-axes, respectively. Observe the strong standing wave patterns with peak heating located somewhere near the center of the brain. The average and maximum heating are found to be 0.3202 and 0.885 in mW/cm^3. The exact solution obtained from Mie theory (see Section 2.8) is shown in Fig. 5.27(b). The average and maximum heating from exact solution are 0.295 and 0.814 mW/cm^3, respectively. A comparison of Figs. 5.27(a) and (b) confirms the accuracy of the numerical procedure. ∎

Example 5.12

Having validated the accuracy of the tensor-integral-equation (TIE) method, determine the induced electric field and specific absorption rate (SAR) of EM energy inside a model of typical human body irradiation (Fig. 5.28), by EM wave at 80 MHz with vertical polarization, i.e.,

$$\mathbf{E} = \mathbf{a}_x \quad \text{V/m}$$

at normal incidence. Assume the body at 80 MHz is that of a high-water content tissue with $\epsilon = 80\epsilon_o$, $\mu = \mu_o$, $\sigma = 0.84$ mhos/m. □

Solution

The body is partitioned into 108 cubic cells of various sizes ranging from 5 cm^3 to 12 cm^3. To ensure accurate results, the cell size is kept smaller than a quarter-wavelength (of the medium). With the coordinates of the center of each cell figured out from Fig. 5.28, the program in Fig. 5.26 can be used to find induced electric field components E_x, E_y, and E_z at the centers of the cells due to an incident electric field 1 V/m (maximum value) at normal incidence. The SAR is calculated from $(\sigma/2)(E_x^2 + E_y^2 + E_z^2)$. Figures 5.29 to 5.31 illustrate E_x, E_y, and E_z at the center of each cell. Observe that E_y and E_z are much smaller than E_x at this frequency due to the polarization of the incident wave.

As mentioned earlier, the model of the human body shown in Fig. 5.28 is due to Chen et al. [52]. An improved, more realistic model due to Gandhi et al. [59]–[61] is shown in Fig. 5.32. ∎

5.8 Concluding Remarks

The method of moments is a powerful numerical method capable of applying weighted residual techniques to reduce an integral equation to a matrix equation. The

```
0001    C*****************************************************************
0002    C  THIS PROGRAM DETERMINED EM POWER ABSORPTION
           OF BIOLOGICAL BODIES
0003    C  PROGRAMMER: JONG A KIEM RAYMOND
0004    C  PROGRAM LIMITATIONS:
0005    C
0006    C     BODIES ARE ASSUMED TO HAVE A PERMEABILITY EQUAL
              TO FREE SPACE
0007    C     MAX NUMBER OF CELLS = 150
0008    C     MAX NUMBER OF CELLS IS SUFFICIENTLY LARGE ELSE G-MATRIX
0009    C     NEED TO BE OBTAINED BY INTEGRATION METHODS
0010    C     THE SHAPE OF A CELL CAN BE APPROXIMATED BY A SPHERE
0011    C
0012    C     DIST = R(M,N) = DISTANCE BETWEEN CENTER OF CELL M AND N
0013    C     E(N) = CONCANTINATED MATRIX OF ALL FIELD INTENSITIES
0014    C     EI(N) = CONCANTINATED MATRIX OF ALL INPUT FIELD INTENSITIES
0015    C
0016    C    NOTE: IN THE CONCANTINATED MATRICES, THE ORDER IN WHICH
                   THE DATA IS
0017    C          STORED IS X,Y,Z I.E. ALL X FIRST, THEN ALL Y,
                   FINALLY ALL Z
0018    C          COORDINATES IN SEQUENTIAL ORDER
0019    C
0020    C            EPS(N) = EPSO*EPSR(N) = PERMITTIVITY OF CELL N
0021    C            EPSO = FREE SPACE PERMITTIVITY
0022    C            F = FREQUENCY
0023    C            G = COEFFICIENT MATRIX
0024    C            J = COMPLEX VALUE
0025    C            KO = FREE SPACE WAVE NUMBER
0026    C            MXCLL = MAXIMUM NUMBER OF CELLS
0027    C            MXCLL3 = MAXIMUM DIMENSION COEFFICIENT
                     MATRIX = 3*MXCLL
0028    C            PZ(I) = POWER ALONG THE Z DIRECTION
0029    C            NCELL = NUMBER OF CELLS
0030    C            SIGMA(N) = CONDUCTIVITY OF CELL N
0031    C            SAR = SPECIFIC ABSORPTION RATE
0032    C            TAU(N) = ARRAY STORING VALUES OF CELL N = E(N)/Jeq(N)
0033    C            UO = FREE SPACE PERMEABILITY
0034    C            V(N) = VOLUME OF CELL N
0035    C            W = RADIAN FREQUENCY
0036    C            X1 = ROW LOCATION IN G-MATRIX
0037    C            X2 = COLUMN LOCATION IN G-MATRIX
0038    C            X(1,N) = X COMPONENT OF CENTER OF CELL N
0039    C            X(2,N) = Y COMPONENT OF CENTER OF CELL N
0040    C            X(3,N) = Z COMPONENT OF CENTER OF CELL N
0041    C
0042    C ------ INPUT DATA MUST OBEY THE FOLLOWING FORMAT ----------- C
0043    C
0044    C    **** DATA ****                  ***** FORMAT *****
0045    C
0046    C    NCELL,F                         FORMAT(1X,I4,E10.4)
0047    C    V(N),X(1,N),X(2,N),X(3,N),
             SIGMA(N),EPS(N)                 FORMAT(1X,E10.5,4F10.5,E10.4)
0048    C    EI(I),EI(I+NCELL),EI(I+2*NCELL) FORMAT(1X,6E12.5)
0049
0050    C ------------ SUBROUTINES AND FUNCTIONS ---------------------- C
0051
0052    C            DELTA = DELTA FUNCTION
0053    C            MAGSQ(C) = MAGNITUDE SQUARED OF COMPLEX NUMBER
0054    C            R(M,N) = DISTANCE BETWEEN CENTERS OF VOLUME M
                     AND VOLUME N
0055    C
```

Figure 5.26

Computer program for Example 5.11 ***(Continued).***

```
0056
0057          IMPLICIT COMPLEX (C), INTEGER (K-N)
0058
0059          PARAMETER (MXCLL=600,MXCLL3=1800,MXCL31=1801)
0060          COMPLEX J,TAU,G,E,EI,G1
0061          REAL KO,COSANGLE,MAGSQ,PZ(10)
0062          INTEGER P,Q,X2,X1
0063
0064          DIMENSION G1(MXCLL3,MXCL31),X(3,MXCLL),SIGMA(MXCLL)
0065    C     DIMENSION EPS(MXCLL)
0066          DIMENSION V(MXCLL),E(MXCLL3),EI(MXCLL3),TAU(MXCLL)
0067
0068
0069    C ---------- STATEMENT FUNCTIONS ------------------------- C
0070
0071          R2(M,N) = (X(1,M)-X(1,N))**2+(X(2,M)-X(2,N))
                        **2+(X(3,M)-X(3,N))**2
0072          R(M,N) = SQRT(R2(M,N))
0073          COSANGLE(P,M,N,DIST)= ( X(P,M) - X(P,N) )/DIST
0074          MAGSQ(C) = (CABS(C))**2
0075
0076          J = (0.,1.)
0077          PI = 4.*ATAN(1.)
0078          EPSO = 1.E-9/(36.*PI)
0079          UO = 4.E-7*PI
0080
0081    C ------------- READ AND GENERATE DATA ----------------- C
0082
0083          READ(5,1) NCELL,F
0084          WRITE(6,1) NCELL,F
0085    1     FORMAT(1X,I4,E10.4)
0086
0087          W = 2.*PI*F
0088          KO = W*SQRT(UO*EPSO)
0089
0090          DO 10 N = 1,NCELL
0091             READ(5,15)  V(N),X(1,N),X(2,N),X(3,N),SIGMA(N),EPS
0092             WRITE(6,15) V(N),X(1,N),X(2,N),X(3,N),SIGMA(N),EPS
0093             TAU(N) = SIGMA(N) + J*W*( EPS - EPSO)
0094    10    CONTINUE
0095    15    FORMAT(1X,E10.5,4F10.5,E10.4)
0096
0097          DO 20 I=1,NCELL
0098              READ (5,25) EI(I),EI(I+NCELL),EI(I+2*NCELL)
0099              G1(I,3*NCELL+1) = -EI(I)
0100              G1(I+NCELL,3*NCELL+1)= -EI(I+NCELL)
0101              G1(I+2*NCELL,3*NCELL+1)= -EI(I+2*NCELL)
0102    20        WRITE(6,25) EI(I),EI(I+NCELL),EI(I+2*NCELL)
0103    25    FORMAT(1X,6E12.5)
0104
0105    C -------- GENERATION OF COEFFICIENT MATRIX  G -------------- C
0106
0107    C ------  M CONTROLS THE NUMBER OF VOLUMES
0108    C ------  P
0109    C ------  Q IS DUE TO DOTPRODUCT
0110    C ------  N IS ALSO DUE TO DOTPRODUCT
0111
0112          C = -J*W*UO*KO
0113          C1 = -2.*J*W*UO/(3.*KO**2)
0114          C2 = 3.*J*W*EPSO
0115
0116          DO 50 P = 1,3
0117             DO 50 Q = 1,3
```

Figure 5.26

(Cont.) **Computer program for Example 5.11** ***(Continued).***

```
0118            X1 = (P-1) * NCELL
0119          DO 50 M = 1,NCELL
0120            X1 = X1 + 1
0121            X2 = (Q-1) * NCELL
0122          DO 50 N = 1,NCELL
0123          X2= X2 + 1
0124          IF (M .EQ. N) THEN
0125            AN = ( 3.*V(N)/(4.*PI) )**(1./3.)
0126            C3 = J*KO*AN
0127            C4 = TAU(N)/C2
0128
0129          G1(X1,X2)=DELTA(P,Q)*( C1*TAU(N)*((1.+C3)
                                *EXP(-C3)-1.)-(1.+C4) )
0130
0131          ELSE
0132            DIST = R(M,N)
0133            IF ( DIST .EQ. 0. ) THEN
0134                PRINT *, 'CELLS HAVE SAME CENTER ',M,N
0135            END IF
0136            AMN = KO*DIST
0137            C3 = ( C*TAU(N)*V(N)*EXP(-J*AMN) )/(4.*PI*(AMN**3))
0138            G1(X1,X2) = C3*( (AMN**2 - 1. - J*AMN)*DELTA(P,Q)
0139         &  +COSANGLE(P,M,N,DIST)*COSANGLE(Q,M,N,DIST)
                                    *(3.-AMN**2+3.*J*AMN))
0140          END IF
0141
0142    50    CONTINUE
0143
0144          CALL GAUSSC(MXCLL3,MXCLL3,MXCL31,3*NCELL,3*NCELL+1,G1,E)
0145
0146          WRITE (6,105)
0147    105   FORMAT (1X,'OUTPUT DATA')
0148          WRITE (6,106)
0149    106   FORMAT(1X,'VOLUME  EX   EY  EZ SAR')
0150
0151          DO 110 I = 1,NCELL
0152           SAR = SQRT(MAGSQ(E(I))+MAGSQ(E(I+NCELL))
                                    +MAGSQ(E(I+2*NCELL)) )
0153           SAR = 0.5 * SIGMA(I) * SAR
0154    110   WRITE(6,115) I,E(I),E(I+NCELL),E(I+2*NCELL),SAR
0155    115   FORMAT(I4,7E10.4)
0156
0157          CLOSE (6)
0158          OPEN (6,FILE='PLHEAD.DAT',STATUS='NEW')
0159    C
0160    C NOTE: THERE ARE 8 CELLS ALONG THE Z-DIRECTION
0161    C       SEE FIG. 5.22 DR. SADIKU'S NOTES
0162    C
0163          PZMAX = -1.E-10
0164          DO 140 I=1,8
0165            PZ(I) = MAGSQ(E(I))+MAGSQ(E(I+NCELL))+MAGSQ(E(I+2*NCELL))
0166            PZ(I) = (SIGMA(I)/2.)*PZ(I)
0167    140     PZMAX = AMAX1(PZ(I),PZMAX)
0168
0169    145   FORMAT(1X,'MAXIMUM POWER FOR CELLS
                      ALONG THE Z-AXIS IS ',F10.5)
0170    146   FORMAT(1X,'NORMALIZED POWER ALONG THE Z-AXIS')
0171          WRITE(6,145) PZMAX
0172          WRITE(6,146)
0173          DO 150 I=1,8
0174            PZ(I) = PZ(I)/PZMAX
0175    150   WRITE(6,155) I,PZ(I)
0176    155   FORMAT(1X,I4,F10.6)
```

Figure 5.26

(Cont.) **Computer program for Example 5.11.** ***(Continued).***

```
0177    C
0178    C AVERAGE POWER CALCULATION
0179    C
0180          SPOW = 0.
0181          SVOL = 0.
0182          PMAX = -1.E-10
0183          DO 160 I=1,NCELL
0184             POWER = MAGSQ(E(I))+MAGSQ(E(I+NCELL))
                                 +MAGSQ(E(I+2*NCELL))
0185             POWER = (SIGMA(I)/2.)*POWER*VOL(I)
0186             PMAX = AMAX1(PMAX,POWER)
0187             IF ( ABS( PMAX - POWER ) .LT. 1.E-6) IVPMAX = I
0188             SVOL = SVOL + V(I)
0189    160      SPOW = POWER + SPOW
0190
0191          WRITE(6,165) SPOW
0192          WRITE(6,170) PMAX/V(IVPMAX)
0193    165   FORMAT(1X,'AVERAGE HEATING IN W/M**3 IS ',E12.6)
0194    170   FORMAT(1X,'MAX HEATING IN W/M**3 IS ',E12.6)
0195          CLOSE (6)
0196          STOP
0197          END
```

```
0001    C*************************************************
0002    C   SUBROUTINE FOR GAUSSIAN ELIMINATION
0003    C  THIS SUBROUTINE SOLVES COMPLEX SIMULTANEOUS EQUATIONS
0004    C  USING GAUSS ELIMIANATION WITH PARTIAL PIVOTING
0005    C  THE ORIGINAL PROGRAM WAS WRITTEN TO HANDLE REAL MATRICES
0006    C  AND CAN BE FOUND IN:
0007    C        APPLIED NUMERICAL METHODS FOR DIGITAL COMPUTATION
0008    C        WITH FORTRAN AND CSMP - SECOND EDITION
0009    C        BY M. L. JAMES, G. M. SMITH, AND J. C. WOLFORD
0010    C  A(I,J) = AUGMENTED MATRIX
0011    C  JJ = PIVOT PURPOSES
0012    C  BIG = VALUE THAT MAY BE USED AS PIVOT ELEMENT
0013    C  CMAX = MAXIMUM DIMENSION OF MATRIX CONTAINING RESULTS
0014    C  CMAX1 = MAXIMUM DIMENSION OF AUGMENTED MATRIX
0015    C  M = NUMBER OF COLUMNS IN AUGMENTED MATRIX = N+1
0016    C  N = NUMBER OF SIMULTANEOUS EQUATIONS
0017    C  RMAX = MAXIMUM ROW DIMENSION OF AUGMENTED MATRIX
0018    C  X(N) = RESULT
0019    C
0020
0021          SUBROUTINE GAUSSC(RMAX,CMAX,CMAX1,N,M,A,X)
0022
0023
0024          COMPLEX A,AB,X,TEMP,QUOT,SUM,BIG
0025          INTEGER RMAX,CMAX1,CMAX
0026          DIMENSION A(RMAX,CMAX1),X(CMAX)
0027
0028          L = N-1
0029          DO 12 K = 1,L
0030          JJ = K
0031          BIG = ABS( A(K,K) )
0032          KP1 = K + 1
0033    C
0034    C  SEARCH FOR THE LARGEST POSSIBLE PIVOT ELEMENT
0035    C
0036          DO 7 I = KP1,N
0037          AB = ABS( A(I,K) )
0038          IF ( ABS(BIG - AB) ) 6,7,7
0039    6     BIG = AB
0040          JJ = I
```

Figure 5.26

(Cont.) **Computer program for Example 5.11.** ***(Continued).***

```
0041    7     CONTINUE
0042    C
0043    C DECISION ON NECESSITY OF ROW INTERCHANGE
0044    C
0045          IF (JJ-K) 8,10,8
0046    C
0047    C ROW INTERCHANGE
0048    C
0049    8     DO 9 J=K,M
0050          TEMP = A(JJ,J)
0051          A(JJ,J) = A(K,J)
0052    9     A(K,J) = TEMP
0053    C
0054    C CALCULATION OF ELEMENTS OF NEW MATRIX
0055    C
0056    10    DO 11 I = KP1,N
0057          QUOT = A(I,K)/A(K,K)
0058          DO 11 J=KP1,M
0059    11    A(I,J) = A(I,J) - QUOT*A(K,J)
0060          DO 12 I = KP1,N
0061    12    A(I,K) = (0.,0.)
0062    C
0063    C FIRST STEP IN BACKSUBSTITUTION
0064    C
0065          X(N) = A(N,M)/A(N,N)
0066    C
0067    C REMAINDER IN BACKSUBSTITUTION
0068    C
0069          DO 14 NN=1,L
0070          SUM = (0.,0.)
0071          I = N-NN
0072          IP1 = I + 1
0073          DO 13 J = IP1,N
0074    13    SUM = SUM + A(I,J)*X(J)
0075    14    X(I) = (A(I,M)-SUM)/A(I,I)
0076          RETURN
0077          END

0001    C**********************************
0002    C   SUBPROGRAM DELTA
0003          FUNCTION DELTA(M,N)
0004
0005          IF (M .EQ. N) THEN
0006                DELTA = 1.
0007          ELSE
0008                DELTA = 0.
0009          END IF
0010          RETURN
0011          END
```

Figure 5.26
(Cont.) **Computer program for Example 5.11.**

solution of the matrix equation is usually carried out via inversion, elimination, or iterative techniques. Although MOM is commonly applied to open problems such as those involving radiation and scattering, it has been successfully applied to closed problems such as waveguides and cavities.

Needless to say, the issues on MOM covered in this chapter have been carefully selected. We have only attempted to cover the background and reference material upon which the reader can easily build. The interested reader is referred to the literature for more in-depth treatment of each subject. General concepts on MOM

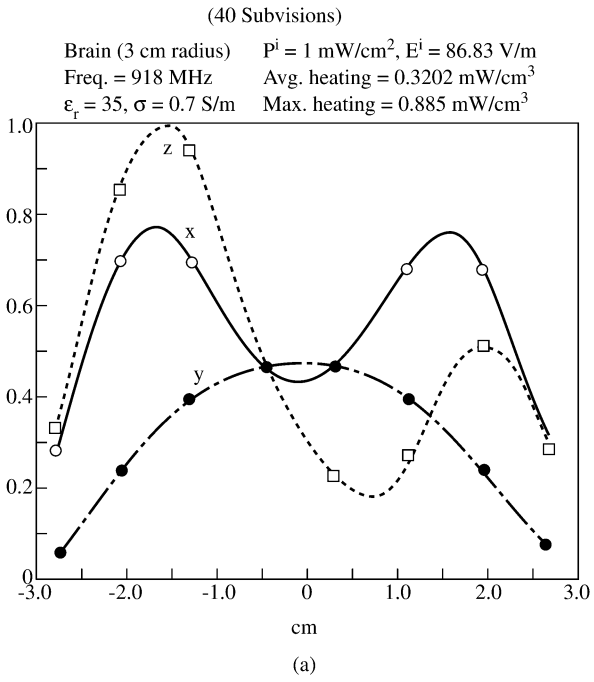

Figure 5.27

Distributions of heating along the x-, y-, and z-axis of a spherical model of an animal brain [57]: (a) MOM solution, (b) exact solution.

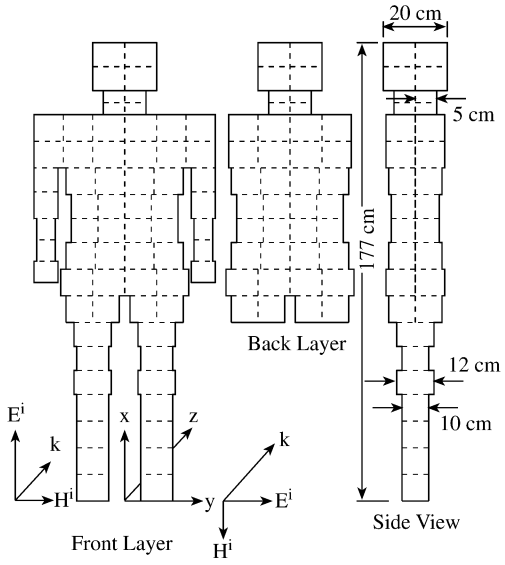

Figure 5.28

Geometry and dimensions of a model of typical human body of height 1.77 m [52].

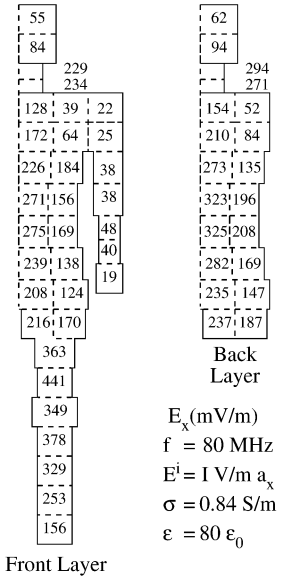

Figure 5.29
Induced E_x (in mV/m) at the center of each cell due to E_x^i of 1 V/m [52].

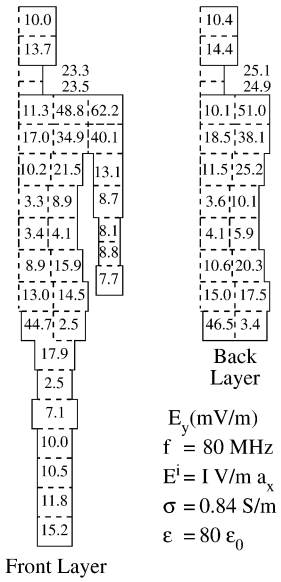

Figure 5.30
Induced E_y (in mV/m) at the center of each cell due to E_x^i of 1 V/m [52].

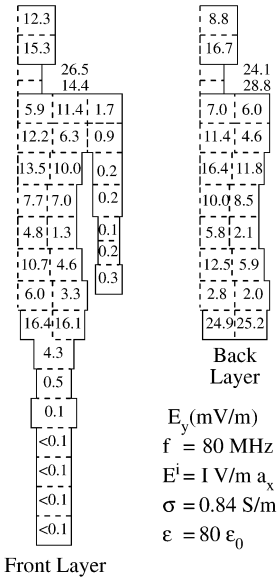

Figure 5.31
Induced E_z (in mV/m) at the center of each cell due to E_x^i of 1 V/m [52].

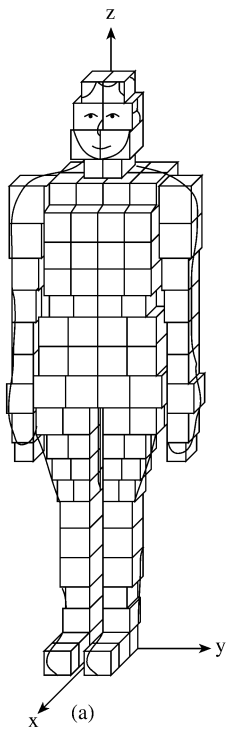

Figure 5.32
A more realistic block model of the human body [59]: (a) In three dimensions *(Continued)*.

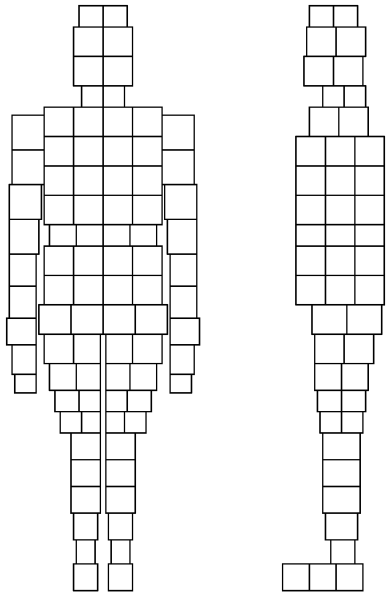

(b)

Figure 5.32
(Cont.) **A more realistic block model of the human body [59]: (b) Front and side views.**

are covered in [10] and [62]. Clear and elementary discussions on IEs and Green's functions may be found in [12], [28]–[30], [62]–[65]. For further study on the theory of the method of moments, one should see [6, 9, 10, 28, 40].

The number of problems that can be treated by MOM is endless, and the examples given in this chapter just scratch the surface. The following problems represent typical EM-related application areas:

- electrostatic problems [31], [66]–[69]
- wire antennas and scatterers [34, 37, 42, 44, 70, 78]
- scattering and radiation from bodies of revolution [79, 80]
- scattering and radiation from bodies of arbitrary shapes [38, 81, 82]
- transmission lines [18]–[20], [23, 24], [83]–[86]
- aperture problems [87]–[89]
- biomagnetic problems [47]–[52], [90]–[92].

A number of user-oriented computer programs have evolved over the years to solve electromagnetic integral equations by the method of moments. These codes

can handle radiation and scattering problems in both the frequency and time domains. Reviews of the codes may be found in [7, 38, 93]. The most popular of these codes is the Numerical Electromagnetic Code (NEC) developed at the Lawrence Livermore National Laboratory [7, 94]. NEC is a frequency domain antenna modeling FORTRAN code applying the MOM to IEs for wire and surface structures. Its most notable features are probably that it is user oriented, includes documentation, and is available; for these reasons, it is being used in public and private institutions. A compact version of NEC is the mini-numerical electromagnetic code (MININEC) [95], which is intended to be used in personal computers.

It is important that we recognize the fact that MOM is limited in application to radiation and scattering from bodies that are electrically large. The size of the scatterer or radiator must be of the order λ^3. This is because the cost of storing, inverting, and computing matrix elements becomes prohibitively large. At high frequencies, asymptotic techniques such as the geometrical theory of diffraction (GTD) are usually employed to derive approximate but accurate solutions [46, 96, 97].

References

[1] L.V. Kantorovich and V.I. Krylov, *Approximate Methods of Higher Analysis* (translated from Russian by C.D. Benster). New York: John Wiley, 1964.

[2] Y.U. Vorobev, *Method of Moments in Applied Mathematics* (translated from Russian by Seckler). New York: Gordon & Breach, 1965.

[3] R.F. Harrington, *Field Computation by Moment Methods*. Malabar, FL: Krieger, 1968.

[4] B.J. Strait, *Applications of the Method of Moments to Electromagnetics*. St. Cloud, FL: SCEEE Press, 1980.

[5] R.F. Harrington, "Origin and development of the method moments for field computation," in E.K. Miller et al., *Computational Electromagnetics*. New York: IEEE Press, 1992, pp. 43–47.

[6] J.H. Richmond, "Digital computer solutions of the rigorous equations for scattering problems," *Proc. IEEE,* vol. 53, Aug. 1965, pp. 796–804.

[7] R.F. Harrington, "Matrix methods for field problems," *Proc. IEEE,* vol. 55, no. 2, Feb. 1967, pp. 136–149.

[8] M.M. Ney, "Method of moments as applied to electromagnetics problems," *IEEE Trans. Micro. Theo. Tech.,* vol. MTT-33, no. 10, Oct. 1985, pp. 972–980.

[9] A.T. Adams, "An introduction to the method of moments," Syracuse Univ., *Report RADC* TR-73-217, vol. 1, Aug. 1974.

[10] M.D. Greenberg, *Application of Green Functions in Science and Engineering*. Englewood Cliffs, NJ: Prentice-Hall, 1971.

[11] A. Ishimaru, *Electromagnetic Wave Propagation, Radiation, and Scattering*. Englewood Cliffs, NJ: Prentice-Hall, 1991, pp. 121–148.

[12] P.M. Morse and H. Feshbach, *Methods of Theoretical Physics*. New York: McGraw-Hill, Part I, Chap. 7, 1953, pp. 791–895.

[13] T. Myint-U, *Partial Differential Equations of Mathematical Physics*. New York: North-Holland, 1980, 2nd ed., Chap. 10, pp. 282–305.

[14] R.F. Harrington, *Time-harmonic Electromagnetic Fields*. New York: McGraw-Hill, 1961, p. 232.

[15] I.V. Bewley, *Two-dimensional Fields in Electrical Engineering*. New York: Dover Publ., 1963, pp. 151–166.

[16] K.C. Gupta, et al., *Computer-aided Design of Microwave Circuits*. Dedham: Artech House, 1981, pp. 237–261.

[17] T. Itoh (ed.), *Numerical Techniques for Microwaves and Millimeterwave Passive Structures*. New York: John Wiley & Sons, 1989, pp. 221–250.

[18] D.W. Kammler, "Calculation of characteristic admittance and coupling coefficients for strip transmission lines," *IEEE Trans. Micro. Tech.,* vol. MTT-16, no. 11, Nov. 1968, pp. 925–937.

[19] Y.M. Hill, et al., "A general method for obtaining impedance and coupling characteristics of practical microstrip and triplate transmission line configurations," *IBM J. Res. Dev.,* vol. 13, May 1969, pp. 314–322.

[20] W.T. Weeks, "Calculation of coefficients of capacitance of multiconductor transmission lines in the presence of a dielectric interface," *IEEE Trans. Micro. Theo. Tech.,* vol. MTT-18, no. 1, Jan. 1970, pp. 35–43.

[21] R. Chadha and K.C. Gupta, "Green's functions for triangular segments in planar microwave circuits," *IEEE Trans. Micro. Theo. Tech.,* vol. MTT-28, no. 10, Oct. 1980, pp. 1139–1143.

[22] R. Terras and R. Swanson, "Image methods for constructing Green's functions and eigenfunctions for domains with plane boundaries," *J. Math. Phys.,* vol. 21, no. 8, Aug. 1980, pp. 2140–2153.

[23] E. Yamashita and K. Atsuki, "Stripline with rectangular outer conductor and three dielectric layers," *IEEE Trans. Micro. Theo. Tech.,* vol. MTT-18, no. 5, May 1970, pp. 238–244.

[24] R. Crampagne, et al., " A simple method for determining the Green's function for a large class of MIC lines having multilayered dielectric structures," *IEEE Trans. Micro. Theo. Tech.,* vol. MTT-26, no. 2, Feb. 1978, pp. 82–87.

[25] R. Chadha and K.C. Gupta, "Green's functions for circular sectors, annular rings, and annular sectors in planar microwave circuits," *IEEE Trans. Micro. Theo. Tech.,* vol. MTT-29, no. 1, Jan. 1981, pp. 68–71.

[26] P.H. Pathak, "On the eigenfunction expansion of electromagnetic dydadic Green's functions," *IEEE Trans. Ant. Prog.,* vol. AP-31, no. 6, Nov. 1983.

[27] R.F. Harrington and J.R. Mautz, "Green's functions for surfaces of revolution," *Radio Sci.,* vol. 7, no. 5, May 1972, pp. 603–611.

[28] C.A. Balanis, *Advanced Engineering Electromagnetics*. New York: John Wiley, 1989, pp. 670–742, 851–916.

[29] E. Butkov, *Mathematical Physics*. New York: Addison-Wesley, 1968, pp. 503–552.

[30] J.D. Jackson, *Classical Electrodynamics,* 2nd ed., New York: John Wiley, 1975, pp. 119–135.

[31] L.L. Tsai and C.E. Smith, "Moment Methods in electromagnetics undergraduates," *IEEE Trans. Educ.,* vol. E-21, no. 1, Feb. 1978, pp. 14–22.

[32] P.P. Silvester and R.L. Ferrari, *Finite Elements for Electrical Engineers*. Cambridge, UK: Cambridge University Press, 1983, pp. 103–105.

[33] H.A. Wheeler, "Transmission-line properties of parallel strips separated by a dielectric sheet," *IEEE Trans. Micro. Theo. Tech.,* vol. MTT-13, Mar. 1965, pp. 172–185.

[34] J.H. Richmond, "Scattering by an arbitrary array of parallel wires," *IEEE Trans. Micro. Theo. Tech.,* vol. MTT-13, no. 4, July 1965, pp. 408–412.

[35] B.D. Popovic, et al., *Analysis and Synthesis of Wire Antennas*. Chichester, UK: Research Studies Press, 1982, pp. 3–21.

[36] E. Hallen, "Theoretical investigations into the transmitting and receiving qualities of antennae," *Nova Acta Regiae Soc. Sci. Upsaliensis,* Ser. IV, no. 11, 1938, pp. 1–44.

[37] K.K. Mei, " On the integral equations of thin wire antennas," *IEEE Trans. Ant. Prog.,* vol. AP-13, 1965, pp. 374–378.

[38] J. Moore and P. Pizer (eds.), *Moment Methods in Electromagnetics: Techniques and Applications*. Letchworth, UK: Research Studies Press, 1984.

[39] H.C. Pocklington, " Electrical oscillations in wire," *Cambridge Phil. Soc. Proc.,* vol. 9, 1897, pp. 324–332.

[40] R. Mittra (ed.), *Computer Techniques for Electromagnetics*. Oxford: Pergamon Press, 1973, pp. 7–95.

[41] C.A. Balanis, *Antenna Theory: Analysis and Design*. New York: Harper & Row, 1982, pp. 283–321.

[42] C.M. Butler and D.R. Wilton, "Analysis of various numerical techniques applied to thin-wire scatterers," *IEEE Trans. Ant. Prog.,* vol. AP-23, no. 4, July 1975, pp. 524–540. Also in [46, pp. 46–52].

[43] T.K. Sarkar, "A note on the choice of weighting functions in the method of moments," *IEEE Trans. Ant. Prog.,* vol. AP-33, no. 4, April 1985, pp. 436–441.

[44] F.M. Landstorfer and R.F. Sacher, *Optimisation of Wire Antenna.* Letchworth, UK: Research Studies Press, 1985, pp. 18–33.

[45] K.A. Michalski and C.M. Butler, "An efficient technique for solving the wire integral equation with non-uniform sampling," *Conf. Proc. IEEE Southeastcon.,* April 1983, pp. 507–510.

[46] R.F. Harrington, et al. (eds.), *Lectures on Computational Methods in Electromagnetics.* St. Cloud, FL: SCEEE Press, 1981.

[47] R. Kastner and R. Mittra, "A new stacked two-dimensional spectral iterative technique (SIT) for analyzing microwave power deposition in biological media," *IEEE Trans. Micro. Theo. Tech.,* vol. MTT-31, no. 1, Nov. 1983, pp. 898–904.

[48] P.W. Barber, "Electromagnetic power deposition in prolate spheroidal models of man and animals at resonance," *IEEE Trans. Biomed. Engr.,* vol. BME-24, no. 6, Nov. 1977, pp. 513–521.

[49] J.M. Osepchuk (ed.), *Biological Effects of Electromagnetic Radiation.* New York: IEEE Press, 1983.

[50] R.J. Spiegel, "A review of numerical models for predicting the energy deposition and resultant thermal response of humans exposed to electromagnetic fields," *IEEE Trans. Micro. Theo. Tech.,* vol. MTT-32, no. 8, Aug. 1984, pp. 730–746.

[51] D.E. Livesay and K.M. Chen, "Electromagnetic fields induced inside arbitrary shaped biological bodies," *IEEE Trans. Micro. Theo. Tech.,* vol. MTT-22, no. 12, Dec. 1974, pp. 1273–1280.

[52] J.A. Kong (ed.), *Research Topics in Electromagnetic Theory.* New York: John Wiley, 1981, pp. 290–355.

[53] C.T. Tai, *Dyadic Green's Functions in Electromagnetic Theory.* Scranton, PA: Intex Educational Pub., 1971, pp. 46–54.

[54] J. Van Bladel, "Some remarks on Green's dyadic infinite space," *IRE Trans. Ant. Prog.,* vol. AP-9, Nov. 1961, pp. 563–566.

[55] B.S. Guru and K.M. Chen, "A computer program for calculating the induced EM field inside an irradiated body," Dept. of Electrical Engineering and System Science, Michigan State Univ., East Lansing, MI, 48824, 1976.

[56] K.M. Chen and B.S. Guru,"Internal EM field and absorbed power density in human torsos induced by 1-500 MHz EM waves," *IEEE Micro. Theo. Tech.,* vol. MTT-25, no. 9, Sept. 1977, pp. 746–756.

[57] R. Rukspollmuang and K.M. Chen, "Heating of spherical versus realistic models of human and infrahuman heads by electromagnetic waves," *Radio Sci.,* vol. 14, no. 6S, Nov.-Dec., 1979, pp. 51–62.

[58] R. Jongakiem, "Electromagnetic absorption in biological bodies," *M. S. Thesis,* Dept. of Electrical and Computer Engr., Florida Atlantic Univ., Boca Raton, Aug. 1988.

[59] O.P. Gandhi, "Electromagnetic absorption in an inhomogeneous model of man for realistic exposure conditions," *Bioelectromagnetics,* vol. 3, 1982, pp. 81–90.

[60] O.P. Gandhi, et al., "Part-body and multibody effects on absorption of radiofrequency electromagnetic energy by animals and by models of man," *Radio Sci.,* vol. 14, no. 6S, Nov.-Dec., 1979, pp. 15–21.

[61] M.J. Hagmann, O.P. Gandhi, and C.H. Durney, "Numerical calculation of electromagnetic energy deposition for a realistic model of man," *IEEE Trans. Micro. Theo. Tech.,* vol. MTT-27, no. 9, Sept. 1979, pp. 804–809.

[62] J.J. Wang, "Generalized moment methods in electromagnetics," *IEEE Proc.,* vol. 137, Pt. H, no. 2, April 1990, pp. 127–132.

[63] G. Goertzel and N. Tralli, *Some Mathematical Methods of Physics*. New York: McGraw-Hill, 1960.

[64] W.V. Lovitt, *Linear Integral Equations*. New York: Dover Publ., 1950.

[65] C.D. Green, *Integral Equation Methods*. New York: Barnes & Nobles, 1969.

[66] R.F. Harrington, et al., "Computation of Laplacian potentials by an equivalent source method," *Proc. IEEE,* vol. 116, no. 10, Oct. 1969, pp. 1715–1720.

[67] J.R. Mautz and R.F. Harrington, "Computation of rotationally symmetric Laplacian," *Proc. IEEE,* vol. 117, no. 4, April 1970, pp. 850–852.

[68] S.M. Rao, et al., "A simple numerical solution procedure for static problems involving arbitrary-shaped surfaces," *IEEE Trans. Ant. Prog.,* vol. AP-27, no. 5, Sept. 1979, pp. 604–608.

[69] K. Adamiak, "Application of integral equations for solving inverse problems in stationary electromagnetic fields," *Int. J. Num. Meth. Engr.,* vol. 21, 1985, pp. 1447–1485.

[70] A.W. Glisson, "An integral equation for electromagnetic scattering from homogeneous dielectric bodies," *IEEE Trans. Ant. Prog.,* vol. AP-33, no. 2, Sept. 1984, pp. 172–175.

[71] E. Max, "Integral equation for scattering by a dielectric," *IEEE Trans. Ant. Prog.,* vol. AP-32, no. 2, Feb. 1984, pp. 166–172.

[72] A.T. Adams, et al., "Near fields of wire antennas by matrix methods," *IEEE Trans. Ant. Prog.,* vol. AP-21, no. 5, Sept. 1973, pp. 602–610.

[73] R.F. Harrington and J.R. Mautz, "Electromagnetic behavior of circular wire loops with arbitrary excitation and loading," *Proc. IEEE,* vol. 115, Jan. 1969, pp. 68–77.

[74] S.A. Adekola and O.U. Okereke, "Analysis of a circular loop antenna using moment methods," *Int. J. Elect.,* vol. 66, no. 5, 1989, pp. 821–834.

[75] E.K. Miller, et al., "Computer evaluation of large low-frequency antennas," *IEEE Trans. Ant. Prog.,* vol. AP-21, no. 3, May 1973, pp. 386–389.

[76] K.S.H. Lee, et al., "Limitations of wire-grid modeling of a closed surface," *IEEE Trans. Elect. Comp.,* vol. EMC-18, no. 3, Aug. 1976, pp. 123–129.

[77] E.H. Newman and D.M. Pozar, "Considerations for efficient wire/surface modeling," *IEEE Trans. Ant. Prog.,* vol. AP-28, no. 1, Jan. 1980, pp. 121–125.

[78] J. Perini and D.J. Buchanan, "Assessment of MOM techniques for shipboard applications," *IEEE Trans. Elect. Comp.,* vol. EMC-24, no. 1, Feb. 1982, pp. 32–39.

[79] J.R. Mautz and R.F. Harrington, "Radiation and scattering from bodies of revolution," *Appl. Sci. Res.,* vol. 20, June 1969, pp. 405–435.

[80] A.W. Glisson and C.M. Butler, "Analysis of a wire antenna in the presence of a body of revolution," *IEEE Trans. Ant. Prog.,* vol. AP-28, Sept. 1980, pp. 604–609.

[81] J.H. Richmond, "A wire-grid model for scattering by conducting bodies," *IEEE Trans. Ant. Prog.,* vol. AP-14, Nov. 1966, pp. 782–786.

[82] S.M. Rao, et al., "Electromagnetic scattering by surfaces of arbitrary shape," *IEEE Trans. Ant. Prog.,* vol. AP-30, May 1966, pp. 409–418.

[83] A. Farrar and A.T. Adams, " Matrix methods for microstrip three-dimensional problems," *IEEE Trans. Micro. Theo. Tech.,* vol. MTT-20, no. 8, Aug. 1972, pp. 497–505.

[84] A. Farrar and A.T. Adams, "Computation of propagation constants for the fundamental and higher-order modes in microstrip," *IEEE Trans. Micro. Theo. Tech.,* vol. MTT-24, no. 7, July 1972, pp. 456–460.

[85] A. Farrar and A.T. Adams, "Characteristic impedance of microstrip by the method of moments," *IEEE Trans. Micro. Theo. Tech.,* vol. MTT-18, no. 1, Jan 1970, pp. 68, 69.

[86] A. Farrar and A.T. Adams, "Computation of lumped microstrip capacitance by matrix methods—rectangular sections and end effects," *IEEE Trans. Micro. Theo. Tech.,* vol. MTT-19, no. 5, May 1971, pp. 495, 496.

[87] R.F. Harrington and J.R. Mautz, "A generalized network formulation for aperture problems," *IEEE Trans. Ant. Prog.,* vol. AP-24, Nov. 1976, pp. 870–873.

[88] R.H. Harrington and D.T. Auckland, "Electromagnetic transmission through narrow slots in thick conducting screens," *IEEE Trans. Ant. Prog.,* vol. AP-28, Sept. 1980, pp. 616–622.

[89] C.M. Butler and K.R. Umashankar, "Electromagnetic excitation of a scatterer coupled to an aperture in a conducting screen," *Proc. IEEE,* vol. 127, Pt. H, June 1980, pp. 161–169.

[90] Special issue on electromagnetic wave interactions with biological systems, *IEEE Trans. Micro. Theo. Tech.,* vol. MTT-32, no. 8, Aug. 1984.

[91] Special issue on effects of electromagnetic radiation, *IEEE Engr. Med. Biol. Mag.,* March 1987.

[92] Helsinki symposium on biological effects of electromagnetic radiation, *Radio Sci.,* vol. 17, no. 5S, Sept.-Oct. 1982.

[93] R.M. Bevensee, "Computer codes for EMP interaction and coupling," *IEEE Trans. Ant. Prog.,* vol. AP-26, no. 1, Jan. 1978, pp. 156–165.

[94] G.J. Burke and A.J. Poggio, *Numerical Electromagnetic Code (NEC)—Method of Moments*. Lawrence Livermore National Lab., Jan. 1981.

[95] J.W. Rockway, et al., *The MININEC System: Microcomputer Analysis of Wire Antennas*. Norwood, MA: Artech House, 1988.

[96] R. Mittra (ed.), *Numerical and Asymptotic Techniques in Electromagnetics*. New York: Springer-Verlag, 1975.

[97] G.L. James, *Geometrical Theory of Diffraction for Electromagnetic Waves,* 3rd ed. London: Peregrinus, 1986.

Problems

5.1 Classify the following integral equations and show that they have the stated solutions:

(a) $\Phi(x) = \dfrac{5x}{b} + \dfrac{1}{2}\displaystyle\int_0^1 xt\Phi(t)\,dt$ [solution $\Phi(x) = x$],

(b) $\Phi(x) = \cos x - \sin x + 2\displaystyle\int_0^x \sin(x-t)\Phi(t)\,dt$ [solution $\Phi(x) = e^{-x}$],

(c) $\Phi(x) = -\cosh x + \lambda\displaystyle\int_{-1}^1 \cosh(x+t)\Phi(t)\,dt$ [solution $\Phi(x) = \dfrac{\cosh x}{\frac{\lambda}{2}\sinh 2 + \lambda - 1}$]

5.2 Solve the following Volterra integral equations:

(a) $\Phi(x) = 5 + 2\int_0^x t\Phi(t)\,dt$,

(b) $\Phi(x) = x + \int_0^x (t - x)\Phi(t)\,dt$

5.3 Find the integral equation corresponding to each of the following differential equations:

(a) $y'' = -y,\ y(0) = 0,\ y'(1) = 1$,

(b) $y'' + y = \cos x,\ y(0) = 0,\ y'(0) = 1$

5.4 Construct the Green's function for the differential equation

$$G_{xx} + k^2 G = -\delta\left(x - x'\right), \quad 0 < x < a$$

subject to $G(0) = G(a) = 0$

5.5 Show that

$$G\left(x, z; x', z'\right) = \frac{j}{a}\sum_{n=1}^{\infty} \frac{\sin(n\pi x/a)\sin\left(n\pi x'/a\right)}{k_n} e^{jk_n(z-z')},$$

where $k_n^2 = k^2 - (n\pi/a)^2$ is the Green's function for Helmholtz's equation.

5.6 Derive the Green's function for

$$\nabla^2\Phi = f, \quad 0 < x, y < 1$$

subject to zero boundary conditions.

5.7 Find the Green's function satisfying

$$G_{xx} + G_{yy} + 2G_x = \delta\left(x - x'\right)\delta\left(y - y'\right), \quad 0 < x < a, 0 < y < b$$

and

$$G(0, y) = G(a, y) = G(x, 0) = G(x, b) = 0$$

5.8 (a) Verify by Fourier expansion that Eqs. (5.79) and (5.80) in Example 5.5 are equivalent.

(b) Show that another form of expressing Eq. (5.79) is

$$G\left(x, y; x', y'\right) = \begin{cases} -\dfrac{2}{\pi}\displaystyle\sum_{m=1}^{\infty} \sinh\frac{m\pi\left(b - y'\right)}{a} \sin\frac{m\pi y}{a} \frac{m\pi x}{a} \frac{m\pi x'}{a}, & y < y' \\ -\dfrac{2}{\pi}\displaystyle\sum_{m=1}^{\infty} \sinh\frac{m\pi y'}{a} \sin\frac{m\pi(b - y)}{a} \frac{m\pi x}{a} \frac{m\pi x'}{a}, & y > y' \end{cases}$$

5.9 The two-dimensional delta function expressed in cylindrical coordinates reads

$$\delta\left(\rho-\rho'\right)=\frac{1}{\rho}\delta\left(\rho-\rho'\right)\delta\left(\phi-\phi'\right)$$

Obtain the Green's function for the potential problem

$$\nabla^2 G=\frac{1}{\rho}\delta\left(\rho-\rho'\right)\delta\left(\phi-\phi'\right)$$

with the region defined in Fig. 5.33. Assume homogeneous Dirichlet boundary conditions.

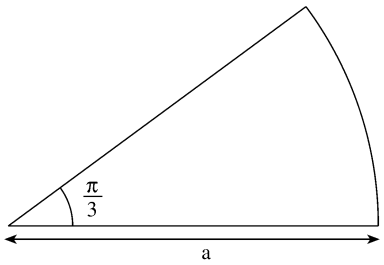

Figure 5.33
For Problem 5.9.

5.10 Consider the transmission line with cross section as shown in Fig. 5.34. In a TEM wave approximation, the potential distribution satisfies Poisson's equation

$$\nabla^2 V=-\frac{\rho_s}{\epsilon}$$

subject to the following continuity and boundary conditions:

$$\begin{aligned}
\frac{\partial}{\partial x}V\left(x,h_1-0\right)&=\frac{\partial}{\partial x}V\left(x,h_1+0\right)\\
\frac{\partial}{\partial x}V\left(x,h_1+h_2-0\right)&=\frac{\partial}{\partial x}V\left(x,h_1+h_2+0\right)\\
\epsilon_1\frac{\partial}{\partial y}V\left(x,h_1-0\right)&=\epsilon_2\frac{\partial}{\partial y}V\left(x,h_1+0\right)\\
\epsilon_2\frac{\partial}{\partial y}V\left(x,h_1+h_2-0\right)&=\epsilon_3\frac{\partial}{\partial y}V\left(x,h_1+h_2+0\right)-\rho_s\left(x,h_1+h_2\right)\\
V(0,y)=V(a,y)&=V(x,0)=V(x,b)=0
\end{aligned}$$

Using series expansion method, evaluate the Green's function at $y=h_1+h_2$, i.e., $G(x,y;x',h_1+h_2)$.

5.11 Show that the free-space Green's function for $L=\nabla^2+k^2$ in two-dimensional space is $-\frac{j}{4}H_0^{(1)}(k\rho)$.

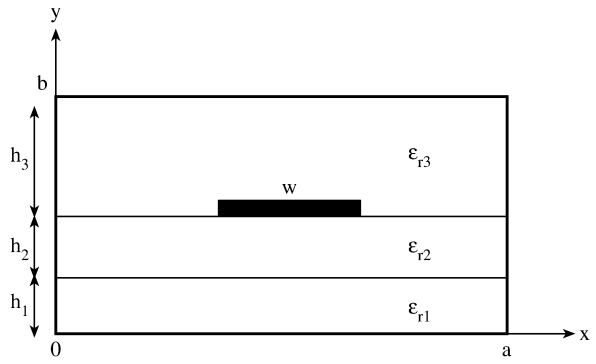

Figure 5.34
For Problem 5.10.

5.12 The spherical Green's function $h_0^{(2)}(|\mathbf{r}-\mathbf{r}'|)$ can be expanded in terms of spherical Bessel functions and Legendre polynomials. Show that

$$h_0^{(2)}\left(\left|\mathbf{r}-\mathbf{r}'\right|\right) =$$

$$\frac{j\exp\left(-j\left|\mathbf{r}-\mathbf{r}'\right|\right)}{(|\mathbf{r}-\mathbf{r}'|)} = \begin{cases} \displaystyle\sum_{n=0}^{\infty}(2n+1)h_n^2\left(\mathbf{r}'\right)j_n(r)P_n(\cos\alpha), & r < r' \\ \displaystyle\sum_{n=0}^{\infty}(2n+1)h_n^2(\mathbf{r})j_n\left(r'\right)P_n(\cos\alpha), & r > r' \end{cases}$$

where $\cos\alpha = \cos\theta\cos\theta' + \sin\theta\sin\theta'\cos(\phi-\phi')$. From this, derive the plane wave expansion

$$e^{-j\,\mathbf{k}\cdot\mathbf{r}} = \sum_{n=0}^{\infty}(-j)^n(2n+1)\,j_n(kr)\,P_n(\cos\alpha)$$

5.13 Given the kernel

$$K(x,y) = \begin{cases} (1-x)y, & 0 \le y \le x \le 1 \\ (1-y)x, & 0 \le x \le y \le 1 \end{cases}$$

Show that

$$K(x,y) = 2\sum_{n=1}^{\infty}\frac{\sin n\pi x\sin n\pi y}{n^2\pi^2}$$

and that

$$\frac{\pi^2}{4} = \sum_{n=1}^{\infty}\frac{1}{n^2}$$

5.14 Derive the closed form solution for Poisson's equation

$$\nabla^2 V = g$$

in the quarter-plane shown in Fig. 5.35 with

$$V = f(x),\ y = 0, \quad \frac{\partial V}{\partial x} = h(y),\ x = 0$$

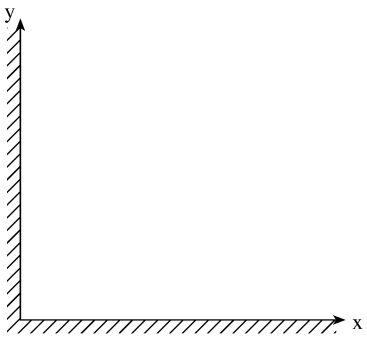

Figure 5.35
For Problem 5.14.

5.15 Consider the cross section of a microstrip transmission line shown in Fig. 5.36. Let $G_{ij}\rho_j$ be the potential at the field point i on the center conductor due to the charge on subsection j. (It is assumed that the charge is concentrated in the filament along the center of the subsection.) G_{ij} is the Green's function for this problem and is given by

$$G_{ij} = \frac{1}{4\pi\epsilon_r}\sum_{n=1}^{\infty}\left[k^{2(n-1)}\ln\frac{A_{ij}^2+(4n-2)^2}{A_{ij}^2+(4n-4)^2} + k^{2n-1}\ln\frac{A_{ij}^2+(4n-2)^2}{A_{ij}^2+(4n)^2}\right]$$

where

$$A_{ij} = \frac{\Delta}{H}|2(i-1)-2(j-1)-1|, \quad k = \frac{\epsilon_r - 1}{\epsilon_r + 1},$$

$\Delta = W/N$, and N is the number of equal subsections into which the center conductor is divided. By setting the potential equal to unity on the center conductor, one can find

$$C = \sum_{j=1}^{\infty}\rho_j \quad \text{(farads/m)}$$

and

$$Z_o = \frac{1}{c\sqrt{C_o C}}$$

where $c = 3 \times 10^8$ m/s and C_o is the capacitance per unit length for an air-filled transmission line (i.e., set $k = 1$ in G_{ij}). Find Z_o for $N = 30$ and:

(a) $\epsilon_r = 6.0, \quad W = 4$ cm, $\quad H = 4$ cm

(b) $\epsilon_r = 16.0, \quad W = 8$ cm, $\quad H = 4$ cm.

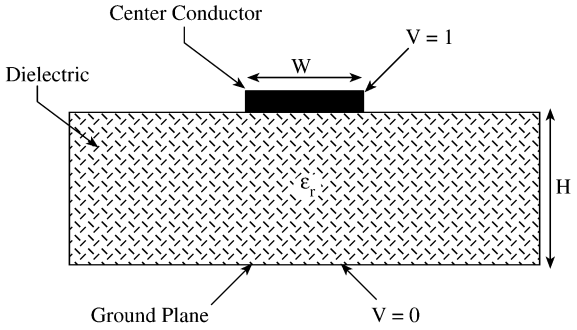

Figure 5.36
For Problem 5.15.

5.16 A rectangular section of microstrip transmission line of length L, width W, and height H above the ground plane is shown in Fig. 5.37. The section is subdivided into N subsections. A typical subsection ΔS_j, of sides Δx_j and Δy_j, is assumed to bear a uniform surface charge density ρ_j. The potential V_i at ΔS_i due to a uniform charge density ρ_j on $\Delta S_j (j = 1, 2, \ldots, N)$ is

$$V_i = \sum_{j=1}^{N} G_{ij} \rho_j$$

where

$$
\begin{aligned}
G_{ij} = & \sum_{n=1}^{\infty} \frac{k^{n-1}(-1)^{n+1}}{2\pi\epsilon_o\,(\epsilon_r+1)} \\
& \Bigg[(x_j - x_i) \ln \frac{(y_j - y_i) + \sqrt{(x_j - x_i)^2 + (y_j - y_i)^2 + (2n-2)^2 H^2}}{(y_j + \Delta y_j - y_i) + \sqrt{(x_j - x_i)^2 + (y_j + \Delta y_j - y_i)^2 + (2n-2)^2 H^2}} \\
& + (x_j + \Delta x_j - x_i) \\
& \quad \ln \frac{(y_j + \Delta y_j - y_i) + \sqrt{(x_j + \Delta x_j - x_i)^2 + (y_j + \Delta y_j - y_i)^2 + (2n-2)^2 H^2}}{(y_j - y_i) + \sqrt{(x_j + \Delta x_j - x_i)^2 + (y_j - y_i)^2 + (2n-2)^2 H^2}} \\
& + (y_j - y_i) \ln \frac{(x_j - x_i) + \sqrt{(x_j - x_i)^2 + (y_j - y_i)^2 + (2n-2)^2 H^2}}{(x_j + \Delta x_j - x_i) + \sqrt{(x_j + \Delta x_j - x_i)^2 + (y_j - y_i)^2 + (2n-2)^2 H^2}} \\
& + (y_j + \Delta y_j - y_i) \\
& \quad \ln \frac{(x_j + \Delta x_j - x_i) + \sqrt{(x_j + \Delta x_j - x_i)^2 + (y_j + \Delta y_j - y_i)^2 + (2n-2)^2 H^2}}{(x_j - x_i) + \sqrt{(x_j - x_i)^2 + (y_j + \Delta y_j - y_i)^2 + (2n-2)^2 H^2}} \\
& - (2n-2) H \tan^{-1} \frac{(x_j - x_i)(y_j - y_i)}{(2n-2) H \sqrt{(x_j - x_i)^2 + (y_j - y_i)^2 + (2n-2)^2 H^2}} \\
& - (2n-2) \\
& \quad H \tan^{-1} \frac{(x_j + \Delta x_j - x_i)(y_j + \Delta y_j - y_i)}{(2n-2) H \sqrt{(x_j + \Delta x_j - x_i)^2 + (y_j + \Delta y_j - y_i)^2 + (2n-2)^2 H^2}} \\
& + (2n-2) H \tan^{-1} \frac{(x_j - x_i)(y_j + \Delta y_j - y_i)}{(2n-2) H \sqrt{(x_j - x_i)^2 + (y_j + \Delta y_j - y_i)^2 + (2n-2)^2 H^2}} \\
& + (2n-2) H \tan^{-1} \frac{(x_j + \Delta x_j - x_i)(y_j - y_i)}{(2n-2) H \sqrt{(x_j + \Delta x_j - x_i)^2 + (y_j - y_i)^2 + (2n-2)^2 H^2}} \Bigg]
\end{aligned}
$$

and $k = \dfrac{\epsilon_r - 1}{\epsilon_r + 1}$. If the ground plane is assumed to be at zero potential while the conducting strip at 1 V potential, we can find

$$C = \sum_{j=1}^{N} \rho_j$$

Find C for:

(a) $\epsilon_r = 9.6, \quad W = L = H = 2$ cm,

(b) $\epsilon_r = 9.6, \quad W = H = 2$ cm , $\quad L = 1$ cm.

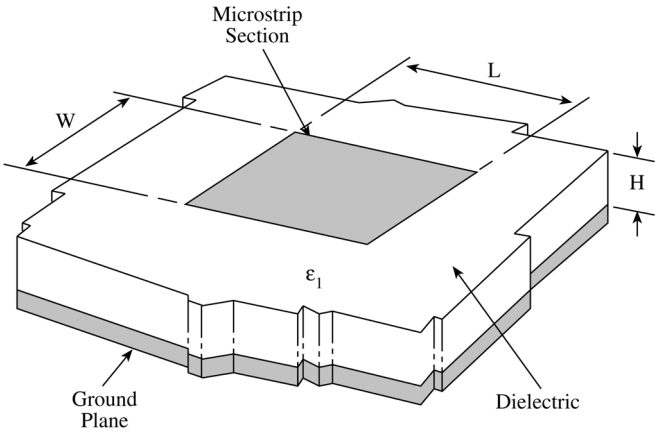

Figure 5.37
For Problem 5.16.

5.17 For a conducting elliptic cylinder with cross section in Fig. 5.38(a), write a program to determine the scattering cross section $\sigma(\phi_i, \phi)$ due to a plane TM wave. Consider $\phi = 0°, 10°, \cdots, 180°$ and cases $\phi_i = 0°, 30°$, and $90°$. Plot $\sigma(\phi_i, \phi)$ against ϕ for each ϕ_i. Take $\lambda = 1\text{m}$, $2a = \lambda/2$, $2b = \lambda$, $N = 18$.

Hint: Due to symmetry, consider only one half of the cross section as in Fig. 5.38(b). An ellipse is described by

$$\frac{x^2}{a^2} + \frac{y^2}{b^2} = 1$$

With $x = r\cos\phi$, $y = r\sin\phi$, it is readily shown that

$$r = \frac{a}{\sqrt{\cos^2\phi + \nu^2 \sin^2\phi}}, \qquad \nu = a/b,\ dl = r d\phi.$$

5.18 Use the program in Fig. 5.17 (or develop your own program) to calculate the scattering pattern for each array of parallel wires shown in Fig. 5.39.

5.19 Repeat Problem 5.17 using the techniques of Section 5.5.2. That is, consider the cylinder in Fig. 5.38(a) as an array of parallel wires.

5.20 Consider the scattering problem of a dielectric cylinder with cross section shown in Fig. 5.40. It is illuminated by a TM wave. To obtain the field $[E]$ inside the dielectric cylinder, MOM formulation leads to the matrix equation

$$[A][E] = \left[E^i\right]$$

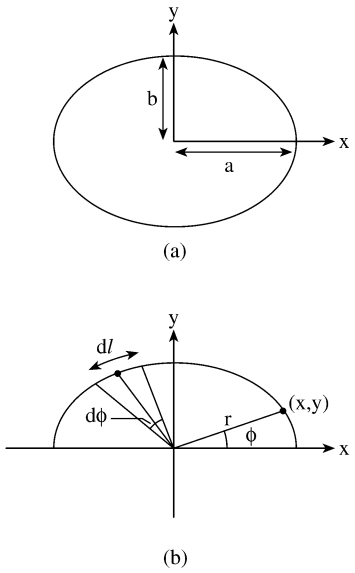

Figure 5.38
For Problem 5.17.

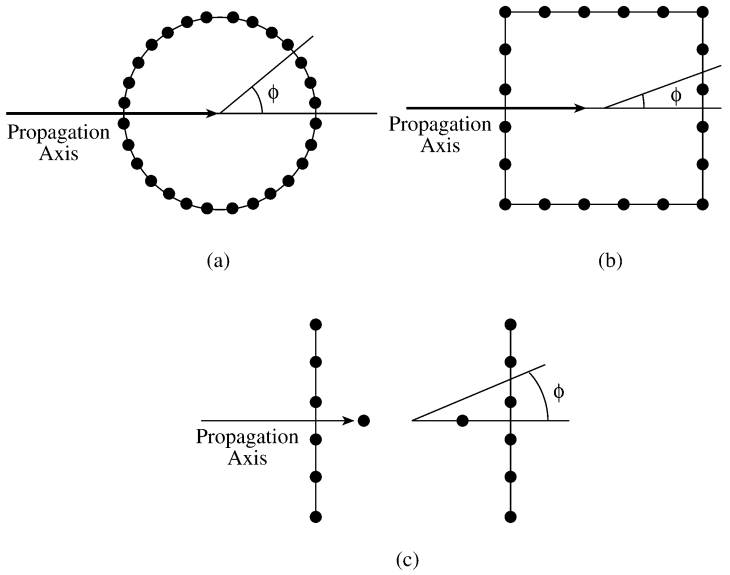

Figure 5.39
Arrays of parallel wires: (a) cylinder, (b) square, (c) I-beam, for Problem 5.18.

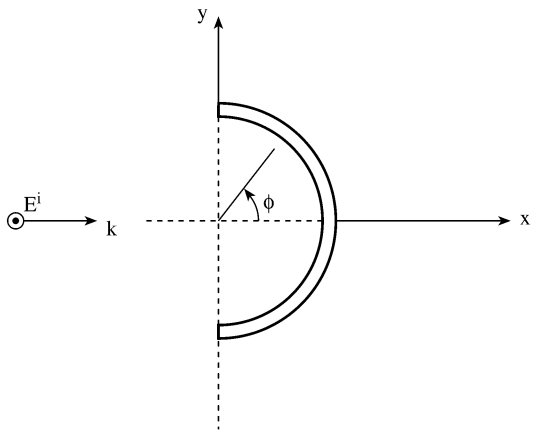

Figure 5.40
For Problem 5.20.

where

$$A_{mn} = \begin{cases} \epsilon_m + j\dfrac{\pi}{2}(\epsilon_m - 1)\, ka_n H_1^{(2)}(ka_m), & m = n \\ j\frac{\pi}{2}(\epsilon_m - 1)\, ka_n J_1(ka_n)\, H_0^{(2)}(k\rho_{mn}), & m \neq n \end{cases}$$

$$E_m^i = e^{jk(x_m \cos\phi_i + y_m \sin\phi_i)}$$

$$\rho_{mn} = \sqrt{(x_m - x_n)^2 + (y_m - y_n)^2},\ m, n = 1, 2, \ldots, N$$

N is the number of cells the cylinder is divided into, ϵ_m is the average dielectric constant of cell m, a_m is the radius of the equivalent circular cell which has the same cross section as cell m. Solve the above matrix equation and obtain $E_n,\ n = 1, 2, \ldots, N$. Use E_n to obtain the echo width of the dielectric cylinder, i.e.,

$$W(\phi) = \frac{\pi^2 k}{\left|E^i\right|^2}\left|\sum_{n=1}^{N}(\epsilon_n - 1)\, E_n a_n J_1(ka_n)\, e^{jk(x_n \cos\phi + y_n \sin\phi)}\right|^2$$

for $\phi = 0°, 5°, 10°, \ldots, 180°$. Plot $W(\phi)$ versus ϕ. For the dielectric cylinder, take $\mu = \mu_o$, $\epsilon = 4\epsilon_o$, inner radius is 0.25λ, outer radius is 0.4λ, and $\lambda = 1$m.

5.21 The integral equation

$$-\frac{1}{2\pi}\int_{-w}^{w} I\left(z'\right)\ln\left|z - z'\right| dz' = f(z), \quad -w < z < w$$

can be cast into matrix equation

$$[S][I] = [F]$$

using pulse basis function and delta expansion function (point matching).

(a) Show that

$$S_{mn} = \frac{\Delta}{2\pi}\left[1 - \ln\Delta - \frac{1}{2}\ln\left|(m-n)^2 - \frac{1}{4}\right| - (m-n)\ln\frac{|m-n+1/2|}{|m-n-1/2|}\right]$$
$$F_n = f(z_n)$$

where $z_n = -w + \Delta(n-1/2), n = 1, 2, \ldots, N, \Delta = 2w/N$. Note that $[S]$ is a Toepliz matrix having only N distinct elements.

(b) Determine the unknowns $\{I_m\}$ with $f(z) = 1, N = 10, 2w = 1$.

(c) Repeat part (b) with $f(z) = z,\ N = 10,\ 2w = 1$.

5.22 A two-term representation of the current distribution on a thin, center-fed half-wavelength dipole antenna is given by

$$I(z) = \sum_{n=1}^{2} B_n \sin\left(\frac{2\pi n}{\lambda}(\lambda/4 - |z|)\right)$$

Substituting this into Hallen's integral equation gives

$$\sum_{n=1}^{2} B_n \int_{-\lambda/4}^{\lambda/4} \sin\left[\frac{2\pi n}{\lambda}\left(\lambda/4 - \left|z'\right|\right]\right. G\left(z, z'\right) dz' + \frac{jC_1}{\eta_o}\cos k_o z$$
$$= -\frac{j}{\eta_o} V_T \sin k_o |z|$$

where $\eta_o = 120\ \pi,\ k_o = \dfrac{2\pi}{\lambda} = \dfrac{2\pi f}{c}$, and $G(z, z')$ is given by Eq. (5.152). Taking $V_T = 1$ volt, $\lambda = 1$ m, $a/\lambda = 7.022 \times 10^{-3}$, and match points at $z = 0, \lambda/8, \lambda/4$, determine the constants B_1, B_2, and C_1. Plot the real and imaginary parts of $I(z)$ against z.

5.23 Using Hallen's IE, determine the current distribution $I(z)$ on a straight dipole of length ℓ. Plot $|I| = |I_r + jI_i|$ against z. Assume excitation by a unit voltage, $N = 51, \Omega = 2\ln\dfrac{\ell}{a} = 12.5$, and consider cases: (a) $\ell = \lambda/2$, (b) $\ell = 1.5\lambda$.

5.24 (a) Show that Pocklington integral equation (5.141) can be written as

$$-E_z^i = \frac{\lambda\sqrt{\mu/\epsilon}}{8j\pi a^2}\int_{-\ell/2}^{\ell/2} \frac{I\left(z'\right)e^{-jkR}}{R^5}\left[(1+jkR)\left(2R^2 - 3a^2\right) + k^2a^2R^2\right]dz'$$

(b) By changing variables, $z' - z = a\tan\theta$, show that

$$-E_z^i = \frac{\lambda\sqrt{\mu/\epsilon}}{8j\pi^2 a^2}\int_{\theta_1}^{\theta_2} I\left(\theta'\right)e^{-jka/\cos\theta'}$$
$$\cdot\left[\left(jka + \cos\theta'\right)\left(2 - 2\cos^2\theta'\right) + k^2a^2\cos\theta'\right]d\theta'$$

$$\text{where } \theta_1 = -\tan^{-1}\frac{\ell/2+z}{a},\ \theta_2 = \tan^{-1}\frac{\ell/2-z}{a}.$$

5.25 Using the program in Fig. 5.26 (or your own self-developed program), calculate the electric field inside a thin conducting layer ($\mu = \mu_o$, $\epsilon = 70\epsilon_o$, $\sigma = 1$ mho/m) shown in Fig. 5.41. Assume plane wave with electric field perpendicular to the plane of the layer, i.e.,

$$\mathbf{E}^i = e^{-jk_o z}\mathbf{a}_x \quad \text{V/m}$$

where $k_o = 2\pi f/c$. Consider only one half of the layer. Calculate $|E_x|/|E^i|$ and neglect E_y and E_z at the center of the cells since they are very small compared with E_x. Take $a = 0.5$ cm, $b = 4$ cm, $c = 6$ cm.

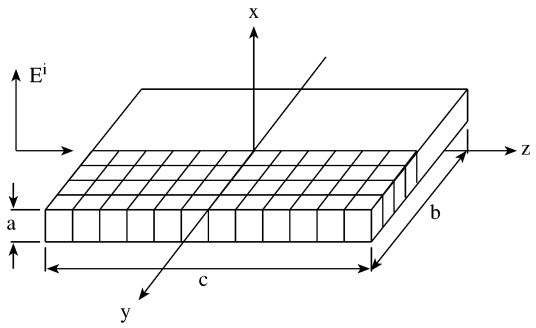

Figure 5.41
For Problem 5.25.

5.26 Consider an adult torso with a height 1.7 m and a shape shown in Fig. 5.42. If the torso is illuminated by a vertically polarized EM wave of 80 MHz with an incident electric field of 1 V/m, calculate the absorbed power density given by

$$\frac{\sigma}{2}\left(E_x^2 + E_y^2 + E_z^2\right)$$

at the center of each cell. Take $\mu = \mu_o$, $\epsilon = 80\epsilon_o$, $\sigma = 0.84$ mhos/m.

5.27 Suppose the dielectric cylinder in Problem 5.20 is a biological body modeled by a cylinder of cross-section 75×50 cm^2, shown in Fig. 5.43. A TM wave of frequency $f = 300$ MHz is normally incident on the body. Compute the fields inside the body using the MOM formulation of Problem 5.20. In this case, take ϵ_m as complex permittivity of cell m, i.e.,

$$\epsilon_m = \epsilon_{rm} - j\,(\sigma_m/\omega\epsilon_o)\,, \qquad m = 1, 2, \ldots, N = 150$$

To make the body inhomogeneous, take $\epsilon_{rm} = 8$ and $\sigma_m = 0.03$ for cells 65, 66, 75, 85, and 86; take $\epsilon_{rm} = 7$ and $\sigma_m = 0.04$ for cells 64, 67, 74, 77, 84, and 87; and take $\epsilon_{rm} = 5$ and $\sigma_m = 0.02$ for all the other cells. Compute E_n.

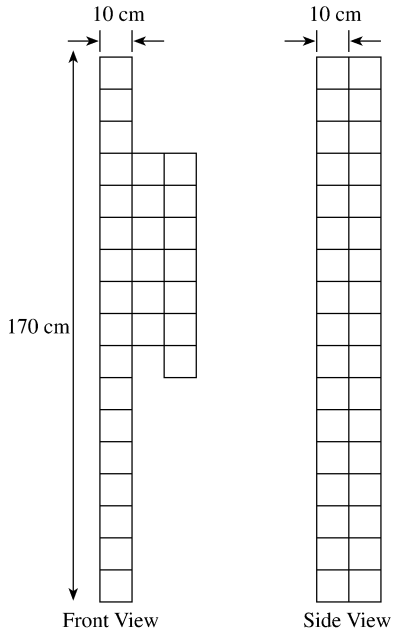

Figure 5.42
An adult torso: for Problem 5.26.

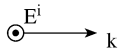

141									150
131									140
121									130
111									120
101									110
91									100
81			84	85	86	87			90
71			74	75	76	77			80
61			64	65	66	67			70
51									60
41									50
31									40
21									30
11									20
1	2	3	4	5	6	7	8	9	10

Figure 5.43
For Problem 5.27.